Efficient Storage Design and Query Scheduling for Improving Big Data Retrieval and Analytics

by

Zhuo Liu

A dissertation submitted to the Graduate Faculty of
Auburn University
in partial fulfillment of the
requirements for the Degree of
Doctor of Philosophy

Auburn, Alabama
May 9, 2015

Keywords: Big Data, Cloud Computing, Hadoop, Hive Query Scheduling, Phase Change Memory, Parallel I/O

Copyright 2015 by Zhuo Liu

Approved by

Weikuan Yu, Chair, Associate Professor of Computer Science and Software Engineering
Saad Biaz, Professor of Computer Science and Software Engineering
Xiao Qin, Associate Professor of Computer Science and Software Engineering

Abstract

With the perpetually increasing requirement and generation of digital data, the human being has been stepping into the Big Data era. To efficiently manage, retrieve and exploit such gigantic amount of data continuously generated by all individuals and organizations of the society, a rich set of efforts has been invested to develop high-performance, scalable and fault-tolerant data storage systems and analytics frameworks. Recently, flash-based solid state disks and byte-addressable non-volatile memories have been developed and introduced into computer system storage hierarchy for substituting traditional hard drives and DRAM due to the faster data accesses, higher density and energy-efficiency. Along with the trend, how to systematically integrate such cutting edge memory technologies for fast system data retrieval becomes a highly concerned issue. In addition, from the users' point of view, some mission-critical scientific applications are suffering from inefficient I/O schemes, thus not able to fully utilize the underlying parallel storage systems. This fact makes the development of more efficient I/O methods appealing. Moreover, MapReduce has emerged as a powerful big data processing engine that supports large-scale complex analytics applications. Most of them are written in declarative query languages such as Hive and Pig Latin. Therefore, it requires efficient coordination of Hive compiler and Hadoop runtime for fast and fair big data analytics.

This dissertation investigates the research challenges mentioned above and contributes efficient storage design, I/O methods and query scheduling for improving big data retrieval and analytics. I firstly aim at addressing the I/O bottleneck issue in large-scale computers and data centers. Accordingly, in my first study, by leveraging the advanced features of cutting-edge non-volatile memories, I have presented and devised a Phase Change Memory (PCM)-based hybrid storage architecture, which provides efficient buffer management and novel wear leveling techniques, thus achieving highly improved data retrieval performance and at the same time solving the PCM's

endurance issue. In the second study, we adopt a mission-critical scientific application, GEOS-5, as a case to profile and analyze the communication and I/O issues that are preventing applications from fully utilizing the underlying parallel storage systems. Through detailed architectural and experimental characterization, we observe that current legacy I/O schemes incur significant network communication overheads and are unable to fully parallelize the data access, thus degrading applications' I/O performance and scalability. To address these inefficiencies, we redesign its I/O framework along with a set of parallel I/O techniques to achieve high scalability and performance. In the third study, I have identified and profiled important performance and fairness issues existing in current MapReduce-based data warehousing system. In particular, I have proposed a prediction based query scheduling framework, which bridges the semantic gap between MapReduce runtime and query compiler and enables efficient query scheduling for fast and fair big data analytics.

Acknowledgments

First and foremost, I would like to sincerely thank my advisor, Dr. Weikuan Yu, for his thorough academic guidance, patient cultivation, encouragement and continuous support during my doctoral study. I have been really fortunate to become his student and conduct interesting and cutting-edge research work in the outstanding academic environment he created in the PASL lab. As my advisor, he has been helping me identify novel research topics and solve critical challenges, and giving me all kinds of precious opportunities to hone my skills, broaden my horizons and shape my professional career. He has also been a most helpful friend of me, helping me in my life and encouraging me during the tough moments. I greatly appreciate his priceless time and efforts for nurturing me during my Ph.D experience.

I wish to thank my collaborators. It has been my true pleasure to work closely with Dr. Jay Lofstead in the Sandia National Laboratories during my summer intern, with Dr. Xiaoning Ding from New Jersey Institute of Technology on the prediction-based query scheduling project, with Dr. Jeffrey Vetter and Dr. Dong Li from Oak Ridge National Laboratory on the non-volatile memory project.

I would also like to thank my committee members: Dr. Saad Biaz and Dr. Xiao Qin and my university reader Dr. Fadel Megahed. Their precious suggestions and patient guidance help to improve my dissertation.

I feel really grateful to my PASL group-mates: Dr. Yandong Wang, Dr. Yuan Tian, Dr. Xinyu Que, Cong Xu, Bin Wang, Teng Wang, Patrick Carpenter, Fang Zhou, Huansong Fu, Xinning Wang, Kevin Vasko, Michael Pritchard, Hai Pham and Bhavitha Ramaiahgari. Their cooperation in work and help in life make Auburn PASL a big and warm family and an excellent place where we learn, create, improve and enjoy.

Finally, I own the deepest gratitude to my mother Cui'e Ding, my grandma Yulian Zhang, my father Jiannong Liu, my grandpa Dirong Liu, my brother Jia Liu, my aunt Zhenfei Liu, my uncle Minxiang Zhou, my parents-in-law Tianqiao Chen and Zhixiang Cao, and my niece Ziyi Liu for their unconditional support, care and love. Eventually, I would like to say thank you to my wife Lin Cao for her everlasting love during my life. Without her being with me, I could not imagine how I could have gone through such a long journey.

Table of Contents

List of Figures

List of Tables

Chapter 1

Introduction

As reported by IDC [39], the digital universe (a measure of all digital data generated, created and consumed in a single year) will rise from about 3,000 exabytes in 2012 to 40,000 exabytes in 2020. To cope with the booming storage and retrieval requirement of such gigantic data, numerous endeavors have been invested. Flash based solid-state devices (FSSDs) have been adopted within the memory hierarchy to improve the performance of hard disk drive (HDD) based storage system. However, with the fast development of storage-class memories, new storage technologies with better performance and higher write endurance than FSSDs are emerging, e.g., phase-change memory (PCM) [6]. Understanding how to leverage these state-of-the-art storage technologies for modern computing systems is important to solve challenging data intensive computing problems.

Even equipped with highly parallel underlying storage systems, some legacy important scientific applications are still being impeded by inefficient I/O aggregation and output schemes. In order to represent the scientific information ranging from physics, chemistry to biology on different longitudes, latitudes and altitudes all over the earth, huge amounts of multi-dimension data sets need to be produced, stored and accessed in an efficient way. However, quite a few important applications still lack efficient I/O methods to deal with such data retrieval issues efficiently. GEOS-5 [8] is one of such applications.

Moreover, 33% of data in the digital universe can be valuable if analyzed [39]. However, currently only 0.5% of total data have been analyzed due to limited analytic capabilities. Thus it requires highly efficient, scalable and flexible approaches to conduct analytics on such gigantic data, where cloud computing plays an increasingly important role. MapReduce [29] is a very popular programming model widely used for efficient, scalable and fault-tolerant data analytics.

In addition, to ease the coding difficulties for each individual MapReduce job, a set of data warehouse systems and query languages are exploited on top of the MapReduce framework, such as Hive [94], Pig [40] and DryadLINQ [117]. In MapReduce based data warehousing system, analytic queries are typically compiled into execution plans in the form of directed acyclic graphs (DAGs) of MapReduce jobs. Jobs in the DAGs are dispatched to the MapReduce processing engine as soon as their dependencies are satisfied. MapReduce adopts a task-level scheduling policy to strive for balanced distribution of tasks and effective utilization of resources. However, there is a lack of query-level semantics in the purely task-based scheduling algorithms, resulting in unfair treatment of different queries, low utilization of system resources, prolonged execution time, and low query throughput.

In this dissertation, I present our studies of PCM-based hybrid storage, I/O optimization for scientific applications, and MapReduce query scheduling framework for improving big data retrieval and analytics. In the rest of this chapter, I first provide a background introduction for my studies. I then give an introduction for my major research contributions. At the end, I provide a brief overview of this dissertation.

1.1 Research Background

1.1.1 Background of Non-Volatile Memories

The explosive growth of data brings both performance and power consumption challenges. To solve these challenges, flash-based Hybrid Storage Drives (HSDs) have been proposed to combine standard hard disk drives (HDDs) and Flash-based Solid-State Drives (FSSDs) into a single storage enclosure [4]. Although flash-based HSDs are gaining popularity, they suffer from several striking shortcomings of FSSDs, namely high write latency and low endurance, which seriously hinder the successful integration of FSSDs into HSDs. Lots of techniques have been proposed to address the issues [90, 88]. However, most of them only target specific usage scenarios and cannot act as a general solution to eliminate FSSDs' drawbacks, which continue to threaten the future success of FSSD-based HSDs. There remains a need of better technologies in the storage market.

Latest storage technologies are bringing in new non-volatile random-access memory (NVRAM) devices such as phase-change memory, spin-torque transfer memory (STTRAM) [57], and resistive RAM (RRAM) [57]. These memory devices support the non-volatility of conventional HDDs while providing speeds approaching those of DRAMs. Among these technologies, PCM is particularly promising with several companies and universities already providing prototype chips and devices [18, 6]. Compared to FSSD, PCM is equipped with a number of performance and energy advantages [26]. First, PCM has much faster read response time than FSSD. It offers a read response time of around 50ns, nearly 500 times faster than that of FSSD. Second, PCM can overwrite data directly on the memory cell, unlike FSSD's write-after-erase. The write response time of PCM is less than 1 us, nearly three orders of magnitude faster than that of FSSD. Third, the program energy for PCM is 6 Joule/GB, 3 times smaller than that of FSSD [26]. Thus, PCM is a viable alternative to FSSDs for building hybrid storage systems.

A number of techniques have used NVRAM as data cache to improve disk I/O [20, 33, 55, 101, 41]. Most of them use LRU-like methods (e.g., Least Recently Written, LRW [33, 41]) to manage small size non-volatile cache to improve performance and reliability of HDD-based storage and file system. However, for GBs of high density PCM cache, using LRU to manage them will cause big DRAM overheads in managing the LRU stack and mapping. In addition, LRU/LRW cannot ensure that destaging I/O traffic be presented as sequential writes to hard disks. CSCAN method used in [41] as a supplement for LRW can ease this issue to some extent but it requires O(log(n)) time for insertion, making it not suitable for large size cache management. Therefore, it is crucial to rethink the current cache management strategies for PCM.

1.1.2 Background of Scientific I/O

Scientific applications are playing a critical role in improving our daily life. They are designed to solve pressing scientific challenges, including designing new energy-efficient sources [5]

and modeling the earth system [8]. To boost the productivity of scientific applications, High-Performance Computing (HPC) community has built many supercomputers [12] with unprecedented computation power over the past decade. Meanwhile, computer scientists are also arduously improving parallel file systems [28, 83] and I/O techniques [66, 67] to bridge the gap between fast processors and slow storage systems. Despite the rapid evolution of HPC infrastructures, the development of scientific applications dramatically lags behind in leveraging the capabilities of the underlying systems, especially the superior I/O performance.

1.1.3 Background of MapReduce-based Data Warehouse Systems

Analytics applications often impose diverse yet conflicting requirements on the performance of underlying MapReduce systems, such as high throughput, low latency, and fairness among jobs. For example, to support latency-sensitive applications from advertisements and real-time event log analysis, MapReduce must provide fast turnaround time.

Because of their declarative nature and ease of programming, analytics applications are often created using high-level query languages. These analytic queries are transformed by compilers into an execution plan of multiple MapReduce jobs, which are often depicted as direct acyclic graphs (DAGs). A job in a DAG can only be submitted to MapReduce when its dependencies are satisfied. A DAG query completes when its last job is finished. Thus the execution of analytic queries is centered around dependencies among DAG jobs and the completion of jobs along the critical path of a DAG. On the other hand, to support MapReduce jobs from various sources, the lower level MapReduce systems usually adopt a two-phase scheme that allocates computation, communication and I/O resources to two types of constituent tasks (Map and Reduce) from concurrently active jobs. For example, the Hadoop Fair Scheduler (HFS) and Capacity Scheduler (HCS) strive to allocate resources among map and reduce tasks to aim for good fairness among different jobs and high throughput of outstanding jobs. When a job finishes, the schedulers immediately select tasks from another job for resource allocation and execution. However, these two jobs may belong

to DAGs of two different queries. Such interleaved execution of jobs from different queries can significantly delay the completion of all involved queries, as we will show in Chapter 2.3.

This scenario is a manifestation of the mismatch between system and application objectives. While the schedulers in the MapReduce processing engine focus on the job-level fairness and throughput, analytic applications are mainly concerned with the query-level performance objectives. This mismatch of objectives often leads to prolonged execution of user queries, resulting in poor user satisfaction. Besides the delayed query completion, the existing schedulers in MapReduce also have difficulties in recognizing the locality of data across jobs. For example, jobs in the same DAG may share their input data [118]. But Hadoop schedulers are unable to detect the existence of common data among these jobs and may schedule them with a long lapse of time. In this case, the same data would be read multiple times, degrading the throughput of MapReduce systems. As Hive and Pig Latin have been used pervasively in data warehouses, the above problem becomes a serious issue and must be timely addressed. More than 40% of Hadoop production jobs at Yahoo! have been Pig programs [40]. In Facebook, 95% Hadoop jobs are generated by Hive [56].

1.2 Research Contributions

1.2.1 PCM-Based Hybrid Storage

In this dissertation, I design a novel hybrid storage system that leverages PCM as a write cache to merge random write requests and improve access locality for HDDs. To support this hybrid architecture, I propose a novel cache management algorithm, named HALO. It implements a new eviction policy and manages address mapping through cuckoo hash tables. These techniques together save DRAM overheads significantly while maintaining constant O(1) speeds for both insertion and query. Furthermore, HALO is very beneficial in terms of managing caching items, merging random write requests, and improving data access locality. In addition, by removing the dirty-page write-back limitations that commonly exist in DRAM-based caching systems, HALO enables better write caching and destaging, and thus achieves better I/O performance. And by

storing cache mapping information on non-volatile PCM, the storage system is able to recover quickly and maintain integrity in case of system crashes.

To use PCM as a write cache, I also address PCM's limited durability. Several existing wear-leveling techniques have shown good endurance improvement for PCM-based memory systems [78, 77, 122]. However, these techniques are not specifically designed for PCM used in storage and file systems, and thus can negatively impact spatial locality of file system accesses, which in turn will degrade read-ahead and sequential access performance of file systems. I propose a wear leveling technique called space filling curve wear-leveling, which not only provides a good write balance between different regions of the device, but also keeps data locality and enables good adaptation to the file system's I/O access characteristics.

Using two in-house simulators, I have evaluated the functionality of the proposed PCM-based hybrid storage devices. Our experimental results demonstrate that the HALO caching scheme leads to an average reduction of 36.8% in execution time compared to the LRU caching scheme, and that the SFC wear leveling extends the lifetime of PCM by a factor of 21.6. Our results demonstrate that PCM can serve as a write cache for fast and durable hybrid storage devices.

1.2.2 I/O Framework Optimization for GEOS-5

This paper seeks to examine and characterize the communication and I/O issues that prevent current scientific applications from fully exploiting the I/O bandwidth provided by underneath parallel file systems. Based on our detailed analysis, we propose a new framework for scientific applications to support a rich set of parallel I/O techniques. Among different applications, we select the Goddard Earth Observing System model, Version 5, (GEOS-5) from NASA [8] as a representative case. GEOS-5 is a large-scale scientific application designed for grand missions such as climate modeling, weather broadcasting and air-temperature simulation. Built on top of Earth System Modeling Framework (ESMF) [42] and MAPL library [89], GEOS-5 incorporates a system of models to conduct NASA's earth science research, such as observing Earth systems, and climate and weather prediction.

GEOS-5 contains various communication and I/O patterns observed in many applications for check-pointing and writing output. Data are organized in the form of either 2 or 3 dimensional variables. In many cases, multiple variables are arranged in the same group, called a bundle. A single variable is a composition of a number of 2-D planes, each of which is evenly partitioned among all the processes in the same application. Although the computation can be fully parallelized, our characterization identifies three inefficient communication and I/O patterns in the current design. First, for each plane of data, a process has to be elected as the *plane root* to gather all the data from all processes in the plane, thus causing a single point of contention. Second, only one process, called the *bundle root*, is responsible for collecting data from all the plane roots and writing the entire bundle to the storage system. This behavior essentially forces all the processes to wait until the bundle root finishes I/O, resulting in not only an I/O bottleneck but also a severe global synchronization barrier. Third, GEOS-5, like many legacy scientific applications, is unable to leverage state-of-the-art parallel I/O techniques due to rigid framework constraints, and continue using serial I/O interfaces, such as serial NetCDF (Network Common Data Form) [9].

To address the above inefficiencies, we redesign the communication and I/O framework in this GEOS-5 application, so that the new framework can allow application to exploit the performance advantages provided by a rich set of parallel I/O techniques. However, our experimental evaluation shows that simply using parallel I/O tools such as PnetCDF [58], cannot effectively enable application to scale to a large number of processes due to metadata synchronization overhead. On the other hand, using another parallel I/O library, called ADIOS (The Adaptable IO System) [66], can improve the I/O performance with the trade-off that it may sacrifice the consistency induced by delayed inter-process written synchronization and complicate the post processing of output files.

To summarize, we have made following three research contributions in this work:

- We conduct a comprehensive analysis of a climate scientific application, GEOS-5, and identify several performance issues with GEOS-5 communication and I/O patterns.
- We design a new parallel framework in GEOS-5 for it to leverage a variety of parallel I/O techniques.

- We have employed PnetCDF and ADIOS for alternative I/O solutions for GEOS-5 and evaluated their performance. Our evaluation demonstrates that our optimization with ADIOS can significantly improve the I/O performance of GEOS-5.

1.2.3 Prediction Based Two-Level Query Scheduling

In this dissertation, I propose a *prediction-based two-level scheduling framework* that can address these problems systematically. Three techniques are introduced including cross-layer semantics percolation, selectivity estimation and multivariate time prediction, and two-level query scheduling (***TLS*** for brevity). First, cross-layer semantics percolation allows the flow of query semantics and job dependencies in the DAG to the MapReduce scheduler. Second, with rich semantics information, I model the changing size of analytics data through selectivity estimation, and then build a multivariate model that can accurately predict the execution time of individual jobs and queries. Furthermore, based on the multivariate time predication, I introduce two-level query scheduling that can maximize the intra-query job-level concurrency, speed up the query completion, and ensure query fairness.

Our experimental results on a set of complex workloads demonstrate that TLS can significantly improve both fairness and throughput of Hive queries. Compared to HCS and HFS, TLS improves average query response time by 43.9% and 27.4% for the Bing benchmark and 40.2% and 72.8% for the Facebook benchmark. Additionally, TLS achieves 59.8% better fairness than HFS on average.

1.3 Publications

During my doctoral study, my research work has contributed to the following publications.

1. Z. Liu, W. Yu, F. Zhou, X. Ding and W. Tsai. Prediction-Based Two-Level Scheduling for Analytic Queries. Under review.

2. Z. Liu, B. Wang and W. Yu. HALO: A Fast and Durable Disk Write Cache using Phase Change Memory. Journal of Cluster Computing (Springer). Under minor revision.

3. C. Xu, R. Goldsone, Z. Liu, H. Chen, B. Neitzel and W. Yu. Exploiting Analytics Shipping with Virtualized MapReduce on HPC Backend Storage Servers. IEEE Transactions on Parallel and Distributed Computing, 2015 [25].

4. T. Wang, K. Vasko, Z. Liu, H. Chen, and W. Yu. Enhance Scientific Application I/O with Cross-Bundle Aggregation. International Journal of High Performance Computing Applications, 2015 [105].

5. X. Wang, B. Wang, Z. Liu and W. Yu. "Preserving Row Buffer Locality for PCM Wear-Leveling Under Massive Parallelism. Under review.

6. B. Wang, Z. Liu, X. Wang and W. Yu. Eliminating Intra-Warp Conflict Misses in GPU. In IEEE Design, Automation and Test in Europe (DATE), 2015 [102].

7. T. Wang, K. Vasko, Z. Liu, H. Chen, and W. Yu. BPAR: A Bundle-Based Parallel Aggregation Framework for Decoupled I/O Execution. International Workshop on Data-Intensive Scalable Computing Systems (DISCS), 2014 [104].

8. Z. Liu, J. Lofstead, T. Wang, and W. Yu. A Case of System-Wide Power Management for Scientific Applications. In IEEE International Conference on Cluster Computing, 2013 [62].

9. Z. Liu, B. Wang, T. Wang, Y. Tian, C. Xu, Y. Wang, W. Yu, C. Cruz, S. Zhou, T. Clune and S. Klasky. Profiling and Improving I/O Performance of a Large-Scale Climate Scientific Application. In International Conference on Computer Communications and Networks (ICCCN), 2013 [63].

10. Y. Tian, Z. Liu, S. Klasky, B. Wang, H. Abbasi, S. Zhou, N. Podhorszki, T. Clune, J. Logan, and W. Yu. A Lightweight I/O Scheme to Facilitate Spatial and Temporal Queries of Scientific Data Analytics. In IEEE Symposium on Massive Storage Systems and Technologies (MSST), 2013 [97].

11. C. Xu, M. G. Venkata, R. L. Graham, Y. Wang, Z. Liu and W. Yu. SLOAVx: Scalable LOgarithmic AlltoallV Algorithm for Hierarchical Multicore Systems. In IEEE/ACM International Symposium on Cluster, Cloud and Grid Computing (CCGrid), 2013 [112].

12. Y. Wang, Y. Jiao, C. Xu, X. Li, T. Wang, X. Que, C. Cira, B. Wang, Z. Liu, B. Bailey and W. Yu. Assessing the Performance Impact of High-Speed Interconnects on MapReduce. In Third Workshop on Big Data Benchmarking (Invited Book Chapter), 2013 [106].

13. Z. Liu, B. Wang, P. Carpenter, D. Li, J. Vetter and W. Yu. PCM-Based Durable Write Cache for Fast Disk I/O. In IEEE International Symposium on Modeling, Analysis and Simulation of Computer and Telecommunication Systems (MASCOTS), 2012 [61].

14. D. Li, J.S. Vetter, G. Marin, C. McCurdy, C. Cira, Z. Liu, W. Yu. Identifying opportunities for byte-addressable non-volatile memory in extreme-scale scientific applications. In International Parallel and Distributed Processing Symposium (IPDPS), 2012 [57].

15. Z. Liu, J. Zhou, W. Yu, F. Wu, X. Qin and C. Xie. MIND: A Black-Box Energy Consumption Model for Disk Arrays. In 1st International Workshop on Energy Consumption and Reliability of Storage Systems (ERSS'11), 2011 [64].

1.4 Dissertation Overview

The focus of this dissertation is on efficient storage design and query scheduling for improving big data retrieval and analytics, which targets at addressing the challenges that origin from explosive data generation and increasing requirements of fast data accesses and analysis. To be specific, this dissertation makes the following research contributions:

- I design a novel hybrid storage system that leverages PCM as a write cache to merge random write requests and improve access locality for HDDs. To support this hybrid architecture, I propose a novel cache management algorithm, named HALO. In addition, I devise two novel wear leveling technique to prolong PCM's life time.

- I profile the inefficiency issue in a mission-critical scientific application called GEOS-5 and address the single point contention and network bottleneck issue by amending its I/O middleware and enabling the integration of parallel I/O interfaces, through which its I/O performance gets significantly improved.

- I design a prediction-based two-level query scheduling framework that can exploit query semantics for resource and time prediction, thus guiding scheduling decisions at two levels: the intra-query level for better job parallelism and the inter-query level for fast and fair query completion.

- Systematic experimental evaluations are conducted to demonstrate our solutions' advantages of improving big data retrieval and analytics efficiency over traditional techniques.

The remainder of the dissertation is organized as follows. In Chapter 2, I present the problem statement, which reveals the challenges in current big data storage and retrieval, and then identifies performance and fairness issues of MapReduce based data warehouse systems. In Chapter 3, I detail the design, implementation and evaluation of PCM-based hybrid storage. In Chapter 4, the design, implementation and evaluation of GEOS-5 I/O optimization are introduced. In Chapter 5, I describe the design, implementation and evaluation of Prediction Based Two-Level Scheduling. I summarize the dissertation and point out future research directions in Chapter 6 and Chapter 7.

Chapter 2

Problem Statement

In this chapter, I firstly analyze I/O systems' challenges for exascale computers, then address and characterize the performance and fairness disadvantages for queries under traditional MapReduce scheduling techniques.

2.1 Challenges in I/O Systems for Exascale Computers

To address existing performance and power consumption issues, a rich set of efforts have been undertaken to bring faster and more energy efficient computing [10], memory [57] and storage [113] hardware to build large-scale supercomputers.

In terms of memory and storage techniques, the new cutting-edge non-volatile random-access memory (NVRAM) attracts many people's focuses. The NVRAM technologies include phase-change memory (PCM), spin-torque transfer memory (STTRAM) [57], and resistive RAM (RRAM) [57], which support the non-volatility of conventional HDDs while providing similar speeds and byte addressability as DRAMs.

Phase-change memory technology has become mature enough to enter the market [18, 6] because of the new discoveries of fast-crystallizing materials such as $Ge_2Sb_2Te_5$(GST) and In-doped Sb_2Te(AIST). Phase-change memory (PCM) is based on a type of chalcogenide-based material made of germanium, antimony or tellurim. The chalcogenide-based material can exist in different states with dramatically different electrical resistivity. The crystalline and amorphous states are two typical states. In the crystalline state, the material has a low resistance and is used to represent a binary 1; while in the amorphous state, the material has a high resistance and is used to represent a binary 0. However, there's still a lack of systematic way to integrate such non-volatile memories

as PCM into our traditional storage hierarchy for addressing the I/O challenges in future exascale computers.

2.2 Challenges in big data retrieval for scientific applications

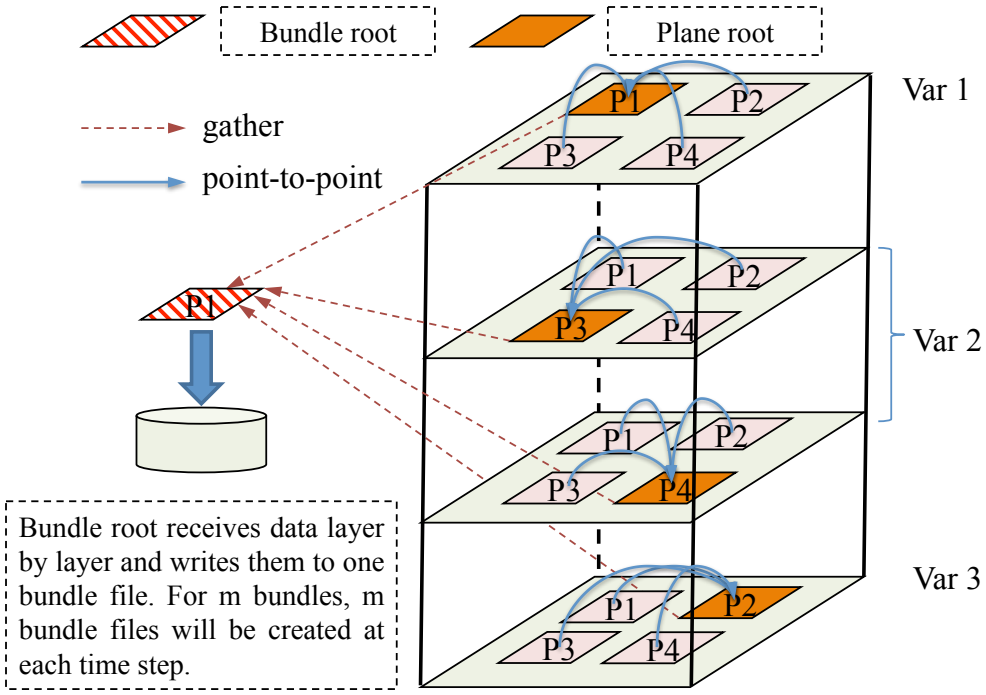

Figure 2.1: Overview of GEOS-5 Communication and I/O

In this section, we first characterize the communication and I/O patterns in GEOS-5, and then examine their impacts on the application performance. The profiling results suggest that it is important to explore an alternative design for the data aggregation and storage for GEOS-5.

2.2.1 Current Data Aggregation and I/O in GEOS-5

GEOS-5 is developed by NASA to simulate climate changes over various temporal granularities, ranging from hours to multiple centuries. Like many legacy scientific applications, GEOS-5 adopts the serial version of NetCDF-4 I/O library [9] for managing its simulation data.

Data variables that describe climate systems are organized as *bundles*, and each bundle represents a physics model such as moisture and turbulence. It contains a varied mixture of many

variables. Each variable has its data organized as a multidimensional dataset, e.g., a 3-D variable transposing internally into latitude, longitude, and elevation. To describe different aspects of the model, multiple 2-D or 3-D variables of state physics are defined, such as cloud condensates and precipitation.

GEOS-5 applies two-dimensional domain decomposition to all variables among parallel processes. 2-D variables have only one level of depth, naturally forming a 2D plane. 3-D variables are organized as multiple 2D planes. The number of 2-D planes is equal to the depth of a 3-D variable. As shown in Figure 2.1, the bundle contains two 2-D variables - *var1* and *var3* and one 3-D variable - *var2*, thus forming a four-layer tube. Each 2-D plane of this bundle is equally divided among four processes so that all four processes can perform simulation in parallel.

At the end of a timestamp, these state variables are written to the underlying file system as history data for future analysis (the real production run lasts for tens or hundreds of timestamps). For maintaining the integrity of the model, all state variables that belong to the same model are written into the same file, called a *bundle file*. As mentioned earlier, each bundle file is stored using the *netcdf* format [9] popular for climatologists.

GEOS-5 currently adopts a hierarchical scheme for collecting data variables and writing them into a bundle file. As shown in Figure 2.1, at the first step, each plane designates a different process as the *plane root* to gather the plane data from all the other processes. Upon the completion of gathering the planar data, one process called *bundle root* is elected to collect the aggregated data from the plane roots. When there are multiple bundles, several bundle roots will aggregate data in parallel from the 2-D planes that belong to their own bundle.

2.2.2 Issues with the Existing Approach

While the existing implementation organizes and stores data variables as bundle files in a convenient format for climatologists, the approach described above faces a number of critical issues for scalable performance.

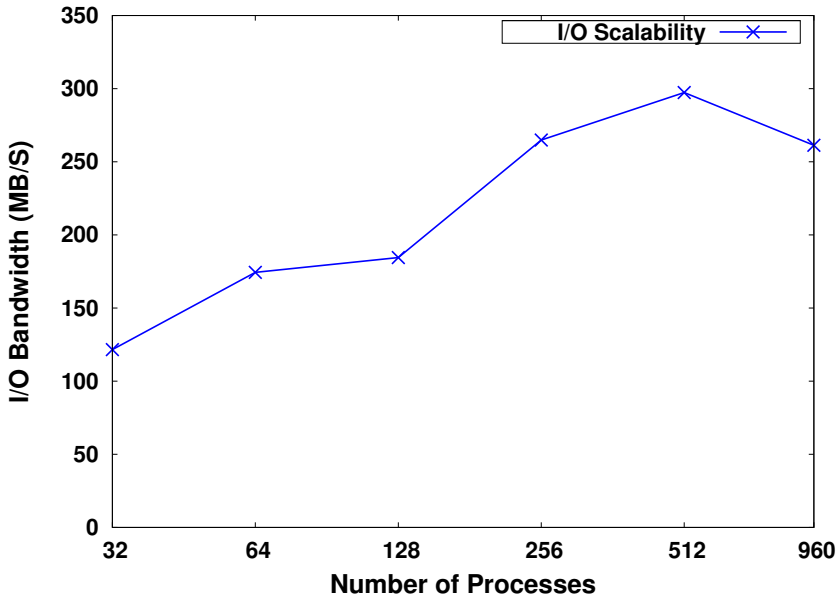

Figure 2.2: I/O Scalability of Original GEOS-5

First, it lacks scalability. With the increase of the number of processes and planes, both plane roots and bundle roots can quickly become points of contention, resulting in communication bottleneck. As demonstrated in Figure 2.2, the application stops scaling when the number of processes increases from 256 to 512 and 960. Although non-blocking MPI (Message Passing Interface) functions are designed to facilitate the overlapping of communication and computation, in current GEOS-5, larger number of processes leads to longer MPI_Wait time as shown in Figure 2.3. Thus simply using non-blocking communication is unable to improve the scalability of the system. Second, increasing the data size of planes can overwhelm the memory capacity of root processes and saturate the network bandwidth of bundle roots, which can be detrimental to the system. Third, such approach leads to a global synchronization barrier among all the processes, since no process can proceed until the bundle root finishes storing all the plane data to the file system. Unfortunately, this point-to-point data transfer between bundle root and I/O server can be very time-consuming, leading to prolonged system running time.

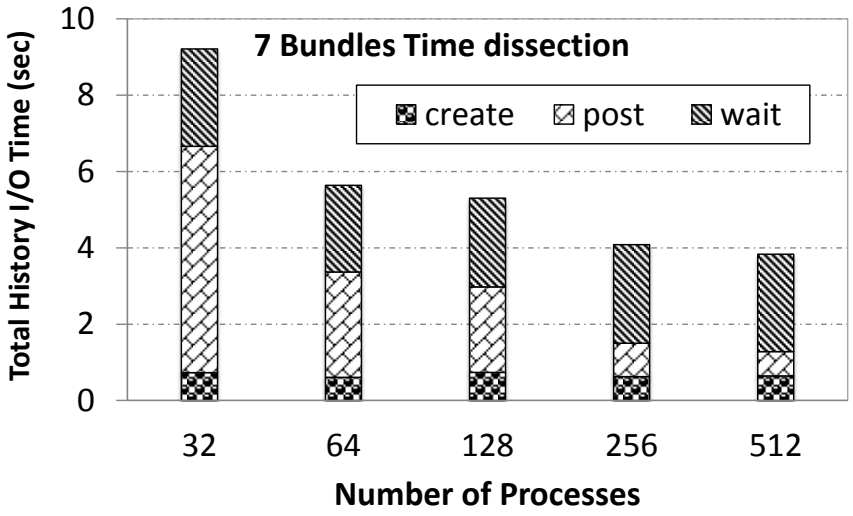

Figure 2.3: Time Dissection of Non-blocking MPI Communication

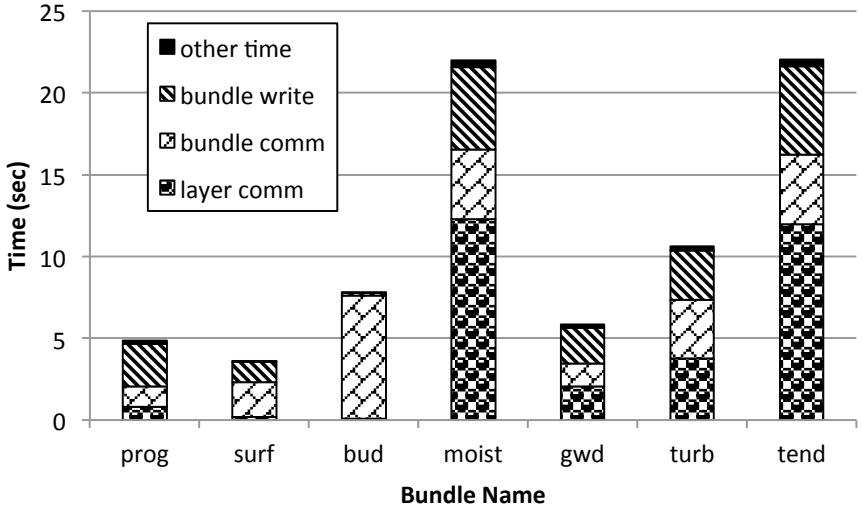

Figure 2.4: Time Dissection for Collecting and Storing Bundles

2.2.3 Performance Dissection of Communication and I/O

To further quantify the communication and I/O time spent on storing history data, we dissect the entire process of collecting and writing 7 bundles in one timestamp. Figure 2.4 shows the results of time dissection. *Moist* and *Tend* are the two largest bundles with 1201 and 1152 planes, respectively. Correspondingly, 55.9% and 54.3% of the time, respectively for Moist and Tend, are spent in collecting the plane data by plane roots. On the other hand, although bundle *Bud* has the fewest number of planes (40), 96.7% of its I/O time is spent on communication between bundle root and plane roots. This is because the plane roots for Bud also play roles as working processes

for other bundles. This delays the progress of plane data collection for the bundle Bud. In addition, on average, the I/O time for writing the bundle into the file system only consumes about 27% of total time of writing the history data.

Gathering data consumes a significant portion of I/O time for the history data as shown in Figure 2.4. Such implementation limits the scalability and is incapable of supporting large datasets. Many parallel I/O techniques are viable to address this issue; however, the hierarchical I/O scheme depicted in Figure 2.1 is unable to leverage these techniques. Therefore, it is critical to overhaul the architecture of scientific application so that it can efficiently run on large-scale cluster with hundreds of thousands of processing cores.

2.3 Performance and Fairness Issues Caused by Semantic Unawareness

In this section, we elaborate the performance and unfairness issues for concurrent queries due to the lack of semantic awareness in the current Hive/Hadoop framework.

2.3.1 Execution Stalls of Concurrent Queries

TPC-H [13] represents a popular online analytical workload. We have conducted a test using a mixture of three TPC-H queries: two instances of Q14 and one of Q17. Q14 evaluates the market response to a production promotion in one month. Q17 determines the loss of average yearly revenue if some orders are not properly fulfilled in time. For convenient description, we name them as QA and QC for the two instances of Q14 and QB for Q17, respectively. Figure 2.5 shows the DAGs for three queries and their constituent jobs. QA and QC are small queries with two short jobs: Aggregate (AGG) and Sort. QB is a large query with four jobs.

In our experiment, we submit QA, QB and QC one after another to our Hadoop cluster. We profile the use of map and reduce slots along with the progress of queries. Figure 2.6 shows the results with the HCS scheduler. J1 and J2 from QB arrive before QA-J2 and QC-J2. They are scheduled for execution, as a result, blocking QA-J2 and QC-J2 from getting map and reduce slots. We can observe that QA-J2 and QC-J2 both experience execution stalls due to the lack of

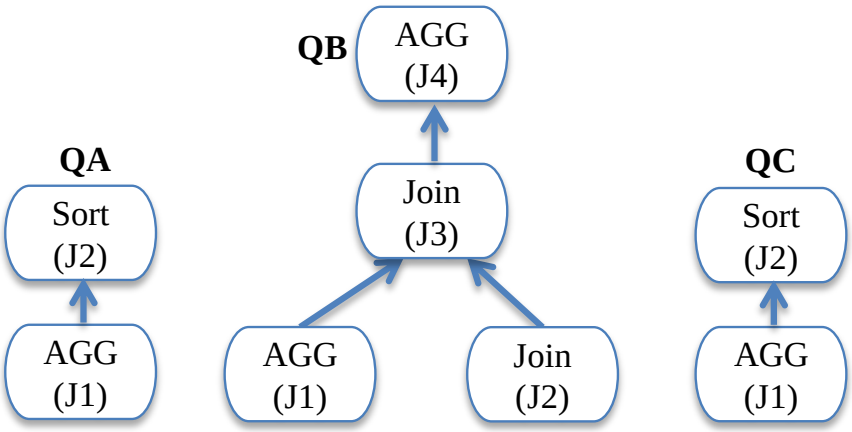

Figure 2.5: A Diagram of Jobs in the DAGs of Three Queries

map slots and reduce slots. Such stalls delay the execution of QA and QC by three times compared to the case when they are running alone.

HFS is known for its monopolizing behavior in causing the stalls to different jobs [107, 92]. We also have conducted the concurrent execution of the same three queries with HFS, and observed similar execution stalls of QA and QC due to the lack of reduce slots. For succinctness, the results are not shown here. Therefore, because of the lack of knowledge on query compositions, Hadoop schedulers cause execution stalls and performance degradation to small queries. In a large-scale analytics system with many concurrent query requests, such issue of execution stalls caused by semantic-oblivious scheduling can become even worse.

2.3.2 Query Unfairness

Besides the stalling of queries and resource underutilization, the lack of query semantics and job relationships at the schedulers can also cause unfairness to different types of queries. For example, some analytic queries possess significant parallelism and they are compiled into DAGs that exhibit a flat star- or tree-like topology, with many branches such as Q18 and Q21. Other queries do not have much parallelism, thus are often compiled into DAGs that have a chain-like linear topology, with very few branches. As depicted in Figure 2.7, we build two groups of queries: Group 1 (*Chain*) composed of Q5, Q9, Q10, Q12 with a chain topology and Group 2

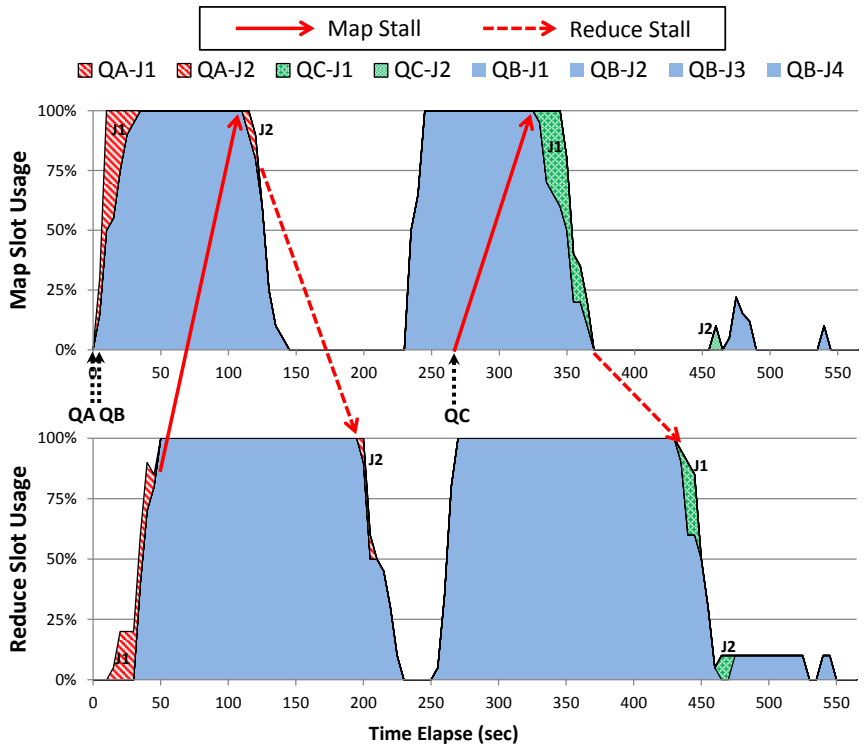

Figure 2.6: Execution Stalls of Queries with HCS

(*Tree*) composed of Q7, Q8, Q17, Q21 with a tree topology. Both groups of queries are from TPC-H and we submit them together for execution.

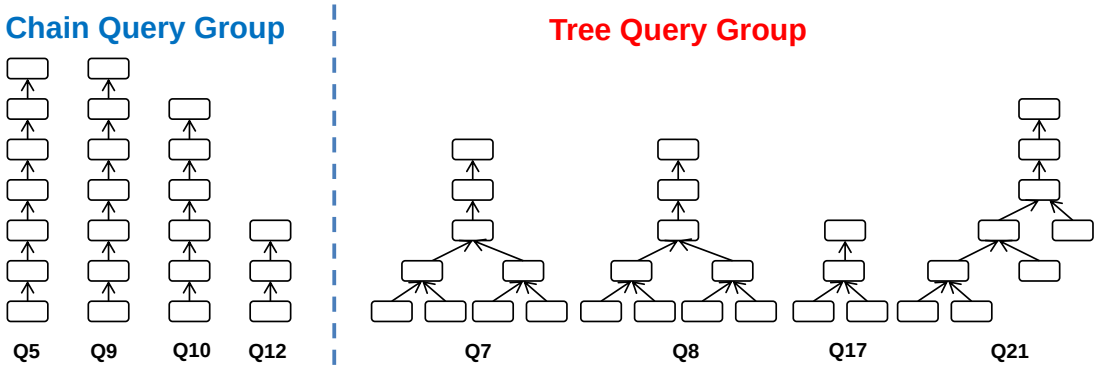

Figure 2.7: Chain Query Group and Tree Query Group

Figure 2.8 shows the average execution slowdown of two groups with different scheduling algorithms. Group 1 has an average slowdown much larger than Group 2, about 2.7× and 2.2× under HCS and HFS, respectively. This is because the Hadoop schedulers are oblivious to high-level query semantics, thus unable to cope with queries with complex, internal job dependencies. Such

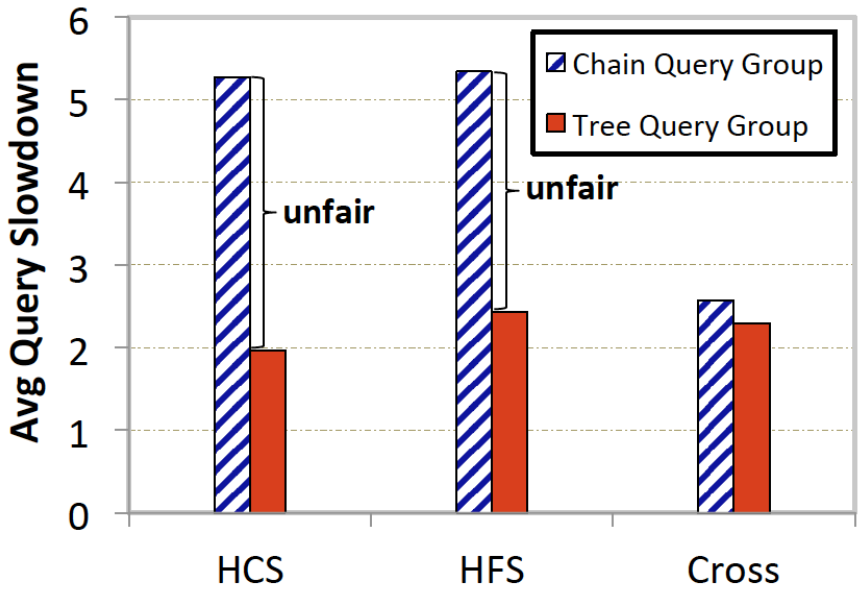

Figure 2.8: Fairness to Queries of Different Compositions

unfair treatment to queries of different compositions can incur unsatisfactory scheduling efficiency for users. A scheduler that is equipped with high-level semantics can eliminate such unfairness. As shown in Figure 2.8, our two-level scheduler (TLS) can leverage the query semantics that is percolated to the scheduler, and complete queries of different DAG topologies under comparable slowdowns.

Chapter 3

PCM Based Hybrid Storage

3.1 Design for PCM Based Hybrid Storage

Hybrid storage devices have been constructed in many different ways. Most HSDs are built using flash-based solid state devices as either a non-volatile cache or a prefetch buffer inside the hard drives. The combination of FSSDs and HDDs offers an economic advantage with low-cost components and the mass production. This composition of hybrid storage devices, as shown in Figure 3.1(a), is currently the most popular.

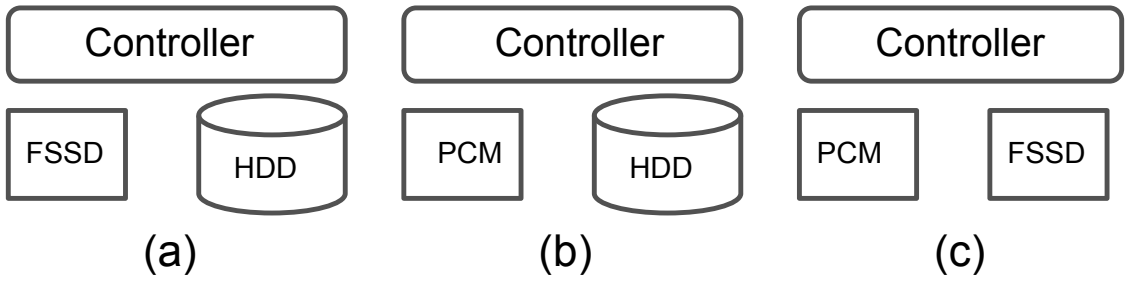

Figure 3.1: Different architectures of hybrid storage devices

Exploring emerging NVRAM devices such as PCM as components in hybrid storage devices has attracted significant research interest. Research in this direction proceeds along two distinct paths. Along the first path, PCM is used as a direct replacement for FSSDs, as shown in Figure 3.1(b). Along the second path, PCM is used in combination with FSSDs to compensate FSSDs' lack of in-place updating, and possibly push HDDs out of hybrid storage devices, as shown in Figure 3.1(c). For example, Sun et al. [90] use this type of hybrid storage devices to demonstrate its capability of high performance and increased endurance with low energy consumption. However, there are two major problems associated with this approach. First, since FSSDs provide primary

data storage space, the erasure-before-write problem still exists, although it happens at lower frequency. This causes significant performance loss for data intensive applications. Second, without HDDs in the memory hierarchy, large volumes of storage space cannot be leveraged at reasonable performance costs. In terms of cost per gigabyte, FSSDs are still about 10 to 20 times more expensive than HDDs.

For the above reasons, we investigate the benefits of leveraging PCM as a write cache for hybrid storage devices that are designed along the first path. As shown in Figure 3.1(b), we use PCMs to completely replace FSSDs while retaining HDDs for their advantages in storage capacity. With the fast development of PCM technologies, we expect that the PCM-based hybrid storage drive will become more popular. In this section, we describe our hybrid storage system - HALO that uses PCM in a write cache for HDDs to improve performance and reliability of HDD-based storage and file systems. Specifically, we first introduce the HALO framework and its basic supportive data structures, and then elaborate on the caching and destaging algorithms.

3.1.1 HALO Framework and Data Structures

Using PCM in caches for HDDs demands efficient caching algorithms. We design a new caching algorithm, referred to as **HALO**, to manage data blocks that are cached in PCM for hard disk drives. HALO is a non-volatile caching algorithm which uses a **HA**sh table to manage PCM and merge random write requests, thereby improving access **LO**cality for HDDs. Figure 3.2 shows the HALO framework. The basic data structure of HALO is a chained hash table used to maintain the mapping of HDD's LBNs (Logical Block Number) to PCM's PBNs (PCM block addresses). Sequential regions on HDDs, in units of 1MB, are managed by one hash bucket. The information associated with sequential regions is used to make cache replacement decisions.

Mapping Management – As shown in Figure 3.3, the chained hashtable includes an in-DRAM array (i.e., the bucketinfo table) and on-PCM mapping structures. Another cuckoo hashtable enables space-efficient fast query. The bucketinfo table stores information for HDD data regions. Each bucket item in the table represents a 1MB region on the disk partition or logical volume.

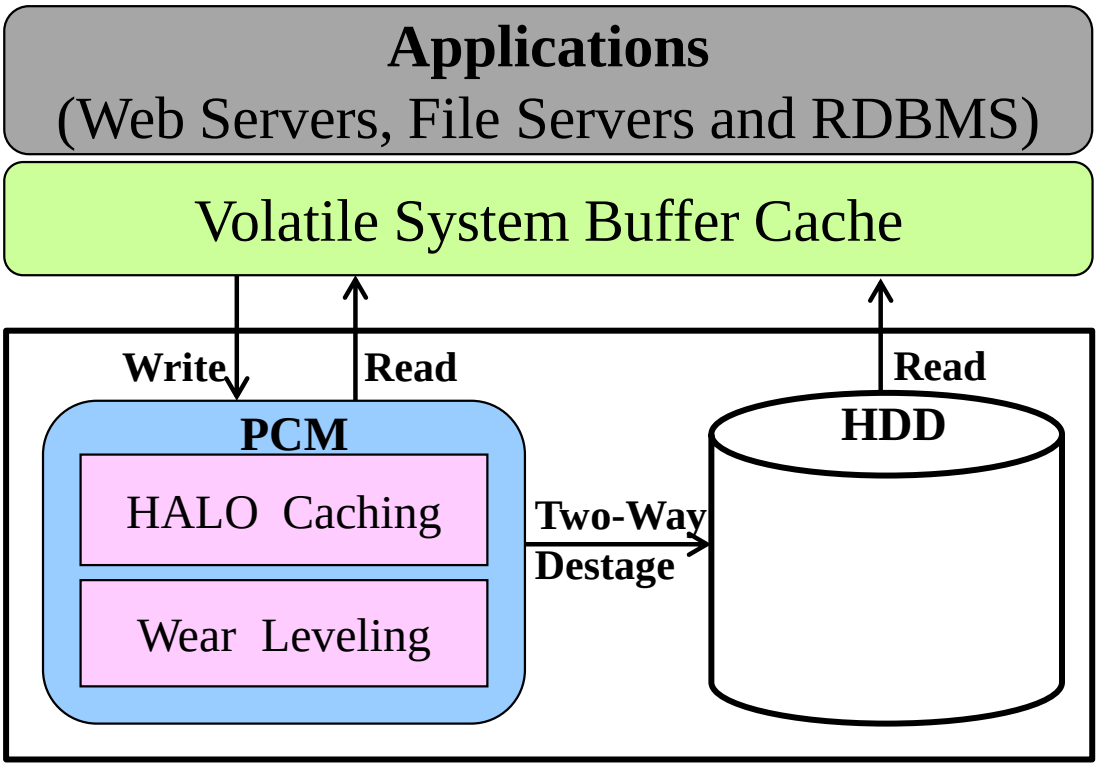

Figure 3.2: Design of the HALO framework

Hence, the number of buckets in the bucketinfo table is determined by the size of the disk volume. Each bucketinfo item, if activated, contains three components: *listhead*, *bcounts*, and *recency*. *listhead* maintains the head block's PBN of a list of cache items that map to the same sequential 1MB disk area, *bcounts* represents the number of caching blocks, and *recency* records the latest access time-stamps for all cache items in this bucket. We use a global request counter to represent the time-stamp; whenever a request arrives, the counter increases by one. The *total_counts* variable records how many HDD blocks have been cached inside PCM, while *activated_bucks* indicates the number of bucketinfo items activated in the bucketinfo table. *buck_scan* is used to search the bucketinfo table for a candidate destaging bucket.

Cache items that are associated with a bucket item do not need to be linked in ascending order of LBNs, because they are only accessed in groups during destaging. Each newly inserted item will be linked to the head of the list. This guarantees insertions to be finished in constant time. Each cache item maintains a 4KB mapping from HDD block address (LBN) to PCM block

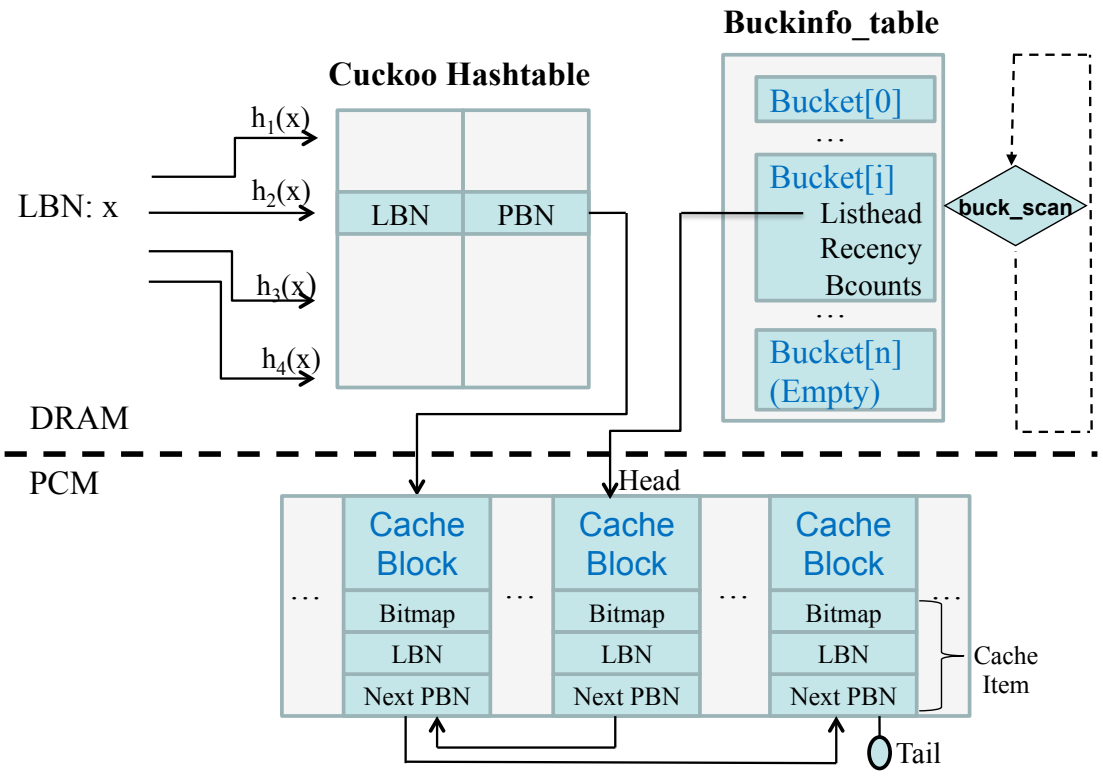

Figure 3.3: Data structures of HALO caching

number (PBN). It contains a LBN (the starting LBN of 8 sequential HDD blocks), the PBN of the next PCM block in the list and an 8-bit bitmap which represents the fragmentation inside a 4KB PCM block. If the 8-bit bitmap is nonzero, the nonzero bits represent cached 512B HDD blocks. Each cache item is stored on each PCM block's meta data section [18].

Cuckoo Hash Table – To achieve fast retrieval of HDD blocks, a DRAM-based cuckoo hash table is maintained using the LBN as the key and the PBN as the value. On a cache hit, the PBN of the cache item is returned, which enables fast access of data information in the PCM. Traditionally, hash tables resolve collisions through linear probing or chained hash and they can answer lookup queries within O(1) time when their load factors are very low, i.e., smaller than $log(n)/n$, where n is the table size. With an increasing load factor, its query time can degrade to O(log(n)) or even O(n). Cuckoo hashing solves the issue by using multiple hash functions [74, 36]. It can achieve fast lookups within O(1) time (albeit a bigger constant than linear hashing), as well as good space efficiency i.e. high load factor. Next, we introduce how we achieve such space efficiency.

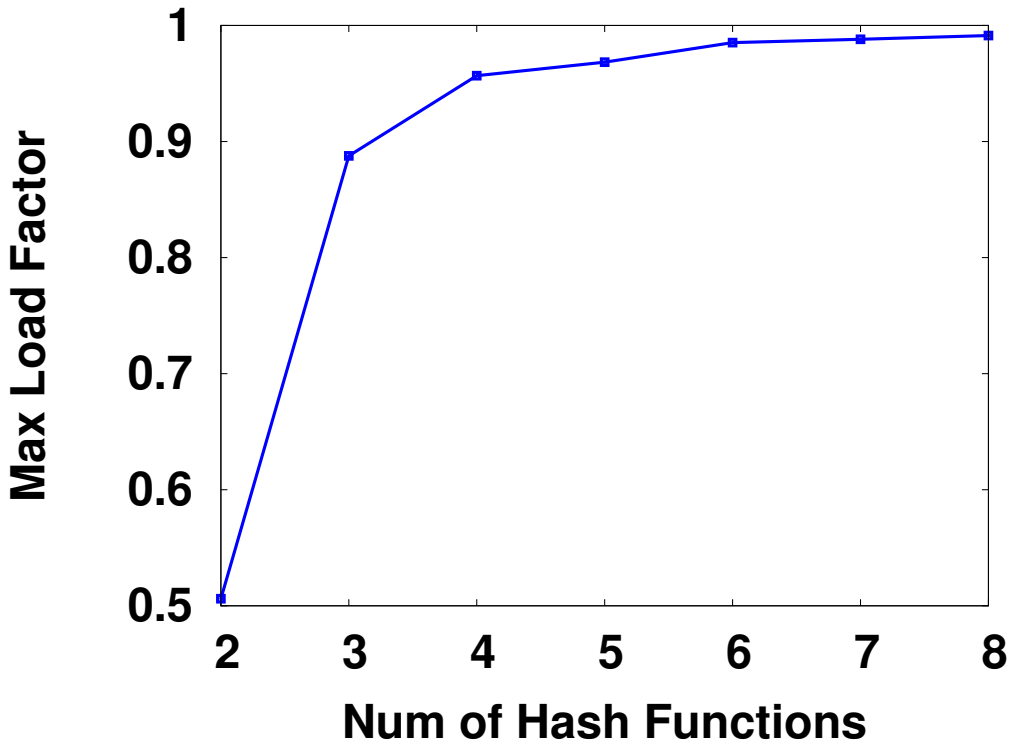

Figure 3.4: Max Load Factors for Different Numbers of Hash Functions

We set 100 as the maximum displacement threshold in the Cuckoo hashtable. When the Cuckoo hashtable cannot find an available slot for a new inserting record within 100 item displacements, it indicates that the hashtable is almost full and requires a larger size table and rehashing. And such critical load factor before rehashing is counted as maximum load factor. Figure 3.4 shows how the number of hash functions influences the average maximum load factor we can achieve for running seven traces above. When the number of functions is two, only 50% load factor can be achieved; as the number of functions increases, the load factor of Cuckoo hash tables initially grows rapidly and then the slope of the curve becomes smaller thus the benefit achieved becomes marginal. Therefore we use four functions in our design since a larger number of functions can in turn bring higher query and computation overheads. In addition, we set a larger initial size of hashtable to keep the load factor lower than 80% percent when PCM cache is fully loaded. In this way we are able to maintain the average displacements per insert below 2 for better performance.

Here, we give a sample calculation of DRAM overhead by the HALO data structures. In total, for a 2 GB PCM cache with 4 KB cache block size, 0.5 M items will placed be in the hashtable. As each item takes 8 Bytes and the load factor of the cuckoo hashtable is 0.8, the total memory overhead of the Cuckoo hashtable is about 5 MB. With the bucketinfo table normally consuming about 6-12 MB DRAM, we need less than 20 MB DRAM to implement HALO cache management for 2 GB PCM and 1 TB hard disk.

Recovery from System Crashes – Mapping information of a PCM block that contains the LBN, the next PBN and the bitmap are stored on non-volatile PCM. Therefore, in case the system crashes, it can first reboot and then either destage the dirty items from PCM to HDD or rebuild the in-DRAM hashtables by scanning information on fixed positions of the PCM meta data sections (to get the cache items' information including LBN, bitmap and next PBN). As the PCM's read performance is similar to that of DRAM, the recovery procedure should only take seconds to rebuild the in-memory mapping data structures. In doing so, we can avoid loss of cached data and guarantee the system integrity.

3.1.2 HALO Caching Scheme

Our caching algorithm is described in Algorithm 1. When a request arrives, the bucket index is computed using the request's LBN. The hash table is then searched for an entry corresponding to the LBN. In the event of a cache hit, the PBNs are returned from the hash table and the corresponding blocks are either written in-place to, or read from, the PCM. The corresponding bucket's recency in the bucketinfo table is also updated to the current time-stamp. In the event of a cache miss on a read request, data is read directly from the HDD without updating the cache. In the event of a cache miss on a write request, a cache item is allocated in the PCM, and data is written to that cache block. Then, if the bucket item of the bucketinfo table for the LBN is empty, it will be activated. After that, the bucket item's list of cache items is updated, the address mapping information is added to the hash table, the recency of this bucket is set to the current time-stamp, and the

bucket's *bcounts* is incremented. The updated access statistic information are used by the two-way destaging algorithm to conduct destaging procedures.

Algorithm 1 Cache Management Algorithm

```
1: Compute the bucket index i from the LBN
2: if this is a write request then
3:    Search the cuckoo hashtable using the LBN
4:    if this is a cache hit then
5:       Write to the PCM block with returned PBN
6:       Bucket[i].recency ← globalReqClock
7:    else
8:       //Cache miss
9:       Allocate and write a PCM block
10:      if Bucket[i] is empty then
11:         Activate Bucket[i]
12:         activate_bucks ← activate_bucks + 1.
13:      end if
14:      Link item to Bucket[i].listhead, add to cuckoo hashtable
15:      Bucket[i].recency ← globalReqClock
16:      Bucket[i].bcounts ← Bucket[i].bcounts + 1
17:      total_bcounts ← total_bcounts + 1
18:   end if
19: else
20:   //This is a read request
21:   Search the cuckoo hashtable.
22:   if cache hit then
23:      Read the PCM block with the returned PBN.
24:      Bucket[i].recency ← globalReqClock.
25:   else
26:      //Cache miss
27:      Read the block from HDD.
28:   end if
29: end if
```

3.1.3 Two-Way Destaging

Since the capacity of PCM cache is limited, we have to destage some dirty data from PCM to HDD in order to spare cache space for accommodating new requests. Therefore, we propose a Two-Way Destaging approach to achieve this target. The Two-Way Destaging approach contains two types of destaging: on-demand destaging and background destaging, which are activated to

evict some data buckets out of PCM. Next, we will introduce when to trigger each destaging and how to select the victim buckets.

The on-demand destaging is activated when the utilization of PCM cache reaches a high percentage, e.g., 95% of the total size. Such on-demand method can sometimes incur additional wait delay to front-end I/O requests, especially when the I/O load intensity is high. To complement this approach and relax such contention, we introduce another destaging method which is triggered when both the PCM utilization is relatively high, e.g., 80%, and the front-end I/O intensity is low (specifically, disk performance utilization smaller than 10%). Through combination of these ways of destaging, PCM space can be appropriately reclaimed with minimal performance impacts to front-end workloads.

For either destaging method, a bucket is eligible to be destaged to HDDs if any of the following two conditions holds: First, the bucket's bcounts needs to be greater than the average value of bcounts plus a constant threshold $TH_{BCOUNTS}$ and the bucket's recency needs to be older than the global request timestamp by a constant $TH_{RECENCY}$. For every unsuccessful round of scan, these two thresholds will dynamically decrease to make sure that victim buckets can be found within a reasonable number of steps. Second, the bucket's recency needs to be older than the global request timestamp by a constant $OD_{RECENCY}$ ($OD_{RECENCY} \gg TH_{RECENCY}$). As soon as a bucket is identified as eligible for destaging, all cache blocks associated with the bucket are destaged to the HDD in a batching manner, the bucket is deactivated and the corresponding items in the cuckoo hash table are deleted. As these cache blocks are mapped to 1MB sequential region of HDD, this batch of write-backs are supposed to only incur one single seek operation to HDD, thus providing good write locality and causing minimal affects to read requests.

We select these two criteria for determining destaging candidates for the following reasons. First, we want to choose a bucket that has enough items to form a large enough sequential write to the HDD to increase spatial locality of write operations, and at the same time it needs to be one that is not recently used in order to preserve temporal locality. Second, for those very old and small buckets, we evict them from the PCM by setting the control variable $OD_{RECENCY}$.

Table 3.1: Parameters Used for Wear Leveling.

LSN	Global Stripe Number (0-64K)
Blk	Offset of blocks in a bank
Seq	Sequence Number in a SFC cube
$Cube$	Cube Number $(0-31)$
S_{stripe}	Number of blocks in a stripe (64)
S_{cube}	Number of stripes in a cube (2048)
N_{cubes}	Number of cubes (32)
N_{ranks}	Number of ranks in a PCM (8)
N_{banks}	Number of banks in a rank (16)
$OS_{inStripe}$	Offset of blocks in a stripe
OS_{inCube}	Offset of stripes in a cube
OS_{inBank}	Offset of stripes in a bank
(R,B,S)	Rank, Bank, Stripe

3.2 Wear Leveling for PCM

Although the write-endurance of PCM is 3-4 orders of magnitude better than that of FSSDs, it is still worse than that of traditional HDDs. When used as storage, excessively unbalanced wearing of PCM cells must be prevented to extend its lifetime. A popular PCM wear leveling technique [77] avoids frequent write requests to the same regions by shifting cache lines and spreads requests through randomization at the granularity of cache lines (256B). This technique is feasible when PCM is used as a part of main memory; however, when PCM is used as a cache for back-end storage, this technique can negatively impact spatial locality of file system requests that are normally several KBytes or MBytes in size. In addition, the use of Feistel network or invertible binary matrix for address randomization requires extra hardware to achieve fast transformation. To address these issues, we propose two wear leveling algorithms for PCM in hybrid devices, namely *rank-bank round-robin* and *Space Filling Curve (SFC)-based wear leveling*. Instead of using 256-Byte cache lines or single bits as wear leveling units, our algorithms use stripes (32KB each). Such bigger units can significantly reduce the number of data movements in wear leveling. In addition, with the fast access time of PCM devices, the time to move a 32KB stripe is quite small (less than 0.1 ms). Hence, the data movement overhead will not affect the response times of front-end requests. The important parameters for our algorithms are listed in Table 3.1.

3.2.1 Rank-Bank Round-Robin Wear Leveling

The rank-bank round-robin wear leveling technique is inspired by the RAID architecture. It adopts a similar round-robin procedure to distribute address space among PCM memory ranks and banks for achieving uniformity in inter-region write traffic. We firstly apply block striping over PCM devices in order to ensure an even distribution of writes at the rank and bank granularity. This scheme iteratively distributes data first over ranks, and then over banks within the same rank. Similarly, consecutive writes to the same rank are distributed over the banks within that rank. This scheme is shown in Figure 3.5. Aside from assuring a good write distribution between ranks and banks, the proposed scheme also takes full advantage of parallel access to all ranks in the PCM. This means that writing N_{rank} blocks of data at the same time is possible, where N_{rank} represents the number of ranks in a particular device. This parallel access translates into improved response times, which is important for data-intensive applications. After block striping, we apply a start-gap rotation scheme inside each bank similar to the method in [77], but different in terms of the size of data units (i.e., in stripes of 32 KB rather than cache lines of 256 B for better spatial locality and less frequent rotations). We illustrate the calculation of LSN, rank index, bank index and logical stripe offset for the address mapping of Rank-Bank round-robin wear leveling in Equation 3.1.

$$\begin{aligned} LSN &= \left\lfloor \frac{PBN}{S_{stripe}} \right\rfloor \\ Rank &= LSN \ mod \ N_{ranks} \\ Bank &= LSN \ mod \ N_{banks} \\ OS_{inBank} &= \left\lfloor \frac{LSN}{N_{ranks}} \times N_{banks} \right\rfloor \end{aligned} \tag{3.1}$$

3.2.2 Space Fill Curve Based Wear leveling

The rank-bank round robin wear leveling algorithm can achieve even distribution among all banks and ranks for most cases as described later in Section 3.3.2. However, under certain workloads, a few intensively accessed banks still reduce lifetime of the PCM device. To solve this

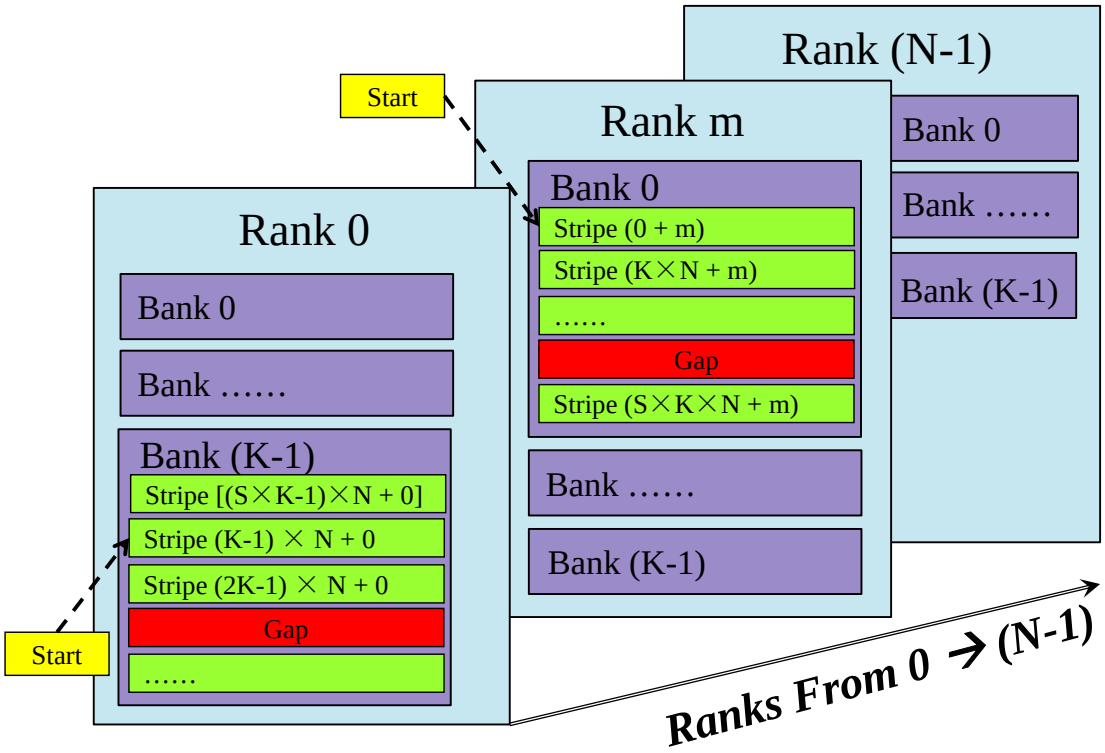

Figure 3.5: Rank-bank round-robin wear leveling

problem, we propose using the Hilbert Space Filling Curve (SFC) to further improve wear leveling. SFCs are mathematical curves whose domain spans across a multidimensional geometric space in a balanced manner [60].

In theory, there are an infinite number of possibilities to map one-dimensional points to multi-dimensional ones, but what makes SFCs suitable in our case is the fact that the mapping schemes of SFCs maintain the locality of data. In particular, points whose 1D indices are close together are mapped to indices of higher dimensional spaces that are still close. In our case, the LBN sequence is represented by the 1D order of points. The 3D space, into which the LBN sequence is mapped, is constructed with a tuple of three elements along the stripe dimension (the offset of stripes in a bank), the bank dimension (the offset of banks in a rank), and the rank dimension (the offset of ranks in a device).

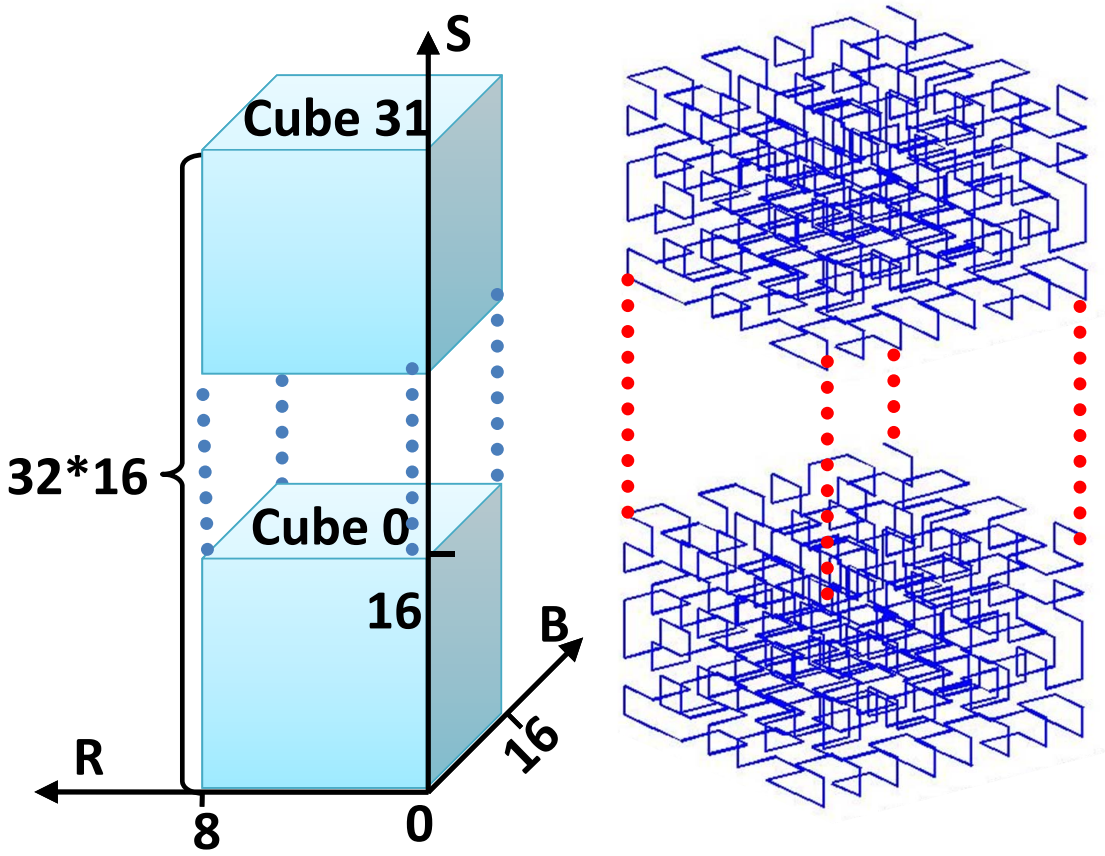

Figure 3.6: Space filling curve based wear leveling

$$
\begin{aligned}
\text{LSN} &= \left\lfloor \frac{\text{PBN}}{S_{stripe}} \right\rfloor \\
OS_{\text{inStripe}} &= PBN \ mod \ S_{stripe} \\
Cube_{\text{no}} &= Stripe \ mod \ N_{cubes} \\
OS_{inCube} &= \left\lfloor \frac{Stripe}{N_{cubes}} \right\rfloor \\
Seq &= StartGapMap(OS_{inCube}) \\
(R,B,S) &= SFCMapFunc(Seq)
\end{aligned}
\tag{3.2}
$$

We have 512 stripes in a bank, 16 banks in a rank and 8 ranks in a device. We evenly split the 3D space into 32 cubes along the stripe dimension. In other words, the number of stripes in each cube is 16 $\times$ 16 $\times$ 8 (i.e., #stripe $\times$ #bank $\times$ #rank). After splitting, we apply the round-robin method to distribute accesses across these cubes. And inside every cube, a start-gap like stripe shifting is implemented, making the 3D SFC cube move like a snake. The consequence is that

consecutive writes in the same cube can only happen for addresses that are 32 stripes away, which dramatically reduces the possibility of intensive writing in the same region. Within each cube, we apply SFC to further disperse accesses. We orchestrate SFC to disperse accesses across ranks as much as possible. This helps exploit parallelism from the hardware.

In summary, using SFC in combination with the round-robin method, we are able to map a 1D sequence of block numbers into a 3D triple of stripe number, rank number and bank number. The address mapping scheme is generally depicted in Figure 3.6. The left figure shows the logical organization of the device with its 32 cubes (or parallelepiped's, to be more precise, because the size is $8 \times 16 \times 16$). The right figure shows a 3-dimensional space filling curve that is used for our work. The mapping scheme starts with PBN provided by the system and ends up with a 3-tuple (R, B, S) calculated based on Equation 3.2. The SFC based wear leveling is designed for a best trade-off among write uniformity, access parallelism and spatial locality.

3.3 Evaluation for PCM-Based Hybrid Storage

To realize our proposed PCM-based write cache for hybrid storage devices we have designed a PCM simulation framework that simulates different caching schemes (HALO and LRU), wear leveling algorithms and PCM devices' characteristics including hardware structure, performance and wearing status. The simulators are written in about 4,300 lines of C.

As we can see from Figure 3.7, during evaluation, the block-level I/O traces are input to the simulators. The I/O requests are then processed by caching and wear leveling schemes, which generate two types of intermediate I/O requests: PCM requests and HDD requests. The PCM requests are processed by the PCM simulator to get response and wear leveling results. The HDD requests come from cache misses and destaging, which are stored as HDD trace files. HDD trace files are then replayed by the blktrace tool [23] on a 500GB, 7200RPM Seagate disk in a CentOS 5 Linux 2.6.32 system with an Intel E4400 CPU and 2.0 GB memory. The DRAM-based system buffer cache is bypassed by the HDD trace replaying process. Traces are replayed in a close-loop way for measuring system service rate.

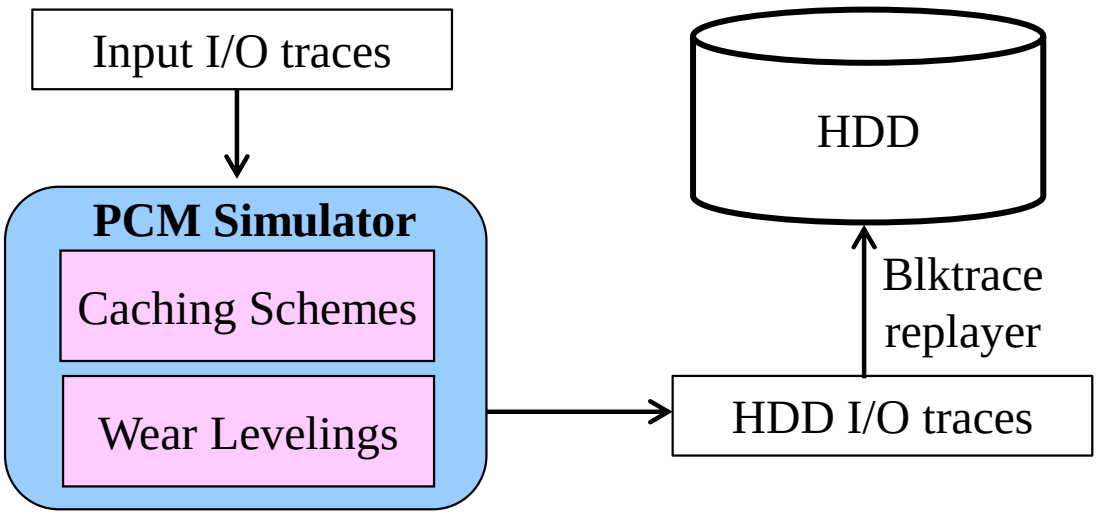

Figure 3.7: PCM Simulation and Trace Replay

Because PCM devices have much higher (more than 10 times) throughput rates and response performance than those of HDDs [18], we reasonably assume that the total execution time of a workload trace is dominated by the replay time of the HDD trace. For example, if the HDD traffic rate is about 10% and the write throughput is about 50 MB/sec, then the PCM cache must have a throughput rate of about 500 MB/sec, which is consistent with the reported performance of current PCM devices [18].

Based on the above discussion, the workload execution time can be calculated as follows: $(Total\_IO\_Size * Traffic\_Rate / Average\_Throughput)$. The traffic rate is calculated as the total number of accessed disk sectors (after the PCM cache's filtering) divided by the total number of requested sectors in the original workloads. This metric is similar to the cache miss rate. The lower the traffic rate we can achieve, the better the cache scheme performs. In order to achieve shorter execution times and better I/O performance, we must minimize the traffic rate and at the same time maximize the average HDD throughput. According to our tests, a standard hard disk can achieve as high as 100 MB/sec of throughput for sequential workloads and only achieve 0.5 MB/sec for workloads with small random requests. We will evaluate whether the HALO caching scheme can reduce the HDD traffic rate while maximizing average throughput of a hard disk by reducing the inter-request seek distance among all disk writes.

To evaluate wear leveling techniques, we define the PCM life ratio metric, which is calculated by dividing the achieved lifetime with the maximum lifetime. The life ratio is significantly affected by the uniformity of write requests. For example, if all write traffic goes to 1% of the PCM area, the life ratio can be reduced to 1% of the maximum life time. The life ratio is directly determined by the region with the maximum write count if there are no over-provisioning regions provided by the device.

Table 3.2: Workload Statistics

	Fin1	Fin2	Dap	Exchange	TPC-E	Mail	Randw
Write Ratio	84.60%	21.50%	54.90%	74%	99.8%	90.10%	100%
Dataset (GB)	18.03	8.85	84.2	163.8	13.2	85	5.9
AvgReqSize (KB)	3.38	2.4	77	13.65	10.48	4	4

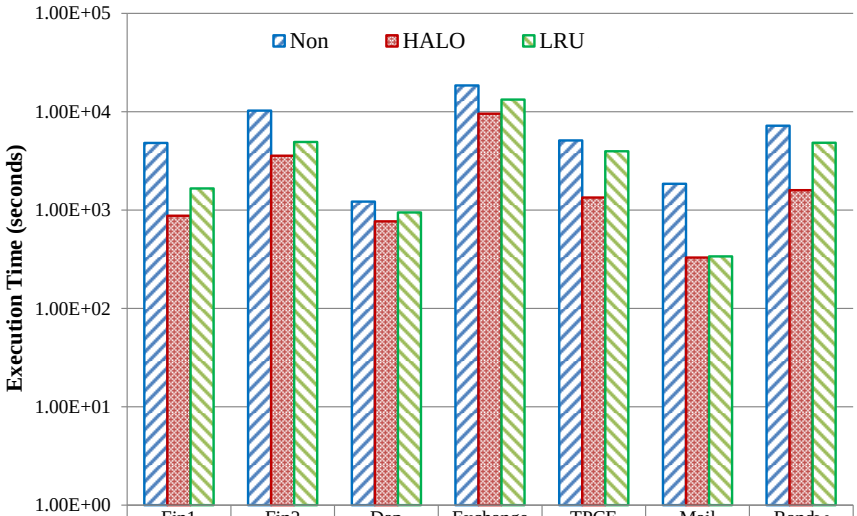

	Fin1	Fin2	Dap	Exchange	TPCE	Mail	Randw
Non	4821	10273	1219	18501	5124	1855	7206
HALO	879	3579	769	9560	1345	330	1592
LRU	1662	4935	949	13328	3968	339	4840
Improve%	47.11%	27.48%	18.97%	28.27%	66.10%	2.65%	67.11%

Figure 3.8: Execution time

Workloads

In our tests, we use seven representative real-world I/O traces. The workload statistics are described in Table 3.2. Specifically, the traces *Fin1* and *Fin2* were collected with the SPC-1

benchmark suite at a large financial organization [14]; the trace *Dap* was collected at a Display Advertisement Platform's payload server; the trace *Exchange* was collected at a Microsoft Exchange 2007 mail server for 5,000 corporate users; the trace *TPC-E* was collected on a storage system of 12 28-disk RAID-0 arrays under an OLTP benchmark, TPC-E [15]; the trace *Mail* was collected on a mail server by Florida International University [15]. The seventh trace *Randw* was collected by us on the target disk while running the IOmeter benchmark with the 4KB-100% random-100% write workload for 2 hours [73].

Table 3.3: The Effects of Cuckoo Hash Function Numbers on Load Factors

func number	2	3	4	5	6	7	8
load factor	0.506082	0.887596	0.956696	0.968351	0.985249	0.988124	0.991324

3.3.1 I/O Performance

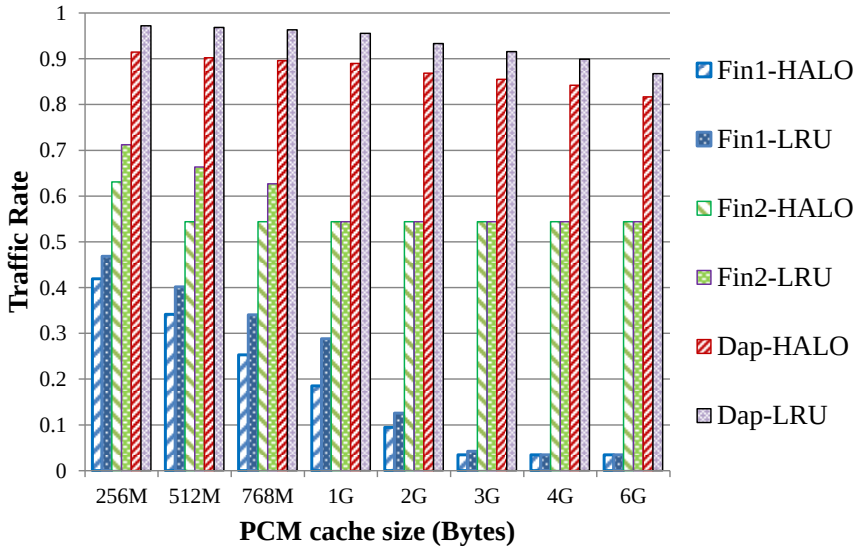

Figure 3.9: Traffic rate for Fin1, Fin2 and Dap

To evaluate execution times of seven traces, we choose 512MB as the cache size for Fin1 and Fin2, and 2GB as the cache size for the other five traces. Figure 3.8 shows the results for Non-cache, HALO-cache and LRU-cache respectively. As we can see, the execution times are reduced greatly for all traces. The execution improvement of HALO caching over LRU caching is 47.11%

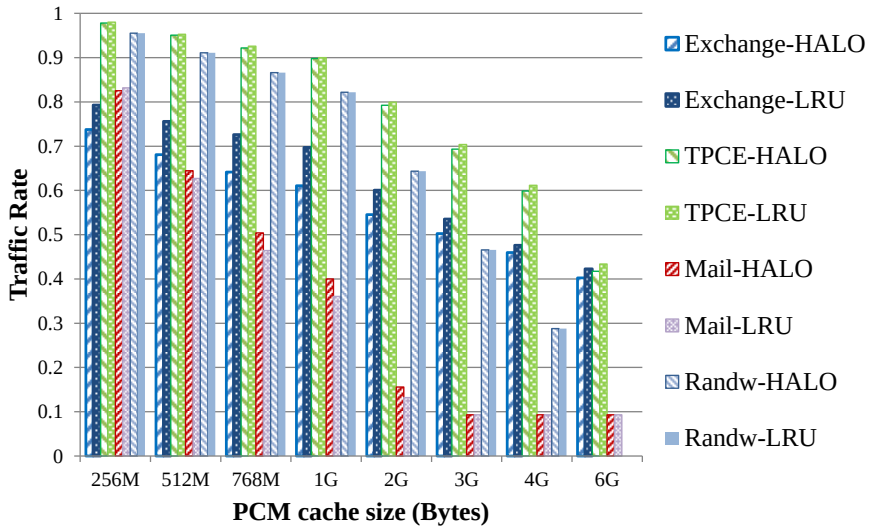

Figure 3.10: Traffic rate for Exchange, TPC-E, Mail and Randw

for Fin1, 27.48% for Fin2, 18.97% for Dap, 28.27% for Exchange, 66.10% for TPC-E, 2.65% for Mail, and 67.11% for Randw. The improvement level is mainly determined by the randomness and write ratio of the traces. Note that for the Mail trace, the improvement is only 2.65%. The reason is that most of write requests in the Mail trace are sequential requests, for which there is not much room for HALO caching to improve on LRU caching. The improvement of execution time comes from two aspects: first, the reduction of traffic rate because of better cache hit; second, the increasing on HDD average throughput due to improved write access sequentiality.

Figures 3.9 and 3.10 show the traffic rates for the seven traces with the HALO cache policy and the LRU cache policy, respectively. In most cases (with the cache size ranging from 256MB to 6GB), HALO consistently achieves 5% - 10% lower traffic rates than LRU. Take the trace Fin1 for an example, HALO achieves 5%, 6%, 9%, 10.3%, 3%, 1% lower traffic rates than LRU, where the cache size varies from 256MB to 3GB. We observe similar results for Exchange and TPC-E. For Dap, because the access repeatability and temporal locality is very poor, the traffic rate for HALO and LRU remains relatively high. However, HALO still gets a 6% lower traffic rate than LRU. For Randw, as it has a completely random write access pattern, all cache schemes can get almost no cache hits. That explains why the traffic rate of HALO and LRU are almost identical. Yet, HALO can still bring significant performance improvement in terms of execution time because

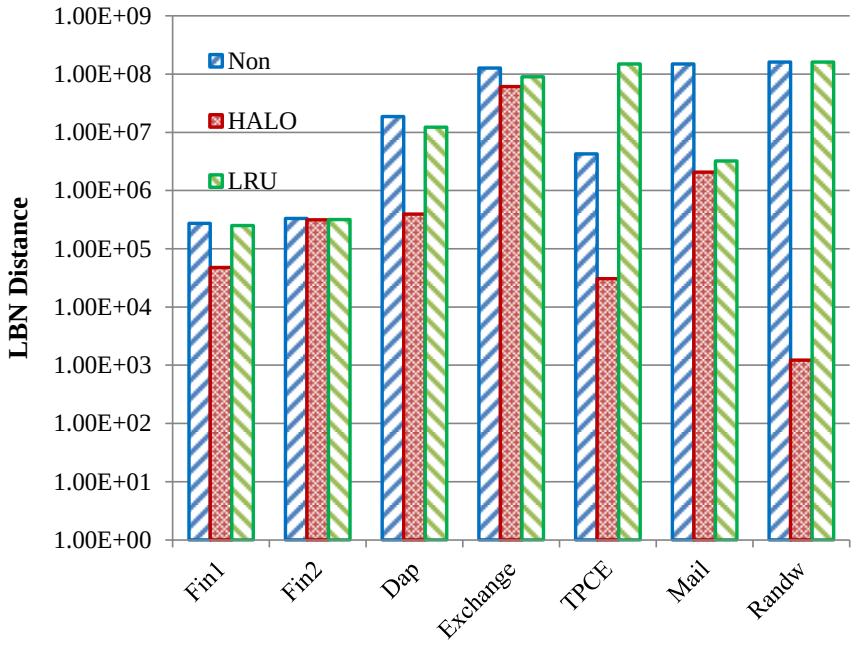

Figure 3.11: Average inter-request LBN distance

of improved write access locality. For Fin2, as the cache size becomes larger, the PCM write cache consistently reduces more traffic until it reaches 768MB. This is due to Fin2's relatively high read ratio (84.60%) and thus the opportunities for optimizing write operations are limited. For Mail, HALO's improvement is more insignificant for larger cache sizes. However, for small cache sizes (512MB–2GB), the traffic rate under LRU caching is about 2% less than that under HALO caching, because most write requests are already in a uniform sequential pattern, so our cache scheme—which is targeted at random-write workload—cannot show good improvement.

We use the average inter-request LBN distance as a metric to evaluate the I/O access sequentiality to HDD, and the results are shown in Figure 3.11. We notice that the average inter-request LBN distance is reduced greatly by HALO caching for almost all traces. This explains why the average disk throughput with HALO is much larger than with Non-cache and with LRU, as shown in Figure 3.12. However, for Fin2, HALO does not reduce the LBN distance, because a majority of Fin2 requests are read requests, and there is little room for HALO to improve performance. As we can see in Figure 3.15, normalized HDD's request response times are demonstrated for LRU and HALO. In terms of geometric mean, HALO averagely leads to 40.1% better request response

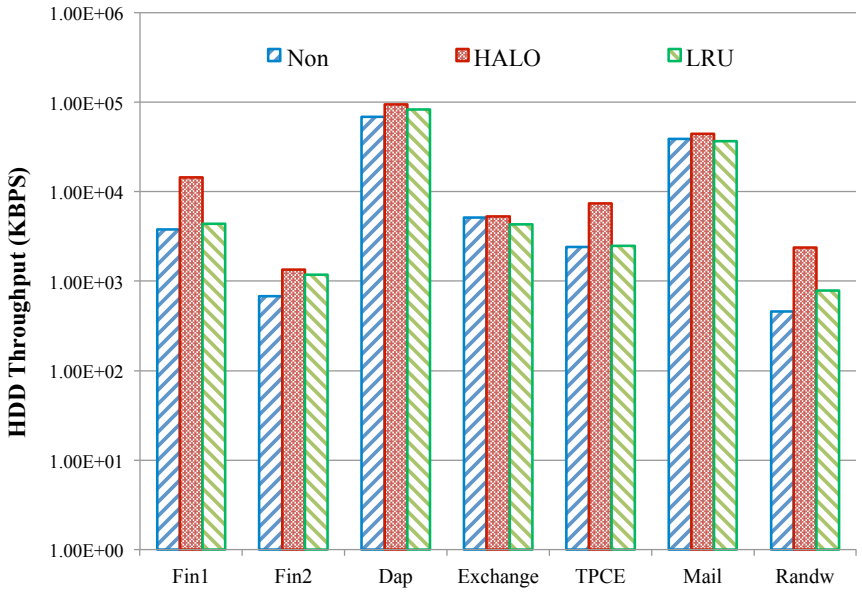

Figure 3.12: HDD throughput rate and HALO's improvement over LRU

time than LRU because of improved access locality and workload intensities achieved by HALO caching and Two-Way destaging algorithms.

We use Figures 3.13 and 3.14 to further explain this. These two figures display how the HALO cache scheme changes the disk access patterns of workloads for Fin1. The x-axis of the figures depicts the request sequence number and the y-axis depicts the LBN address of every request. As shown in the figure, the original access pattern is almost random. It stretches through the whole address space over time. Moreover, with HALO, the number of disk access requests drops from 5 million to 0.6 million and the access pattern becomes very regular. Especially for write requests, periodical batched writes range from lower LBNs to higher LBN as the buck_scan pointer moves (Section 3.1.1). This explains why the disk throughput is remarkably improved, especially for workloads with intensive random-writes.

3.3.2 Wear Leveling Results

Table 3.4 and Figure 3.16 illustrate the wear leveling results for different wear leveling schemes. SG-max represents the maximum bank write count deviations for non-randomized region-based start-gap wear leveling (SG). Avg-counts represents the average bank write counts of all 128 banks.

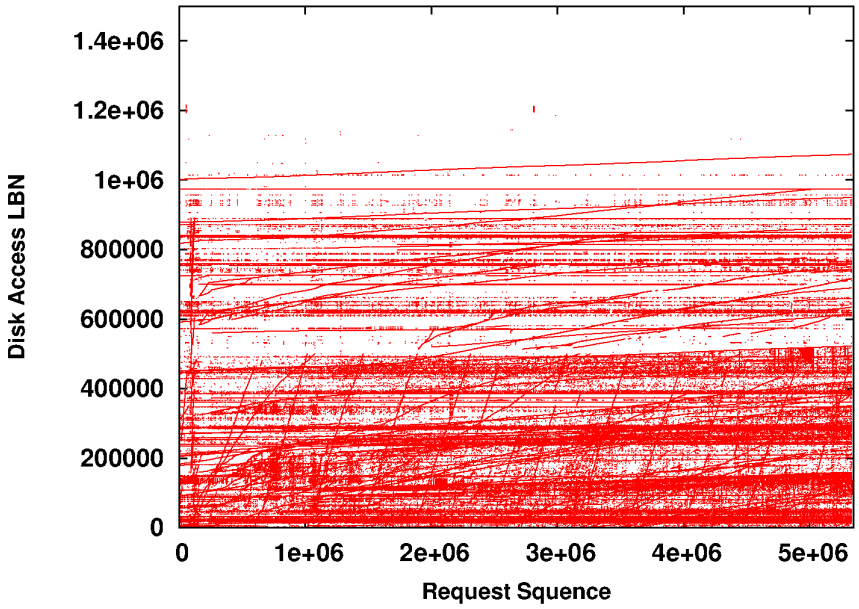

Figure 3.13: Original LBN distribution of Fin1

NAME-life represents the life ratio compared to perfect wear leveling, which can be calculated by $\frac{1}{(NAME\text{-}max/Avg\text{-}counts+1)}$. The "lifetime improvement" column gives an indication of the SFC wear leveling technique's lifetime improvement compared to that of SG. In terms of arithmetic mean, the average life ratio is 0.9255 for SFC-based wear leveling (SFC), 0.619 for rank-bank round-robin wear leveling (Rank-Bank RR or RR), and 0.0598 for SG. The average lifetime improvement with our scheme (SFC) for all traces is 21.60 $\times$. In terms of geometric mean, the life ratios for SFC and SG are 0.9214 and 0.0478 respectively, and the average lifetime improvement for all traces is 19.29 $\times$.

Table 3.4: Wear leveling Results

	SFC-max	RR-max	SG-max	Avg-cnt	SFC-life	RR-life	SG-life	Imprv
Fin1	113921	5094200	44559020	1799300	0.9405	0.261	0.0388	23.23
Fin2	38507	195648	7510848	202822	0.8404	0.509	0.0263	30.96
Dap	90802	1820127	13999887	285233	0.7585	0.1355	0.02	36.99
Exch	193633	9699420	1.87E+08	5765866	0.9675	0.3728	0.0299	31.36
TPC-E	3148	56823	13154423	1665767	0.9981	0.967	0.1124	7.88
Mail	32278	1320622	37488462	2678274	0.9881	0.6698	0.0667	13.82
Randw	12762	23859	6135289	871481	0.9856	0.9734	0.1244	6.92

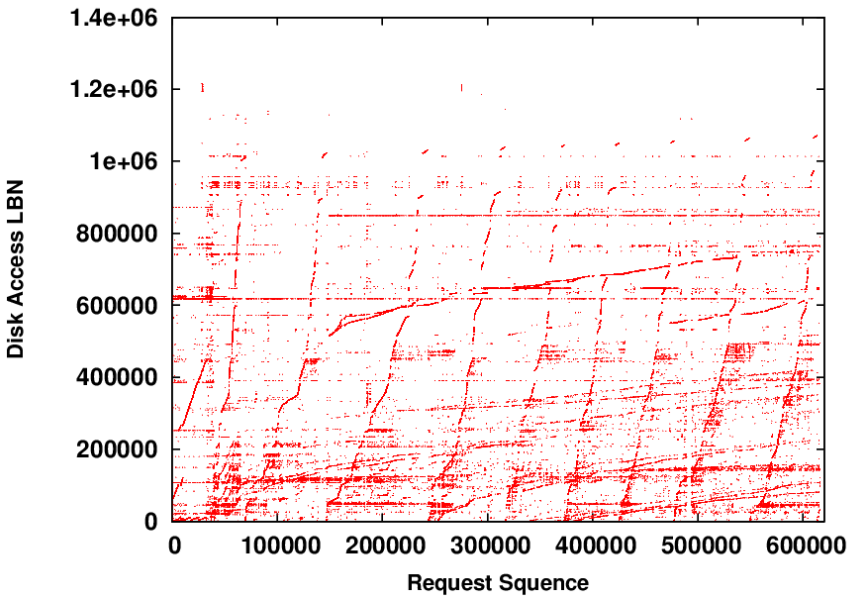

Figure 3.14: LBN distribution of Fin1 after applying the HALO caching

Figure 3.17 shows the bank write count deviations for RR and SFC under Fin2 workload. The x-axis is the bank number for 8 ranks * 16 banks per rank. The y-axis is the deviation of wear counts among all banks. We observe that SFC can achieve very good wear uniformity and very low deviations for all banks. This is very helpful for extending the life ratio and thus the lifetime of a PCM device. Bank deviations for other traces are similar and not shown here to conserve space. Deviation results for other traces are pretty similar and not shown here for space limit.

3.4 Related Studies on Hybrid Storage and NVM

Hybrid Storage/Memory Systems: While NVRAM has non-volatility and energy benefits over DRAM and has great performance advantages over HDDs, it has limitations such as short device endurance and asymmetric access latency. To overcome these limitations, researchers have combined conventional memory systems with NVRAM to avoid these limitations and leverage the benefits of both HDDs and NVRAM. Ramos et al. [79] and Zhang et al. [120] place PCM and DRAM side-by-side behind the bus to build a hybrid system. Ramos et al. [79] have introduced hardware extensions to the memory controller (MC) to monitor popularity and write intensity of memory pages. They migrate pages between DRAM and PCM, and let operating systems (OS) in

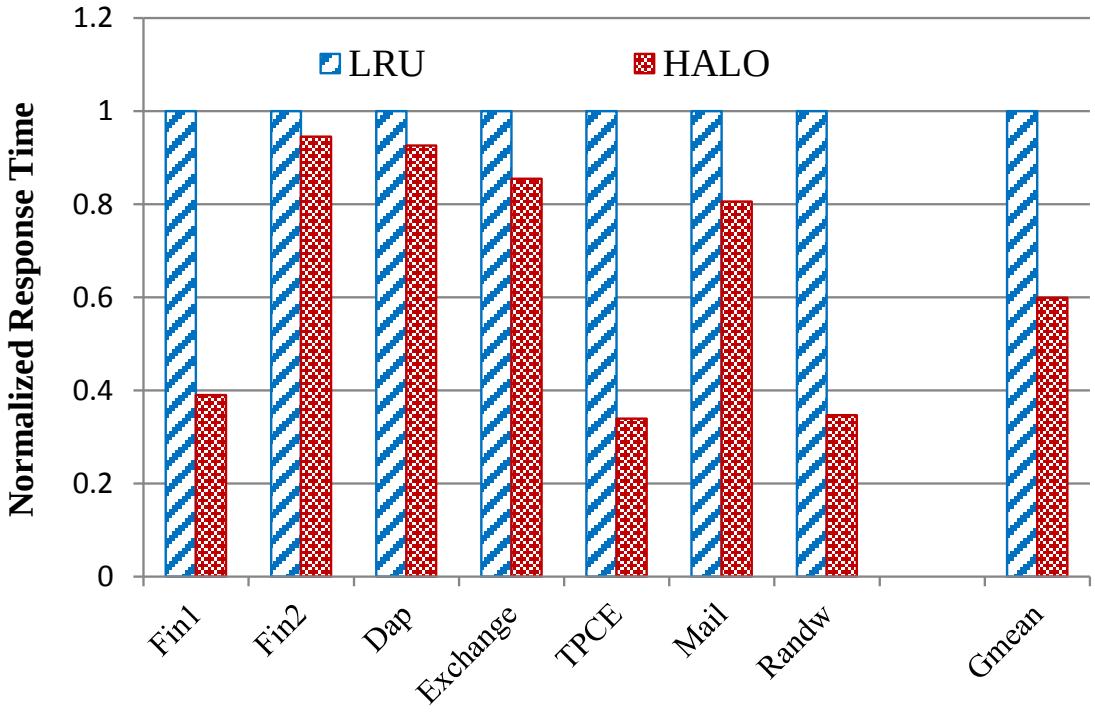

Figure 3.15: Response time

charge of updating memory mapping, such that performance-critical pages and frequently written pages are placed in DRAM, while non-critical pages and rarely written pages are in PCM. Zhang et al. [120] also rely on the MC to monitor access pattern. Their work differs from [120] by completely relying on OS to manage pages and treating DRAM as an OS-managed write partition. Over time, frequently written pages are placed into DRAM to reduce writes to PCM. Shi et al. present a flash+PCM hybrid nonvolatile disk cache system where flash is used mainly as read cache and PCM is used as write cache [86]. In [54], non-volatile memory is used as both buffer cache and journaling layers for ext4 file system. Our work aims at combining PCM and HDDs as a back-end storage device. Instead of relying on hardware and/or online detection mechanisms to partition data between PCM and HDDs, we store data blocks based on logical block numbers and record the mapping with hash tables, which avoids the involvement of OS in monitoring data access patterns and the need of additional hardware.

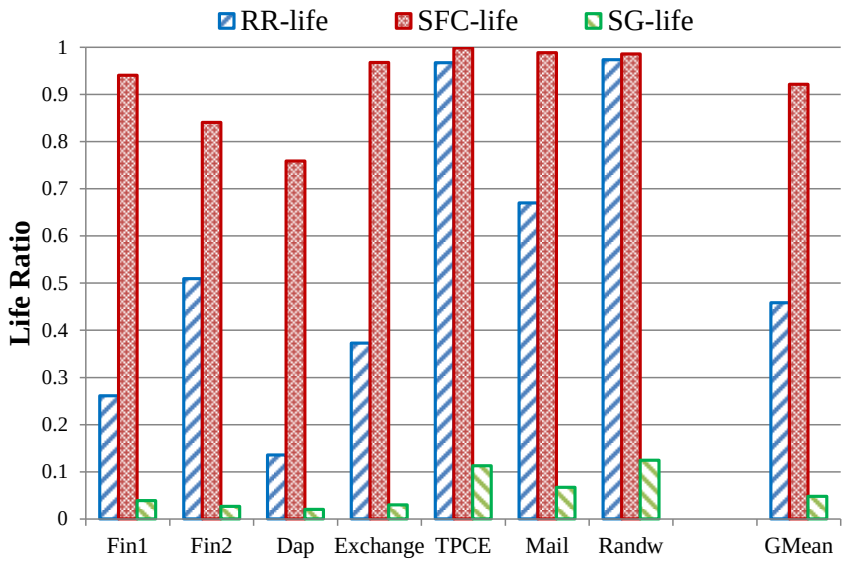

Figure 3.16: Life ratio comparison between different wear leveling techniques

Caching and Logging: Least recently used (LRU) and least frequently used (LFU) are common cache replacement policies. LRU-k [72], LRFU [52], MQ [123] and LIRS [48] are important improvements to the basic LRU policy. They consider inter-access time, access history and access frequency to improve hit ratios. DULO [47] and DISKSEEN [31] complement LRU by leveraging spatial locality of data access. DULO gives priority to random blocks by evicting sequential blocks (those with similar block addresses and timestamps). However, the limited sequential bank size and volatility of DRAM prevents DULO from detecting sequences within a larger global address space and over a longer time scale. For this reason, DULO is not positioned to attain performance improvements over LRU for random access workloads in storage and file systems.

Logging is a method that aims to mitigate random writes to hard drives [80] and flash-based SSDs [110]. When data blocks are appended to early blocks rather than updated in place, the garbage collection is necessary and becomes a critical issue. DCD [71] uses a hard disk as a log disk for improving the random write performance of hard disks. However, it does not solve issues such as random reads from the log disk and suffers from expensive destaging operations (still random writes) under heavy workloads. Several techniques employ non-volatile devices to

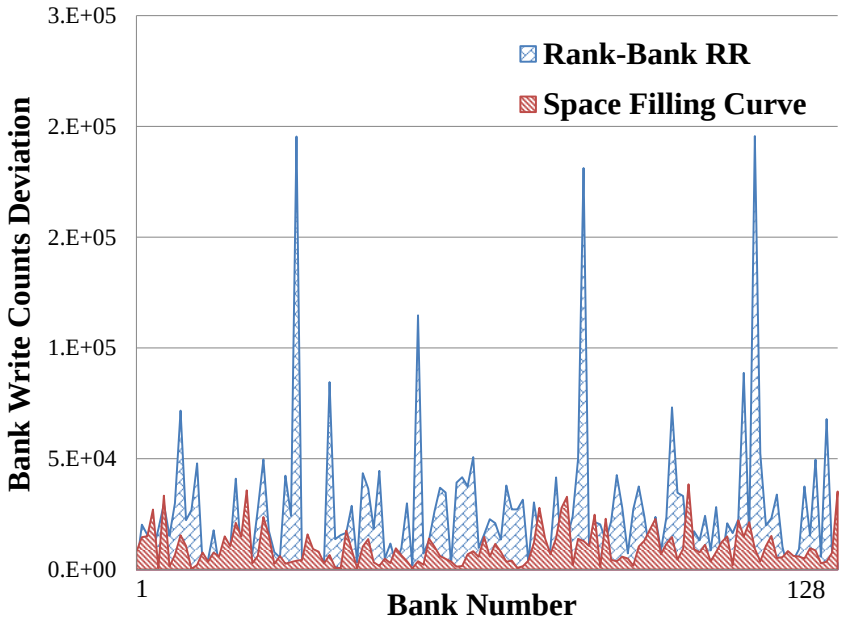

Figure 3.17: Write deviations among banks for Fin2

boost the performance of storage and file systems. Some use NVRAM as the file system metadata storage [32, 33, 75], while others use NVRAM as LRU/LRW caches in file and storage systems [20, 55, 101]. However, these techniques have limitations. For example, they can only boost performance for certain types of file systems; they also cannot ensure the sequential write-back to HDDs due to the usage of LRU policy to manage cache replacement. The HALO scheme as proposed in our hybrid storage system addresses both of these limitations.

Wear Leveling for PCM: Many research efforts have been invested in studying wear leveling in order to extend the lifetime of PCM. Qureshi et al. [78] make the writes uniform in the average case by organizing data as rotating lines in a page. For each newly allocated page, a random number is generated to determine the detailed rotation behavior. Seong et al. [84] use a dynamic randomized address mapping scheme that swaps data using random keys to prevent adversaries. Zhou et al. [122] propose a wear-leveling mechanism that integrates two techniques at different granularities: a fine-grained row shifting mechanism that rotates a physical row one byte at a time for a given shift interval, and a coarse-grained segment swapping mechanism that swaps the most frequently written segment with the less frequently written segments. Their work suffers

from the overhead of hardware address mapping and the overhead of periodical sorting to pick up appropriate segments for swapping. Ipek et al. [45] propose a solution to improve the lifetime of PCM by replicating a single physical memory page over two faulty, otherwise unusable PCM pages. With modifications to the memory controller, TLBs and OS, their work greatly improves the lifetime of PCM. In [103], Wang et al. provide inter-set and intra-set wear-leveling techniques to uniform write operations to ReRAM which is used as on-chip caches. Our wear leveling work is distinguished from these prior efforts. We regard the global address space as a multidimensional geometric space and employ a novel space filling curve-based algorithm to evenly distribute accesses across different dimensions. Compared with existing work, our approach significantly extends the lifetime of PCM in hybrid storage devices.

3.5 Summary

In this paper, we propose a new hybrid PCM+HDD storage system that leverages PCM as a write cache to merge random write requests and improve access locality for the storage system. Along with this, we also design a cache scheme, named HALO, which utilizes the fast access and non-volatility features of PCM to improve system I/O performance with guaranteed reliability. Results from a diverse set of workloads show that HALO can achieve lower traffic rates to HDDs due to better caching and achieve higher system throughput led by smarter destaging techniques. Therefore, our approaches reduce execution times significantly, 36.8% on average. This hybrid storage organization is especially beneficial for workloads with intensive random writes. We also design two wear leveling schemes, rank-bank round-robin wear leveling and space filling curve based wear leveling, to extend the lifetime of PCM in the proposed hybrid devices. Our results show that SFC-based wear leveling improves the life time of PCM devices by as much as 21.6 times. Also, we have integrated an in-house PCM simulator into DiskSim 4.0 [24] as a new hardware model.

Chapter 4

I/O Optimization for a Large-Scale Climate Scientific Application

4.1 An Extensible Parallel I/O Framework

To overcome the limitations of existing design, especially to improve the performance at large scale, a new framework that can support parallel I/O is imperative. One alternative approach to enable parallel I/O is to have all the participating processes write their own output independently. However, such approach can generate a large number of small files, making it extremely difficult, if not impossible, for post-processing software, such as visualization tool, to analyze the simulation results. In addition, many parallel file systems, such as GPFS, provide poor performance on managing small files due to high metadata overhead. Therefore, in this work, we take another approach to designing a generalized framework that can leverage a rich set of state-of-the-art parallel I/O techniques to eliminate the data gathering bottleneck in the original system, thereby accelerating the output of simulation data. Figure 4.1 illustrates the new framework. Different from original design in which root processes need to gather either plane data or bundle data before writing the output into the file system, our new framework eliminates such limitation by enabling all the participating processes to write their own data into a shared file in the parallel file system.

4.1.1 A Generalized and Portable Architecture

Different platforms have been optimized for different file formats. For example, many laboratories have meticulously tuned PVFS [11] to efficiently support NetCDF format. Therefore, to provide high portability across different platforms, we redesign the communication and I/O framework of GEOS-5 as shown in Figure 4.1 to support three parallel I/O techniques, including parallel NetCDF, NetCDF-4, and ADIOS. Despite the striking differences among these techniques, our

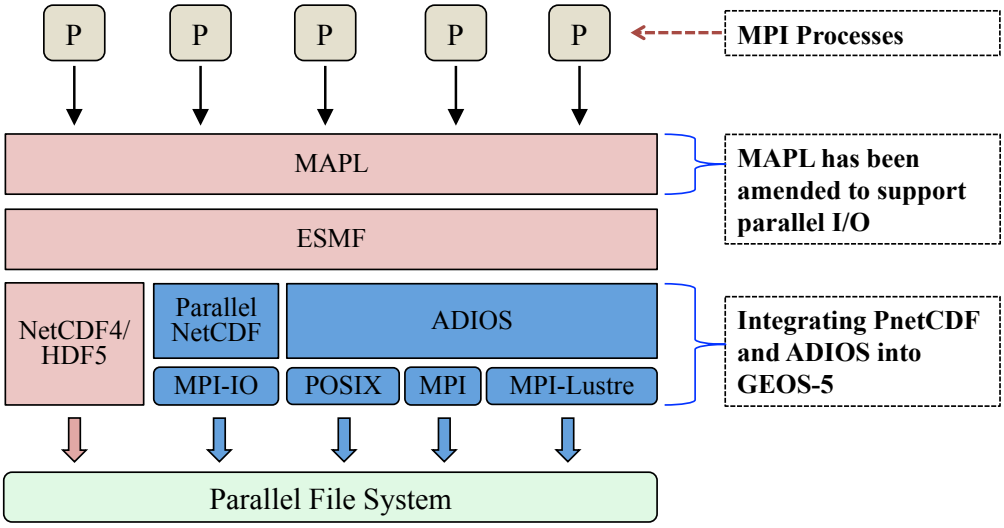

Figure 4.1: Parallel I/O Based System Architecture

new MAPL library and the ESMF framework together can hide such complexities and provide a set of uniform interfaces for upper layer MPI processes, who perform equivalently to conduct basic file operations, such as *open*, *write*, and *close*, *etc*. Within this design, each process can communicate with available I/O servers of file system via I/O middleware independently to transfer data. As a result, when data size is large, it can efficiently utilize the aggregated bandwidth to accelerate data transfers. Most importantly, such design eliminates the scalability bottleneck caused by plane roots and bundle roots described in Section 2.2.1. In the following sections, we provide a detailed description about how different scientific file formats are supported in the new framework.

4.1.2 Leveraging Parallel NetCDF

NetCDF is one of the most widely adopted formats used by many scientific applications. Its file structure contains a file header and multidimensional data arrays. File header includes metadata that describes the dimensions, attributes, and variable IDs. Data arrays store the concrete variable values, which can be either fixed-size or varied-size. Built on top of MPI-IO, parallel NetCDF (PnetCDF) [58] overcomes the inefficiency within the serial NetCDF [9] and provides parallel semantics to operate shared files in the file system.

Our new framework strives to leverage the strength of PnetCDF. Each MPI process performs computation on a chunk of plane data (as described in Section 2.2.1). At the end of each timestamp, instead of sending the data to the roots, each process directly writes the data into the shared NetCDF file through specifying the offset to the starting point of the data array. The starting point of the variable array is determined at the variable defining phase, which is conducted during the file open phase. During the data writing, we adopt collective I/O methods provided by PnetCDF in the current design. This means many I/O requests for non-contiguous portions of a file are merged together by either I/O servers or working processes before being processed. Such approach significantly reduces the number of I/O requests that need to be processed by the file system, thus improving the performance. At the file open and close phases, NetCDF metadata, such as dimension definition, variable attributes and lengths, needs to be synchronized among all of the participating processes in the group. To achieve this, one process is elected as the leader of the group to take charge of broadcasting the changes whenever metadata is modified. However, our evaluation results show that maintaining strong metadata consistency can cause high overhead when doing small bundle operations.

4.1.3 Integration of ADIOS

In order to leverage the asynchronous I/O of ADIOS to improve GEOS-5's performance, we integrate ADIOS into GEOS-5 as an ESMF component. ADIOS is able to provide the flexibility of switching back-end I/O methods at ease, such as the universal POSIX and MPI-IO methods. Meanwhile, ADIOS provides the easy-to-use plug-in mechanism to add new file system or platform-specific I/O methods for optimal performance, such as MPI-Lustre.

Along with the integration of ADIOS, we use the BP file format [66] for processes to write data to a shared file. BP is a self-describing and metadata rich file format that consists of a number of process groups (each process group maintains data for one individual process) and a footer containing the file's metadata and index information. It can be easily transformed into other scientific file formats, e.g., HDF5 and NetCDF.

In contrast to the current implementation that stores each bundle's data into a separate file at each time step, our ADIOS implementation dumps all bundle data into a single file at each time step, which greatly reduces the number of files created. At each time step, every process writes its portion of bundle data into a single shared file image. Instead of immediately writing a sub-plane at a time, the ADIOS method buffers all the variable data for different bundles in memory and asynchronously writes out the buffered data when buffer is full. Compared to the original NetCDF I/O, ADIOS can save file opening/closing overheads significantly and increase the possibility of locally aggregating small data portions for reduced number of random disk accesses. In addition, the non-contiguous data layout of ADIOS format also contributes to the performance improvement. As no inter-process communication for aggregating data is needed in ADIOS I/O, the communication and synchronization overheads can be saved thus reducing the overall I/O time significantly.

4.2 Experimental Evaluation

In this section, we conduct a systematic evaluation of our parallel I/O based framework with PnetCDF and ADIOS, respectively. All experiments are performed five times and the average is presented in the paper. Our experiments are carried out on the Discover cluster [7] at the NASA Goddard Space Flight Center. Discover is one of the major computing platforms in NASA. It is equipped with 128 compute nodes, each of which contains two 6-core 2.8GB Intel Xeon CPUs and 24 GB memory. The compute nodes are connected with a 5PB GPFS parallel storage system via InfiniBand.

4.2.1 Performance with PnetCDF

We begin our evaluation through assessing the performance when PnetCDF is used. In this experiment, we measure the I/O time via using a single bundle Moist whose size is 1GB. Total number of timestamps is 10 so that the application outputs bundle results for 10 times. Meanwhile, we increase the number of processes from 32 to 960. Figure 4.2 shows the evaluation results.

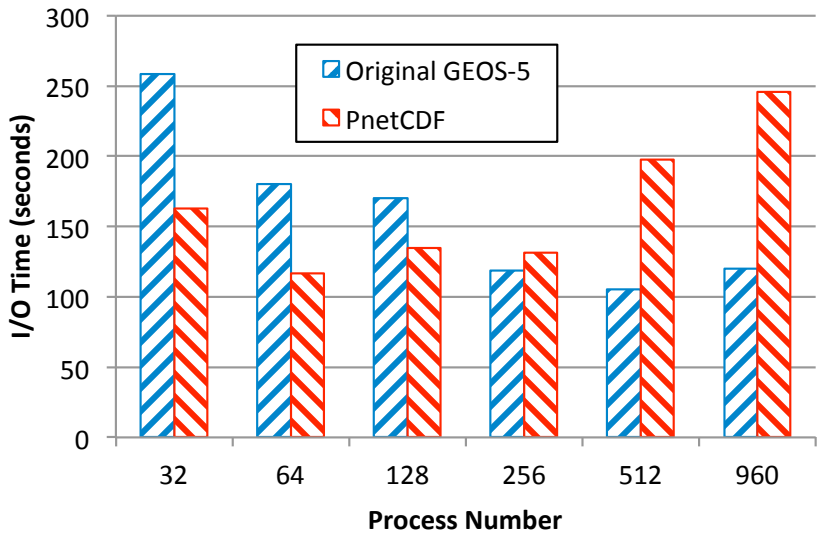

Figure 4.2: Comparison between Serial NetCDF and PnetCDF

However, we observe that compared to the original design called *CFIO*, although using PnetCDF can efficiently reduce the I/O time by up to 36.9% when the number of processes is less than 128, PnetCDF fails to provide improvement when the number of processes increases beyond 256, and unexpectedly degrade the performance by as much as 110% when the number reaches 960.

To investigate the cause, we dissect the I/O time. We measure the time consumed by *file creation*, *file write* and *close wait*, respectively. As shown in Figure 4.3, within the given experimental configuration, the original design constantly incurs negligible *file creation* but high *close wait* overheads, while PnetCDF incurs much higher *file creation* and drastically increases *close wait* overheads for maintaining the consistency of metadata and aggregating data variables. In addition, the *file write* time of both the original design and PnetCDF I/O decreases with an increasing number of processes because of higher aggregated bandwidth. Though PnetCDF achieves several times higher write bandwidth than CFIO, its performance degrades as the total process count increases, because the total I/O time has been dominated by the overheads of *file creation* and *close wait* at large-scale for small bundles. For example, when the number of processes reaches 960, the two overheads cost almost 99% of total I/O time when PnetCDF is used. Note that PnetCDF incurs much higher *file create* and *close* overheads due to the metadata synchronization and aggregation of variable data so that the NetCDF format can be strictly consistent all the time. As a summary,

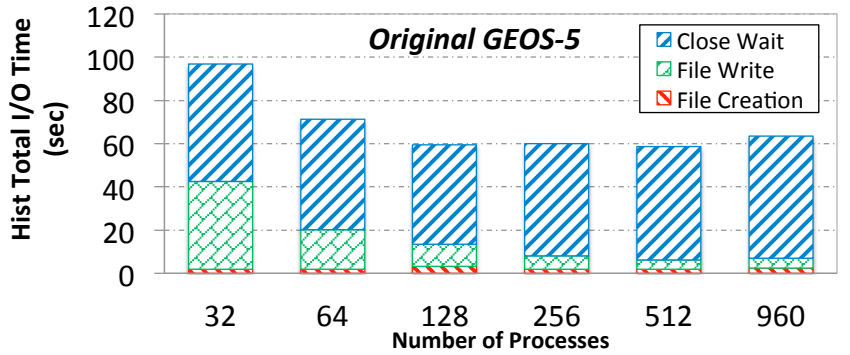

a) CFIO Dissection

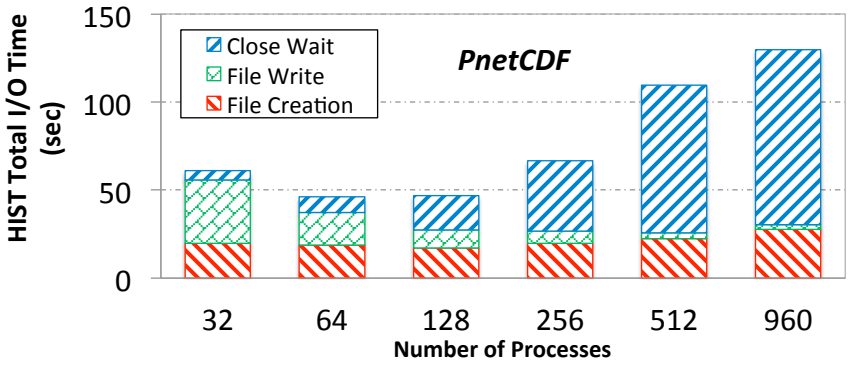

b) PnetCDF Dissection

Figure 4.3: Time dissection of CFIO and PnetCDF

these results explain why PnetCDF fails to outperform the original serial CFIO at scale. They also demonstrate that the mitigation of the overhead caused by *file creation* and *close wait* is critical to the successful adoption of any parallel I/O technique into scientific applications.

4.2.2 Performance with ADIOS

To evaluate the performance of GEOS-5 with ADIOS, we select two ADIOS methods, MPI and POSIX, for writing GEOS-5 bundle files. Figures 4.4 and 4.5 show the results of evaluation, in which we use 7 bundles and 30 timestamps and increase the number of processes from 32 to 960. As shown in Figure 4.4, compared to the original design, using ADIOS with MPI significantly reduces the I/O time, up to 58.2% when the number of processes is 960. More importantly, ADIOS with MPI shows efficient scalability for a large number of processes (from 256 to 960). On the contrary, although ADIOS with POSIX shows effective improvement over the original design in

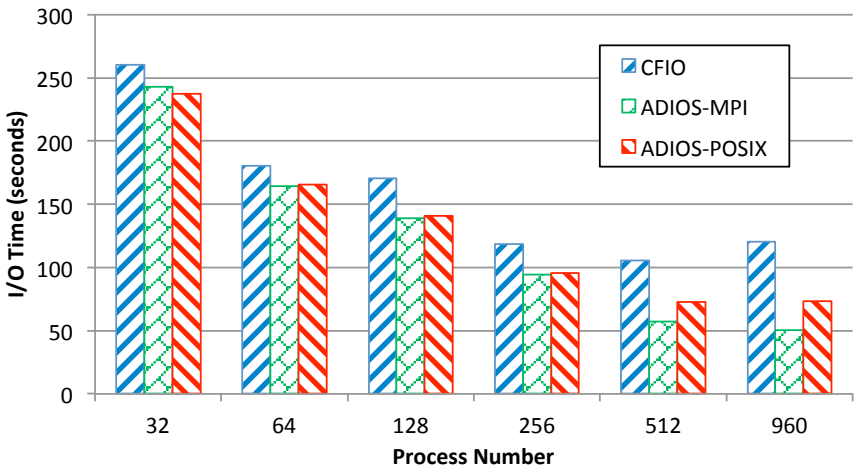

Figure 4.4: Comparison between CFIO and ADIOS

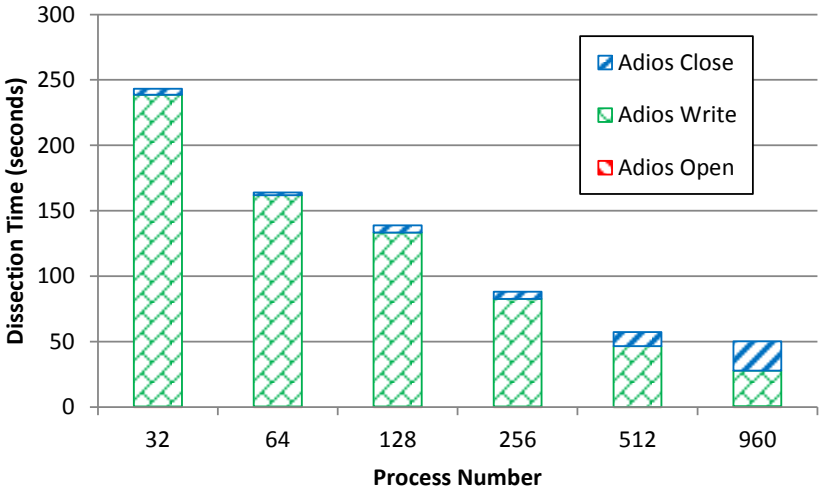

Figure 4.5: Time Dissection of ADIOS-MPI

terms of I/O time reduction, it stop scaling when the number of process increases from 512 to 960 due to consistency semantics rooted in POSIX interfaces.

Figure 4.5 shows the time dissection of using ADIOS-MPI. Similar to the approach used in Section 4.2.1, we analyze the time spent on *open*, *write*, and *close*, respectively. As shown in the figure, ADIOS incurs almost zero overheads when conducting file open, and negligible overhead for file close. This is because the file open call returns immediately with the use of open-on-write. And when writing out the data, buffered data is frequently flushed to the underlying file system, thus causing little waiting time when file is being closed. In addition, ADIOS with MPI shows

scalable file writing with an increasing number of processes, decreasing from 90% of I/O time to 56% of I/O time. This is because of the higher aggregated bandwidth achieved with a large number of processes. Compared with PnetCDF, using ADIOS efficiently mitigates the overhead of maintaining the metadata of shared file, thus achieving better scalability and performance at large-scale.

4.3 Related Studies on I/O optimizations for scientific applications

There is a large body of research literature on improving the I/O performance of scientific applications on large-scale supercomputing systems. Many I/O techniques have been designed to exploit the best I/O performance from underlying file systems. These include NetCDF-4 [98], HDF-5 [93, 67], PnetCDF [58] and ADIOS [1]. Built on top of these techniques, more efforts have been taken to study optimizations such as data buffering [61], file striping [116], subfiling [22, 27], staging [16] and data reorganization for multidimensional data structure [82, 87, 95, 96, 97]. Some of the techniques have been adopted into various I/O middleware libraries.

There is also a rich set of literatures on the performance characterization of HPC systems, spanning a wide variety of aspects such as inter-process communication [112], interconnect technologies, parallel file systems, reading patterns [65] and power management. Many studies are closely related to ours. [35, 44, 114, 115] reported scaling trends of the performance for various I/O patterns on Cray XT platforms. [53] described the challenges to improve the I/O performance and scalability on IBM Blue Gene/P systems. [81] characterized the I/O performance of NASA applications on Pleiades. Our work is different from the aforementioned studies. We focus on a climate application GEOS-5 that has a communication and I/O pattern representative of various climate and earth modeling applications. For this pattern, we introduce an extensible parallel framework that can employ different parallel I/O techniques such as PnetCDF and ADIOS and optimize the I/O performance of climate application.

4.4 Summary

In this work, we target at identifying and addressing influential factors that can hinder current scientific applications from achieving efficient I/O. By adopting the GEOS-5 climate modeling application as our case study, we analyze the typical communication and I/O patterns in representative scientific applications. And we discover that many legacy scientific applications employ similar hierarchical network aggregation to collect data portions for multi-dimensional variables from all processes and then dump the aggregated data into persistent storage. Through comprehensive measurements on the NASA discover cluster, we quantitatively profile and dissect the network communication and I/O costs by such I/O schemes. In order to address the drawbacks of single point of network contention and under-parallelized I/O patterns, we modify the current I/O framework of GEOS-5, enabling the applications to take advantage of state-of-art parallel I/O techniques like PnetCDF and ADIOS. Experimental results demonstrate that the integrated parallel I/O techniques supported by our I/O framework can improve the application I/O time at various scales. This performance improvement come from the elimination of huge amounts of network aggregation and significantly promoted I/O concurrency.

In the future, we plan to study asynchronous I/O schemes and efficient burst buffering techniques for further I/O performance improvements of scientific applications.

Chapter 5

Prediction Based Two-Level Query Scheduling

5.1 Cross-layer Scheduling Framework

In the current Hadoop-based query processing framework, Hive queries are first processed by the parser and the semantic analyzer, and then a physical execution plan is generated as a DAG of MapReduce jobs. For all jobs in a DAG, Hive submits one job to the JobTracker when that job's dependency has been satisfied. Jobs from various queries are linearly ordered at the JobTracker, which then selects map and reduce slots based on either HCS or HFS.

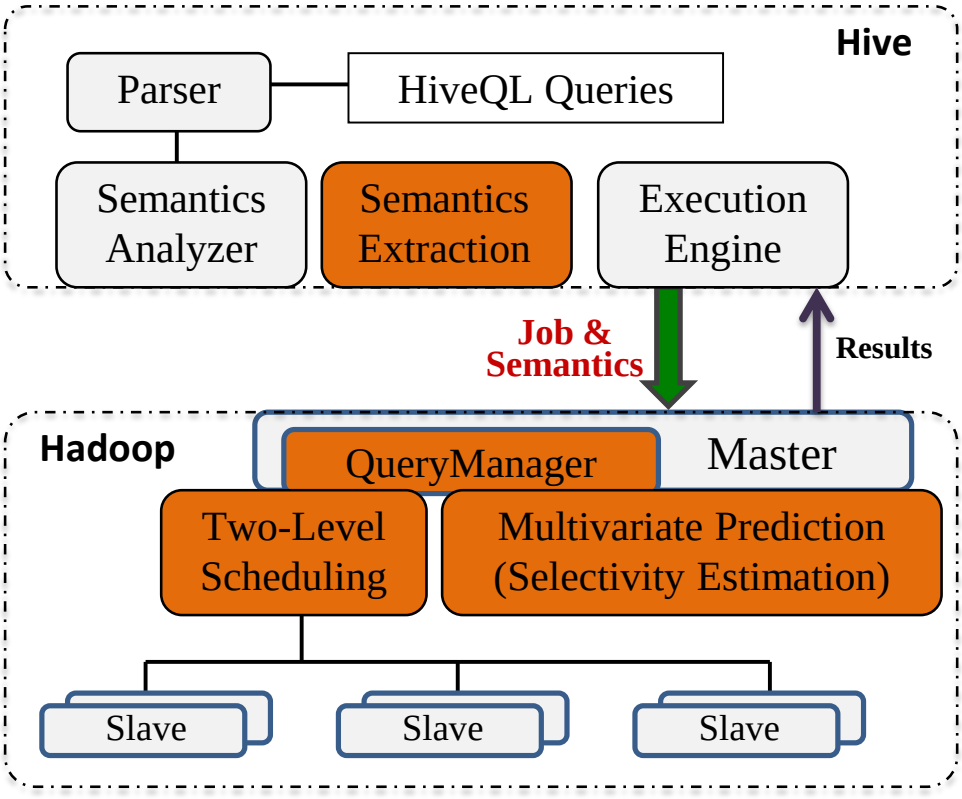

Figure 5.1: Prediction-Based Two-Level Scheduling Framework

Clearly, all the query-level semantics is lost when Hadoop receives a job from Hive. In addition, the Hadoop JobTracker can only see the presence of individual jobs, not their parent queries. As a result, there is no coordination among jobs to ensure the best overall progress for the query, not just that of the individual jobs.

To address the aforementioned challenges systematically, we propose a *cross-layer two-level scheduling framework*. As shown in Figure 5.1, three techniques are introduced including semantics extraction and percolation, multivariate execution-time prediction with selectivity estimation, and two-level query scheduling.

Semantics Extraction and Percolation: First, we introduce a component for semantics extraction and percolation in Hive during the query compilation and its execution plan construction. To bridge the semantic gap between Hive and Hadoop, we extract the semantics from each query's logical and physical plans. This includes these query attributes: the DAG of jobs, the dependencies among jobs, the operators and predicates of jobs, and the input tables. When Hive submits a job to Hadoop, it includes its semantics information as part of the job configuration file. Instead of directly queuing a job, our framework maintains a queue of all queries, and adds each job along with related semantics to its parent query.

Second, across both Hive and Hadoop layers, we introduce a scheme for multivariate execution-time prediction. This scheme includes a selectivity estimator that can evaluate query predicates and estimate the changing size of data during the query execution, and a regression model that predicts the job execution time. The percolated semantics is leveraged by both the selectivity estimator and the regression model.

Finally, at the Hadoop layer we introduce two-level query scheduling to (1) manage the admission and concurrency of queries to ensure efficient resource utilization and fair progress among different queries at a coarse-grained inter-query level; and (2) leverage percolated semantics and estimate the progress of jobs at the intra-query level, and accordingly prioritize jobs on the critical path of a query DAG for execution.

Multivariate time prediction and two-level query scheduling are described in detail in Sections 5.2 and 5.3, respectively.

5.2 Query prediction model

To achieve the objective of efficient two-level query scheduling, accurate prediction of the execution time and resource usage for a query is a crucial prerequisite. We apply a job-oriented time estimation rather than a query-oriented time estimation approach [38] in MapReduce because of two reasons. First, in MapReduce-based data warehouses, a query is divided into multiple MapReduce jobs, each with a separate scan of its input tables, materialization and de/serialization; second, intra-query job parallelism can affect query execution time. Therefore, job-oriented time estimation/modeling can gain insights about execution statistics and dynamic behaviors of jobs inside a query, therefore presents a better fit.

In order to have an accurate prediction of job execution time, we need to decide what semantics to include as parameters in the model. In addition, there are multiple steps of data movement during the execution of a job, and the data size changes inside a job and along the DAG of a query. Thus a good prediction model also needs to reflect such dynamics of data [34]. To this end, we first describe the selectivity estimation of MapReduce jobs and then elaborate the integration of selectivity estimation into the prediction.

5.2.1 Selectivity Estimation

As shown in Figure 5.2, for a MapReduce job in a query DAG, the output of its map tasks provides the input for its reduce tasks. One job's output is often taken as part of the input of its succeeding job in the same DAG. The input size of a job directly affects its resource usage (number of map and reduce tasks) during execution in MapReduce. In addition, the data size of map output (intermediate data) also significantly affects the execution time of reduce tasks, and indirectly affects the execution of the downstream jobs in the query. An accurate prediction of

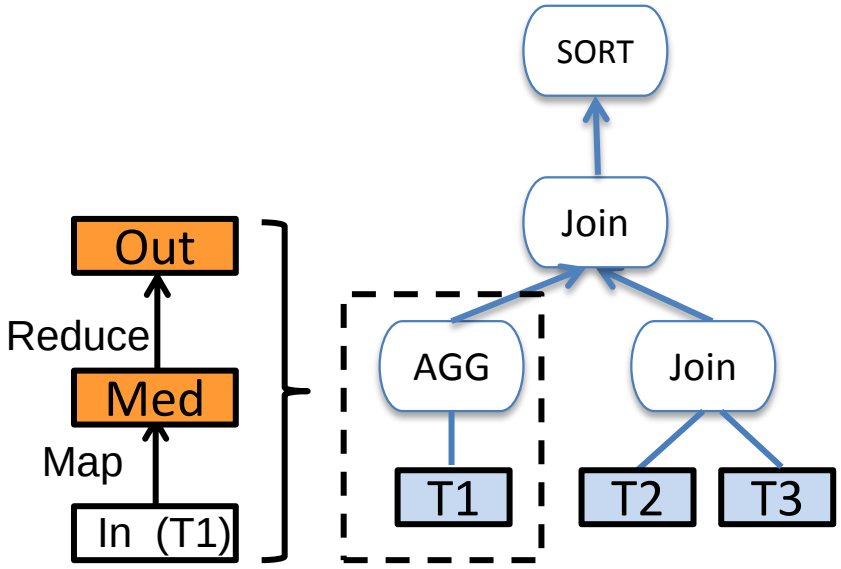

Figure 5.2: Intermediate and Final Selectivity Estimation

execution for the job and/or the query requires a good estimation of the dynamic data size during execution.

We divide this requirement into two metrics: the growth estimation of intermediate data (Intermediate Selectivity) and the growth estimation of a job's output (Final Selectivity). Let us denote the input of a job as D_{in}, D_{med} as the intermediate data, and D_{out} as the output. The Intermediate Selectivity (IS) is defined as the ratio between D_{med} and D_{in}, and the final selectivity (FS) as the ratio between D_{out} and D_{in}.

Intermediate Selectivity

In general, a job's intermediate selectivity is determined by the semantics of its predicate and projection clauses on the input tables. For some jobs with a local combine step in its map tasks, e.g., groupby, their intermediate selectivity needs to take into account the impact of combination. A local combine in MapReduce happens at the end of an individual map task to merge the output key-value pairs that share the same key. The selectivity of a project clause, S_{proj}, can be calculated

as the ratio between the average width of the selected attributes and the average tuple size in a table. We rely on the table statistics information for estimating S_{proj}.

Let us denote $|In|$ and $|Med|$ as the numbers of tuples in the input table and the intermediate data, respectively. The selectivity of a predicate clause, S_{pred}, can be calculated as $S_{pred} = |Med|/|In|$ if there is no local combine operation in the map tasks. We build off-line histograms for the attributes of the input table for estimating S_{pred}. Assuming piece-wise uniform distribution of attribute values, equi-width histograms [76] are built on tables' attributes to be filtered through a MapReduce job and stored on HDFS. An equi-width histogram is built by first splitting the domain of an attribute uniformly into a given number of buckets and then recording the number of values and distinct values in each bucket [76]. For scale values, such as integer, double and date, we compute the selectivity of predicate clauses by counting the number of tuples in the matching buckets. For text values, such as string, we avoid complex and expensive structures such as suffix trees, and only record the numbers of distinct and total values, as well as history selectivities if possible, for a best-effort selectivity estimation. For a conjunctive predicate formed by multiple predicate clauses that filter multiple tables on different attributes, we assume the distribution independence of attributes and compute the overall selectivity S_{pred} as the product of selectivities from all predicate clauses.

Hive and Pig queries are compiled into DAGs of operators. In these DAGs, the operators for global shuffle/aggregation will be converted into separated MapReduce jobs. We term such operators as *major operators*, e.g., groupby, orderby and join. Other operators will be carried out with the map phase of a job. We term such operators as *minor operators*, e.g., normal range and equality predicates. We categorize jobs into three types with respect to their major operators: groupby, join and extract (including orderby and all other major operators).

We elaborate further on our estimation of IS. Our discuss focuses on the aforementioned three operations: extract, groupby and join. Other operations can be considered as simple or composite derivatives of these three.

Extract: An extract operation usually scans one input table, we calculate its intermediate selectivity as $IS = S_{pred} * S_{proj}$.

Groupby: In a groupby operation, its local combine can further reduce the intermediate data. Let S_{comb} denote the combination selectivity. We can calculate its intermediate selectivity as $IS = S_{comb} * S_{proj}$. The calculation of S_{comb} needs to be elaborated further with an example. Suppose a job performs a groupby operation on Table T's key x and key y. Let $T.d_{xy}$ denote the product from the numbers of distinct keys for x and y. If the groupby keys are all clustered in the table, S_{comb} is calculated as $S_{comb} = min(1, \frac{T.d_{xy}}{|T|*S_{pred}}) * S_{pred} = min(S_{pred}, \frac{T.d_{xy}}{|T|})$. Otherwise, if the groupby keys are randomly distributed, S_{comb} is then calculated as $S_{comb} = min(S_{pred}, \frac{T.d_{xy}}{|T|/N_{maps}})$, where N_{maps} denotes the number of map tasks of the job. We omit the calculation for other minor cases.

Join: A join operation may select tuples from two or more input tables. We describe the calculation of IS for a simple join job of two tables. Let r_1 represent the percentage of one table's data in the total input of a job, $r_2 = (1 - r_1)$ for the other table. We can calculate IS for a join job with two input tables as: $IS = S_{pred1} * S_{proj1} * r_1 + S_{pred2} * S_{proj2} * (1 - r_1)$.

Final Selectivity

Let us denote $|Out|$ as the number of tuples and W_{out} the average width of tuples in the output (Out), a job's final selectivity is calculated as $FS = |Out| * W_{Out}/D_{In}$. The key of calculating FS is to compute $|Out|$. Our discussion focuses on three common operations including extract, groupby and join.

Extract: In Hive, there are two common extract operations, "$limit\ k$" and "$order\ by$". For the former, $|Out| = min(|In|, k)$; and for the latter, $|Out| = |In|$.

Groupby: A groupby operation may use one or more keys. The number tuples in the output is determined by the cardinalities of the keys and the predicates on the keys. We show the calculation for an example operation with one key. For a table T, let us denote the cardinality of a key x as $T.d_x$. A groupby operation on key x will have $|Out| = min(T.d_x, |T| * S_{pred})$.

Join: There are many variations of join operations. Multiple operations may hierarchically formulate as a join tree. We focus on a few common join operations with two or three tables to illustrate the calculation and the most important case: equi-join between a primary key and a foreign key (and tables should obey referential integrity).

An equi-join operation from these two tables T_1 and T_2 will have $|Out| = |T_1 \bowtie T_2| = |T_1| * |T_2| * \frac{1}{max(T_1.d_x,\, T_2.d_x)}$ if join keys follow uniform distribution [91]. However, uniform distribution is rare in practical cases; in addition, this approach only applies for multiple joins that share a common join key. In our work, we assume piece-wise uniform distribution, where in each equi-width bucket keys follow uniform distribution. Let T_{1i} denote the i-th bucket of in the equi-width histogram for a join operation on Key x. Then we can calculate the number of tuples in a join job's result set as:

$$|T_1 \bowtie T_2| = \sum_{i=1}^{n} |T_{1i}| * |T_{2i}| * \frac{1}{max(T_{1i}.d_x,\, T_{2i}.d_x)} \tag{5.1}$$

Since $(T_{1i} \bowtie T_{2i}).d_x = min(T_{1i}.d_x,\, T_{2i}.d_x)$, the equation above can be evolved to calculate the join selectivity for shared-key joins on three or more tables.

For chained joins with unshared keys, e.g., T_1 and T_2 joining on Key x and T_2 and T_3 joining on Key y, we leverage the techniques introduced in [21] by acquiring the updated piece-wise distribution of Key y after the first join for selectivity estimation of cascaded joins. For natural joins (each operator joins one table's primary key with another table's foreign key) with local predicates on each table, selectivities are accumulated along branches of the join tree, thus the number of tuples in the result set can be approximated as:

$$\begin{aligned} &|T_1.pred_1 \bowtie T_2.pred_2 \bowtie \cdots \bowtie T_n.pred_n| \\ &\qquad = S_{pred\,1} S_{pred\,2} \ldots S_{pred\,n}\, max(|T_1|, |T_2|, \ldots, |T_n|) \end{aligned} \tag{5.2}$$

An Example of Selectivity Estimation

We use a modified TPC-H [13] query Q11 as an example to demonstrate the estimation of selectivities. Figure 5.3 shows the flow of selectivity estimation. This query is transformed into

two join jobs and one groupby job. In Job 1, the predicate on the nation table has a predicate selectivity of 96% and it is relayed to the upcoming jobs along the query tree. Thus we can predict *IS* and *FS* for Job 1 and Job 2 according to the equations above. In Job 3, since the groupby key (partkey) has a cardinality of 200,000 that is much less than input tuples of this job, the output tuples of Job 3 is approximated as 200,000.

```
SELECT ps_partkey, sum(ps_supplycost*ps_availqty)
FROM nation n JOIN supplier s ON
  s.s_nationkey=n.n_nationkey AND n.n_name<>'CHINA'
JOIN partsupp ps ON
  ps.ps_suppkey=s.s_suppkey
GROUP BY ps_partkey;
```

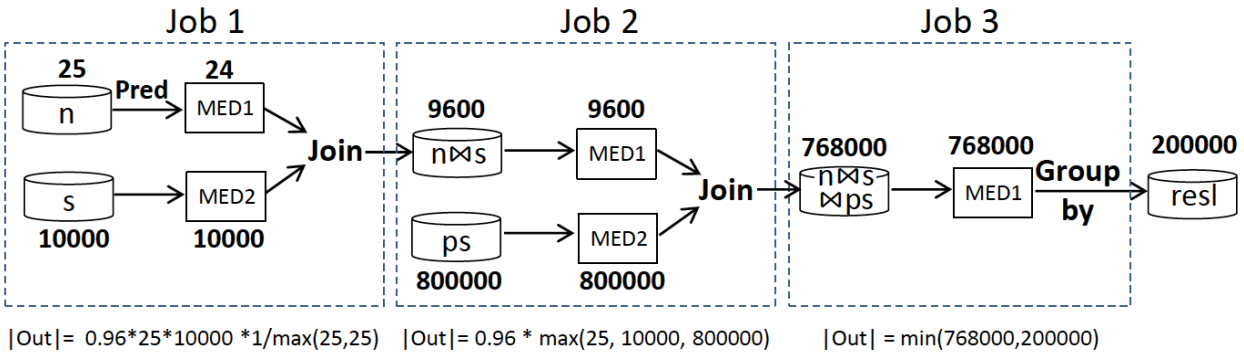

Figure 5.3: An Example of Selectivity Estimation

5.2.2 A Multivariate Regression Model

Based on the estimation of selectivities, we build a multivariate regression model for execution time prediction. We focus on the three operations as we have discussed in Section 5.2: extract, groupby and join. As listed in Table 5.1, we rely on several input features to predict the execution time. First, for simple jobs with the groupby or extract operator, we include three parameters D_{in}, D_{out} and D_{med} can provide good enough modeling accuracy. Second, different types of jobs display

distinct selectivity characteristics. Thus we include the operator type as part of our multivariate model.

Table 5.1: Input Features for the Model

Name	**Description**
O	The Operator Type: 1 for Join, 0 for others
D_{in}	The Size of Input Data
$D_{avg\,med}$	Avg Intermediate Data Per Reduce Task
D_{out}	The Size of Output Data
$P(1-P)D_{med}$	The Data Growth of Join Operators

However, for a join job, these parameters are not enough to reflect the growth of data sizes because the number of tuples can be the Cartisian product of input tables. Let $|T_1|$ and $|T_2|$ denote the number of tuples for the two input tables of a join operator. We define P as the ratio between the number of tuples in the larger filtered table and that of the final Cartisian product, i.e.,

$$P = \frac{max(|T_1|S_{pred1}, |T_2|S_{pred2})}{|T_1|S_{pred1} + |T_2|S_{pred2}},\ 0 < P < 1 \tag{5.3}$$

So $P(1-P)$ reflects the factor of a join operator, $P(1-P) \in (0, \frac{1}{4}]$. In our model, we include an additional parameter about the data growth for better estimation accuracy.

Based on these input features, we formulate a linear model with a set of coefficients $\vec{\theta} = [\theta_0, \theta_1, ..., \theta_m]$ to predict the job execution time (ET) as

$$ET = \theta_0 + \theta_1 D_{in} + \theta_2 D_{avg\,med} + \theta_3 D_{out} + \theta_4 O * P(1-P)D_{med}. \tag{5.4}$$

Note that $\vec{\theta}$ is trained separately for each of the three different operation types.

More features may lead to better prediction accuracy [111]. However, they can cause more monitoring overhead and are difficult to obtain in real-time. Thus the rationale behind our choice of features is to balance the need of accuracy with the complexity of extracting input features. Note that in the paper we concentrate on selectivity prediction for analytic queries, for other non-relational workloads such as User-Defined Functions (UDFs), there are some available solutions

in recent work [68, 100]. Next we validate the accuracy of our predicted execution time for jobs and queries.

Validation of Job Execution Prediction

To validate our model, we build up a training set using queries from TPC-H and TPC-DS benchmarks [13]. The data size ranges from 1 GB to 100 GB. Our validation test uses about 1,000 queries, which are converted into 5,647 MapReduce jobs. Among them, 7/8 of queries are used as the training set while the rest are used as the part of the test set. In addition, we further add 200 GB and 400 GB scale queries into the test set for assessing the model's scalability.

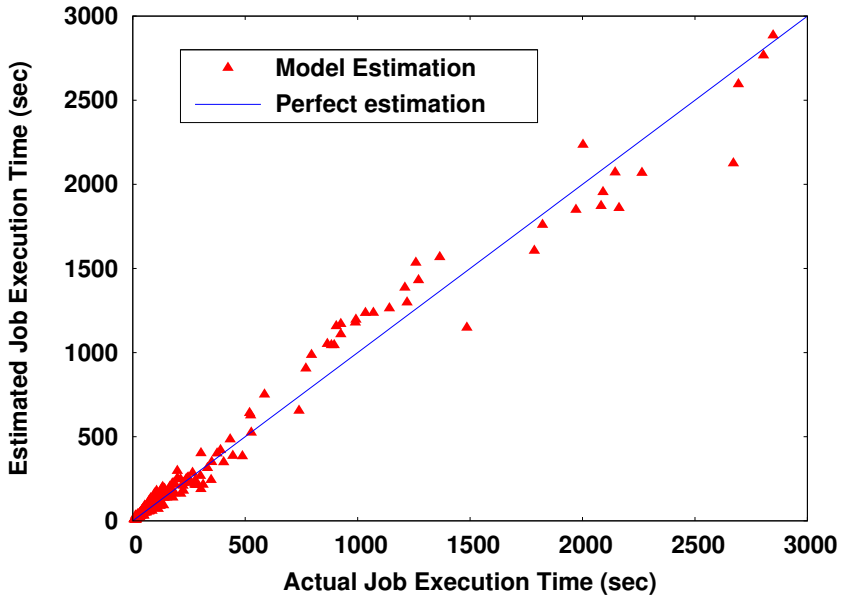

Figure 5.4: Accuracy of Job Execution Prediction

The accuracy of our job-level time prediction is shown in Figure 5.4. As we can see, x-axis indicates the actual job execution time while y-axis indicates the estimated job execution time. And the straight line represents a perfect prediction. We can observe that our model can accurately predict the execution time of MapReduce jobs through a careful process of selectivity estimation based on a few input parameters. Table 5.2 further summarizes the R-squared accuracy and the average error rate of our model for each operator. The average error rate for the test set of jobs is 13.98%.

Table 5.2: Accuracy Statistics for Job Execution Prediction

Types	R-squared accuracy	Avg Error
Groupby	96.75%	8.63%
Join	92.71%	14.40%
Extract	84.64%	9.38%
TestSet	N/A	13.98%

Validation for Predicted Query Execution

The execution time of a query can be approximated as the sum of execution times of all jobs along the critical path of its DAG and other large jobs which are able to use up the system's resource. Such jobs may include some that are yet to be submitted and others that are actively running. We directly use our multivariate model to predict the execution time of jobs that have not been submitted. For the active jobs, we further improve the prediction accuracy of their execution time by taking into account runtime statistics, such as the execution time and intermediate data size of completed tasks.

We compare the actual execution time and estimated execution time of 100 GB TPC-H queries. As shown in Figure 5.5, the average prediction error rate can be as low as 8.3%. Again, this error rate adequately validates the accuracy of our prediction model and its strength from selectivity estimation.

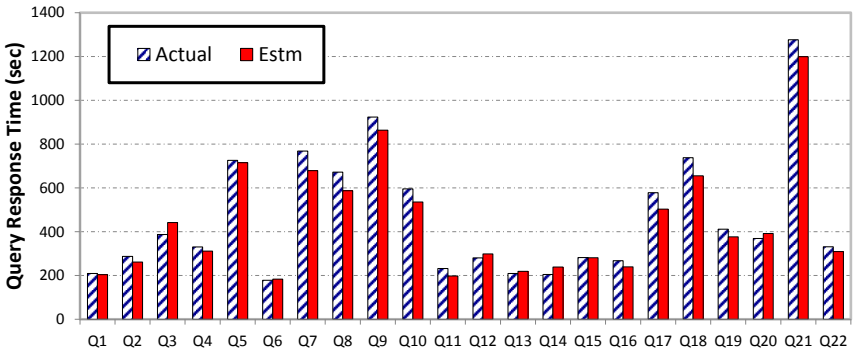

Figure 5.5: Accuracy of Query Response Time Prediction

5.3 Two-level Query Scheduling

Based on the multivariate query model, our objective is to schedule the queries for better resource utilization, efficiency and fairness. We propose to schedule queries and their internal tasks and jobs at two levels. At the coarse-grained query level, an inter-query scheduler selects queries for system efficiency and ensures fairness among concurrent queries. At the fine-grained job level, an intra-query scheduler leverages the DAG semantics in a query and prioritizes critical-path jobs based on our multivariate model.

5.3.1 Inter-Query Scheduling

When analytic queries are first submitted to our scheduling framework, we admit the query and initialize the structure to keep track of its runtime information according to our multivariate model. A query queue (L_{act}) is maintained for the active queries each of which contains a DAG of runnable or running jobs. We apply our selectivity estimation and multivariate model recursively from the largest depth of the query DAG to the smallest depth, i.e. the root node. To be specific, D_{In}, IS, D_{Med}, FS and D_{Out} are initialized based on the job type, predicate and projection selectivities as mentioned in Section 5.2. When one task has completed, we will update the number of remaining tasks for this query. When one job is completed, we recursively update our estimation of input, output and execution time for the downstream jobs along the DAG.

Selection Metric – Weighted Resource Demand

We need to ensure all queries be fairly treated with comparable slowdown ratios so that small queries can turn around faster while big queries still get their fair share of time and resources for execution if delayed by a certain degree. However, in selecting queries that are organized as DAGs of jobs, we cannot solely rely on the temporal resource demand of a query, i.e. its remaining time that can be estimated from our multivariate model. A query and all of its jobs often employ a dynamic number of tasks during its execution. Each task may have its own execution time, CPU, memory and I/O resource demand. Therefore, we introduce a simple metric to take into account

of the time and resource demand of a query or a job called **W**eighted **R**esource **D**emand (*WRD*). *WRD* is intended as a metric to estimate how much system resource will be required to complete a query or a job. A query's *WRD* is calculated as: $WRD = \sum_{i=1}^{n} MT_i * N_{Mi} + RT_i * N_{Ri}$, where MT_i denotes the predicted map task time, N_{Mi} denotes the remaining number of map tasks, RT_i denotes the predicted reduce task time and N_{Ri} the remaining number of reduce tasks, for an arbitrary job i of the query.

Table 5.3: Accuracy for Task Execution Prediction

Types	Map Task	Join	Groupby	Extract
R-squared accuracy	87.05%	85.83%	98.82%	90.03%

Even though we have a job-level multivariate model, the parameters' value ranges for various tasks can sometimes go far beyond our training set [59]. To deal with such issue, we empirically develop an estimation scheme for the execution time of MapReduce tasks based on the task type, the operator type, the input size and the output size. Table 5.3 summarizes the R-squared accuracy for map tasks and reduce tasks with three different operators. Such close estimation of task execution also allows us to determine the WRDs of all queries. We can then select the best query for execution.

Query Scheduling for Efficiency and Fairness

We have introduced an inter-query scheduling algorithm for Query Efficiency and Fairness (QEF) management. It strives to reconcile efficiency and fairness among concurrent queries within L_{act}. For optimal scheduling efficiency at inter-query level, we adopt an **SWRD** policy that prioritizes the query with the *Smallest WRD* in L_{act}. This heuristic algorithm is expected to achieve comparable query scheduling performance as SRPT does in M/G/1 scheduling (see a brief proof in Section 5.3.1). As shown in Algorithm 2, QEF includes the SWRD-based selection policy and a fairness guarantee policy, which addresses potential starvation and fairness issues among queries.

All the queries are sorted within L_{act} according to their WRD requirement (Line 2). Our algorithm selects the query with the least WRD (Line 16). However, to ensure fairness, we check

L_{act} for a query that has been severely slowed down and prioritize it (Lines 5-8). Meanwhile, a query with slow progress is also put into another list L_{slow} (Lines 9-11). QEF checks the size of L_{slow} to decide in which list of queries to select the next query.

To measure the slowdown experienced by each query, we consider query's sojourn time $T_{sojourn}$ and estimated remaining execution time T_{rem}. Specifically, the slowdown is defined as $slowdown = \frac{T_{sojourn}+T_{rem}}{T_{alone}}$. T_{alone} denotes the estimated execution time when it runs alone in the system. T_{rem} and T_{alone} are predicted based on our multivariate model. Meanwhile, the threshold $D_{threshold}$ that determines whether a query has been unfairly treated is computed as $\frac{1}{1-\rho}$, where ρ is the accumulated load on the system. Such threshold exhibits expected slowdown with the Processor-Sharing (PS) policy as proven by M/G/1 model [109].

Algorithm 2 Query Efficiency and Fairness Management

1: L_{act}: {a list of queries in the ascending order of WRD.}
2: L_{slow}:{a list of queries that have exceeded the slowdown threshold in the ascending order.}
3: **for all** $Q \in L_{act}$ **do**
4: **if** $(Q.slowdown > 2 \times D_{threshold})$ **then**
5: Schedule Q via Algorithm 3
6: Return
7: **end if**
8: **if** $(Q.slowdown > D_{threshold})$ **then**
9: L_{slow}.add(Q)
10: **end if**
11: **end for**
12: **if** $sizeof(L_{slow}) > Limit_{slow}$ **then**
13: $Q_{sched} \leftarrow$ {last query in L_{slow}}
14: **else**
15: $Q_{sched} \leftarrow$ {first query in L_{act}} //SWRD
16: **end if**
17: Schedule Q_{sched} via Algorithm 3

Proof for SWRD

According to Little's Law [51], a schedule for minimizing average response time translates to a schedule for minimizing the average query number in a system. Let $N(t)^{SWRD}$ and $N(t)^{\varphi}$ denote the number of queries residing in the system for SWRD scheduling policy and any other policy. For

the J queries with largest WRD and $J <= min(N(t)^{SWRD}, N(t)^{\varphi})$, we have $\sum_{i=1}^{J} WRD_i^{SWRD} <= \sum_{i=1}^{J} WRD_i^{\varphi}$ because SWRD favors the queries with smallest WRD. With the assumption of not considering the possible resource utilization difference caused by job phase independence and intra-query job dependence, the remaining workloads (WRD) at any time should be the same for any scheduling algorithm, thus we have $\sum_{i=1}^{N(t)^{SWRD}} WRD_i^{SWRD} = \sum_{i=1}^{N(t)^{\varphi}} WRD_i^{\varphi}$. Therefore, $N(t)^{SWRD} <= N(t)^{\varphi}$.

5.3.2 Intra-Query Scheduling

At the intra-query level, our target is to minimize the makespan of a query that consists of a DAG of MapReduce jobs. This problem is analogous to the multiprocessor scheduling problem for a DAG of tasks. The HLFET algorithm [17] is able to achieve the best makespan for the scheduling of DAGs of parallel tasks. The *level* of a task is calculated as the total execution time of all constituent tasks along its longest path and the task at the highest level is prioritized in HLFET. However, the execution of DAGs for analytic queries on MapReduce systems is very different from the DAGs of parallel tasks on a multiprocessor environment because each job in a query's DAG requires a collection of map and reduce tasks, i.e., causing rounds of resource allocation and task scheduling. Therefore, the HLFET algorithm is not a good fit to achieve the minimal makespan for DAGs of analytic queries. It can cause insufficient job parallelism and underutilization of system resources.

Depth-First Algorithm: Based on the internal complexity of MapReduce jobs in the DAGs, we design an algorithm that would first prioritize the job with the largest depth. In addition, for jobs of the same depth, our algorithm prefers the job with a larger WRD of the path from this job to the root node. We refer to this algorithm as the Depth-First Algorithm. As shown in Figure 5.6, a query is compiled into a DAG of six jobs. J2 and J4 are big jobs with highest levels in the HLFET algorithm. Thus HLFET schedules jobs J2, J4 and J5 in sequence according to their levels. In four steps of job scheduling, it can only achieve a job parallelism of 1.75 on average. System resources can be under-utilized with very low job parallelism. In contrast, DFA chooses the jobs

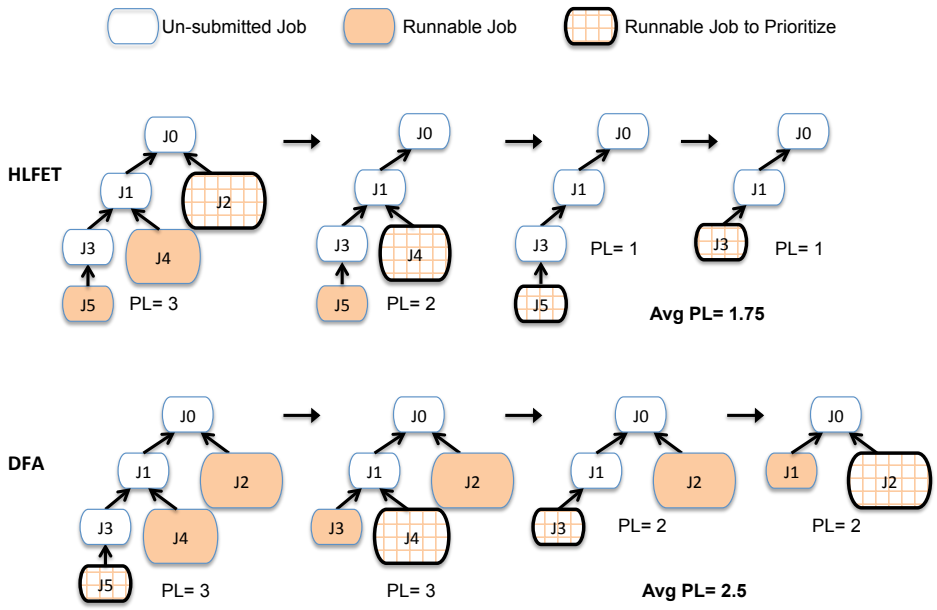

Figure 5.6: Comparison between HLFET and DFA Algorithms

with higher depths, whose results are needed by more downstream jobs. In the same number of steps, DFA achieves a job parallelism of 2.5 on average. When prioritizing one job with the biggest depth, the remaining slots can be leveraged by other concurrent jobs for boosting the progress of the whole query. Thus DFA recognizes and leverages a query's DAG structure to achieve better job parallelism, thereby speeding up query execution.

Locality through Input Sharing: To further strengthen DFA, we exploit input-sharing opportunities for better memory locality. For example, as shown in Figure 5.7, the TPC-H query Q21 contains two groupby (AGG) jobs and a join job that share the *lineitem* table as their input, an opportunity for intra-query table sharing. This input locality can be exploited to achieve better memory locality and reduce disk I/O. Note that input tables can be shared across different queries, e.g., between Q21 and Q17 (not shown for succinctness). Exploiting inter-query input sharing would complicate our design with diminishing returns. We focus on intra-query input sharing opportunities in this paper.

Combined Algorithm: We propose a Locality-Based Depth-First Algorithm (LoDFA) to combine both ideas. As shown in Algorithm 3, LoDFA first initializes the depth, WRD and input tables for each job (Lines 5-6). In addition, for each input table, it creates a set that includes the

Algorithm 3 Locality-Based Depth-First Algorithm

Initialization:
$DAG(Q), Ready(Q), IT(Q) \leftarrow$ {Query Q's DAG, Runnable jobs, Input Tables}
$LA(e)$: {Jobs sharing Table e, first empty.}
for all $j \in DAG(Q)$ **do**
    $Depth_j, WRD_j, Input_j \leftarrow$ {Job j's depth, WRD, tables}
    Insert Job j into $Ready(Q)$ if its dependencies are ready.
    for all $e \in IT(Q)$ **do**
        if $e \in Input_j$ and $e.size > Input_j.size/2$ **then**
            Insert Job j into $LA(e)$ in descending WRD.
        end if
    end for
end for
Method:
A heartbeat from Node n about Task t's completion
Find Task t's host job *Job i*
$e \leftarrow$ the max table in $Input_i$
if $LA(e) <> null$ **then**
    Select a demanding Job k with max WRD in $LA(e)$
    Schedule MapTask s from Job k to node n
    Check and update WRD_k and $Ready(Q)$
    Return
end if
Select jobs with the highest depth from $Ready(Q)$ as L_{todo}
Select Job k with the largest WRD in L_{todo}
Schedule Task s from Job k to node n
Check and update WRD_k and $Ready(Q)$

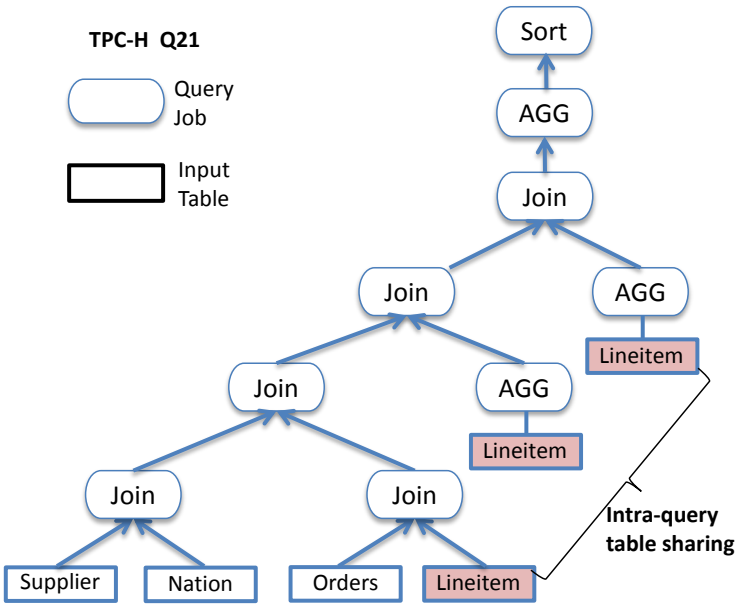

Figure 5.7: An Example of Table Sharing for a TPC-H Query

jobs that share the table (Lines 7-11). Upon a heartbeat notification about the completion of a map task t, it finds the sets of jobs that share the input table (e) with task t, and schedules a task from the job with the largest WRD (Lines 14-22). This allows LoDFA to exploit the benefit of input sharing between the recently completed task t and the newly scheduled task s for memory locality. If such a task is not found, LoDFA then follows the DFA algorithm to select the job with the highest depth and then the largest WRD (Lines 23-26). For a reduce task, we directly schedule the task according to the DFA policy in Lines 23-26.

5.4 Evaluation for MapReduce Query Scheduling

We have implemented our cross-layer scheduling framework in Hive v0.10.0 and Hadoop v1.2.1. In this section, we carry out extensive experiments to evaluate the effectiveness of the framework with a diverse set of analytic query workloads.

5.4.1 Experimental Settings

Testbed: Our experiments are conducted on a cluster of 9 nodes, one of which dedicatedly serves as both the JobTracker of Hadoop MapReduce and the namenode of HDFS. Each node features two 2.67GHz hex-core Intel Xeon X5650 CPUs, 24GB memory and two 500 GB Western Digital SATA hard drives. According to the resource available on each node, we configure 8 map slots and 4 reduce slots per node. The heap size for map and reduce tasks is set as 1GB and the HDFS block size as 256 MB. All other Hadoop parameters are the same as the default configuration. We employ Hive with the default configuration, while allowing the submission of multiple jobs into Hadoop.

Table 5.4: Workload Characteristics

Bin	**Input Size**	**Number of Queries**		
		Bing	**Facebook**	**QMix**
1	1-10 GB	44	85	85
2	20 GB	8	4	4
3	50 GB	24	8	8
4	100 GB	22	2	2
5	>100 GB	2	1	1

Benchmarks and Workloads: We choose a wide spectrum of benchmarks to conduct experiments. We first choose a few TPC-H queries with tree-structure execution plans to examine the efficacy of the intra-query scheduling. Then, we test the overall performance of the two-level scheduling under large-scale workloads with concurrent queries. For this purpose, with the TPC-H and TPC-DS queries, we first build two workloads based on the workload composition on Facebook and Bing production systems characterized in [19]. We name them *Bing workload* and *Facebook workload*, respectively. Though our framework is mainly targeted for Hive queries, we also test the feasibility of the framework on scheduling mixed workloads consisting of UDF jobs and Hive queries. For these experiments, we build the *QMix workload*, which mixes TPC queries with non-Hive benchmarks (Terasort, WordCount and Grep, processed as single-job queries).

Table 5.4 summarizes the composition of the Bing, Facebook and QMix workloads. Each workload has 100 queries with different input sizes and these queries are divided into 5 bins based

on their input sizes. We carefully tune the scales of the data sets and select queries, such that the numbers of queries in each bin follow a similar distribution as that described in [19]. While Facebook workload has a dominant portion of queries with small input sizes, Bing workload's queries are more uniformly distributed in the bins. The QMix workload is built by replacing 20 Hive queries in the Facebook workload with 20 non-Hive MapReduce jobs such that the QMix workload follows a long-tailed distribution similar to the Facebook workload. The queries are submitted into the system following a random Poisson distribution of inter-arrival times.

Metrics: One of the major objectives of the paper is to improve user experience. Thus, in the experiment, we collect query response times perceived by users. For each of scheduling schemes (HCS, HFS, and TLS), we run each benchmark 5 times and calculate average query response times. To show the performance advantage of TLS, we compare the query response times when the system uses TLS against those with other scheduling schemes.

In addition to query response times, we are also interested in how queries are slowed down when they run concurrently with other queries. Thus, we collect the response time of each query when it uses the whole system dedicatedly, and compare the response time against that with other concurrent queries to calculate the slowdown of the query. By comparing the slowdowns of different queries, we measure the capability of the different schemes on scheduling queries fairly.

5.4.2 Intra-Query Scheduling Evaluation

To test the effectiveness of the intra-query scheduling algorithm LoDFA, we collect the response time of each query when it uses the whole system dedicatedly. While queries with chain-structured execution plans usually have similar response times under LoDFA as they do under conventional Hadoop schedulers HCS and HFS. We found that LoDFA can effectively reduce the response times for queries with tree-structured execution plans. Figure 5.8 illustrates the response times of a few representative TPC-H queries of 200 GB scale under LoDFA and conventional Hadoop schedulers.

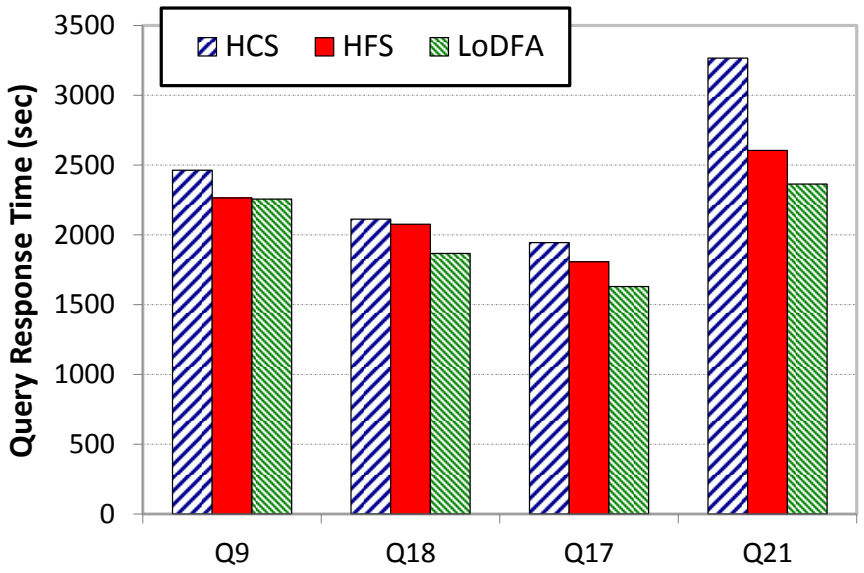

Figure 5.8: Query Response Times of Q9, Q18, Q17, and Q21 when They Use System Resources Alone.

Compared to HCS, LoDFA reduces the response times of Q9, Q18, Q17, and Q21 by 8.4%, 11.6%, 16.2% and 27.6%, respectively. Compared to HFS, LoDFA reduces the response times of Q18, Q17 and Q21 by 10.1%, 9.9% and 9.3%, respectively. LoDFA improves the performance of Q9 and Q18 mainly because it preferentially schedules jobs that can maximize the number of concurrent jobs in these queries to fully utilize resources. LoDFA improves the performance of Q17 and Q21 mainly because it is aware of the data sharing between the jobs in each query and schedules the jobs in a way that can exploit memory locality for efficient execution.

Specifically, the execution plan of Q9 is an unbalanced tree structure. On one side of the tree is a long chain of small jobs. Each small job may not fully utilize all the resources in the system due to their small input sizes. On the other side of the tree is mainly a time-consuming join operation. With HCS, the join job monopolizes the system resources and thus significantly delays the processing of small jobs, including those on the critical path. When the join job finishes, the lack of concurrency between unfinished small jobs makes the system underutilized and increases the overall response time. With HFS, small jobs can get a fair amount of resources and make progress concurrently with the job carrying out the join operation. According to the LoDFA algorithm,

small jobs on the long chain are preferentially scheduled according to the LoDFA algorithm. Thus, HFS and LoDFA achieve better performance than HCS.

Q18 shows the performance advantage of DFA acquired by prioritizing the jobs with large depths and WRDs. Usually, jobs with large depths and WRD are on critical paths and there are other pending jobs depending on their results. Prioritizing these jobs reduces the delay to other jobs and helps "releasing" more jobs to increase concurrency. Thus, LoDFA achieves better performance than HCS and HFS.

Since in Q17 and Q21 the jobs on the leaf nodes of their execution plans share the same big table (lineitem), the sharing-aware scheduling in LoDFA can consecutively execute the tasks of jobs sharing the same data sets and improve data access' temporal locality for these jobs. Such strategy reduces the amount of data to be read from disks and accelerates the execution of map and reduce tasks. Take Q17 as an example. When HCS is replaced by LoDFA, the data read from disks is reduced by 37.1% in each of its execution. This translates to the 44.2% and 19% reductions of the aggregated execution time for map operations and reduce operations respectively.

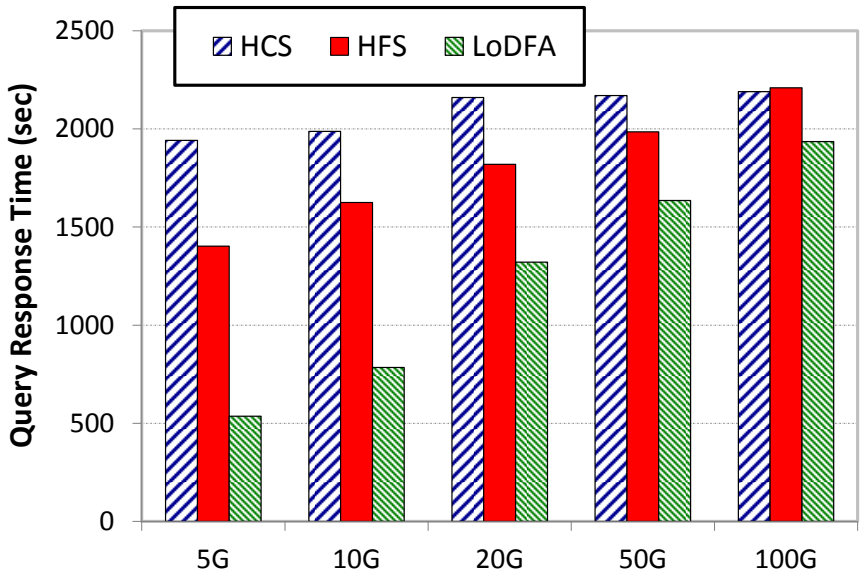

Figure 5.9: Query Response Times of 5 Instances of Q21 with Different Input Sizes.

When queries run concurrently and contend for resources, the intra-query scheduling algorithm - LoDFA becomes more effective in reducing query response times, especially for small

queries. At the same time, it improves the data temporal locality among jobs that share data and hence increases system throughput. To prevent the interferences from irrelevant factors, we submit 5 queries with the same query number (i.e. same execution plans) but with different input sizes (from 5GB to 100GB) simultaneously to the system.

We measure and compare the response times of each query under different scheduling schemes. The system throughput is determined by the response time of the query that finishes the last. Figure 5.9 shows the performance advantage of LoDFA over the two conventional Hadoop schedulers for the queries with Q21. With HCS, five queries have similar response times. This is because the executions of the queries with small inputs are significantly delayed by the jobs from the queries with large inputs and the execution priority is turned around among all five queries. The HFS scheduler ameliorates this situation. It shortens the response times of small queries at the cost of slightly increased response time for the largest query (and the system throughput). Compared to HFS, LoDFA further reduces the response times of small queries by large percentages (up to 61.8% for the query with the input size of 5GB). In addition, LoDFA reduces the response time even for the largest query, which also indicates the increase of the system throughput. Overall, LoDFA on average reduces the response time by 34.2% and increases system throughput by 11.6% compared with HFS. These improvements are mainly caused by the facts that TLS tends to increase locality by not assigning resources in an interweaving manner among queries and LoDFA can effectively exploit the data-sharing opportunities among jobs. In doing so, we not only accelerate the execution of each individual query, but also bring global benefits by reducing the contention for resources.

5.4.3 Overall Performance

In this section, we use Bing, Facebook and QMix workloads to test the overall performance of TLS. This evaluation helps us to understand how TLS performs under large-scale workloads, in which different types of queries with a wide range of input sizes are submitted by multiple independent users.

Table 5.5: Average Query Response Times

Workload	Average Response Time (s)		
	HFS	HCS	TLS
Bing	1028.79	794.635	576.965
Facebook	732.463	1609.71	438.235
QMix	1516.62	3455.44	819.557

Query Response Time

Table 5.5 summarizes the average query execution times of the Bing, Facebook and QMix workloads under three scheduling schemes. For all the workloads, TLS achieves the best performance. For Facebook and Bing workloads, TLS effectively improves performance by leveraging the semantics information and prediction results for efficient query scheduling. Compared to HFS, TLS reduces the average query response times by 40.2% and 43.9%, respectively; compared to HCS, TLS reduces the average query response times by 72.8% and 27.4%, respectively. For QMix workload, TLS reduces the average query response time by 45.96% and 76.28% respectively, relative to HFS and HCS. This clearly demonstrates the capability of TLS to handle workloads consisting of queries with and without semantic information.

Figures 5.10 and 5.11 plot the CDFs of the query response times for these scheduling schemes under Bing and Facebook workloads. As we can observe, TLS consistently reduces the response times for almost all the queries.

Allocating more resources to small jobs sacrifices the performance of large jobs. This can be confirmed with the HFS curves in Figure 5.10(c) and Figure 5.10(d). Thus, the Bing workload, which has more queries with large inputs, exhibits larger average response time with HFS than it does with HCS.

In the Facebook workload, most queries have small input sizes and thus have small jobs. With the HCS scheduler, the executions of the small jobs are significantly delayed due to the interleaving of the execution of large queries. The HFS scheduler reduces the response times for small queries by allocating a fair amount of resources to small jobs (Figure 5.11(b)). This is why the average query response time is smaller with HFS than that with HCS. Our TLS outperforms

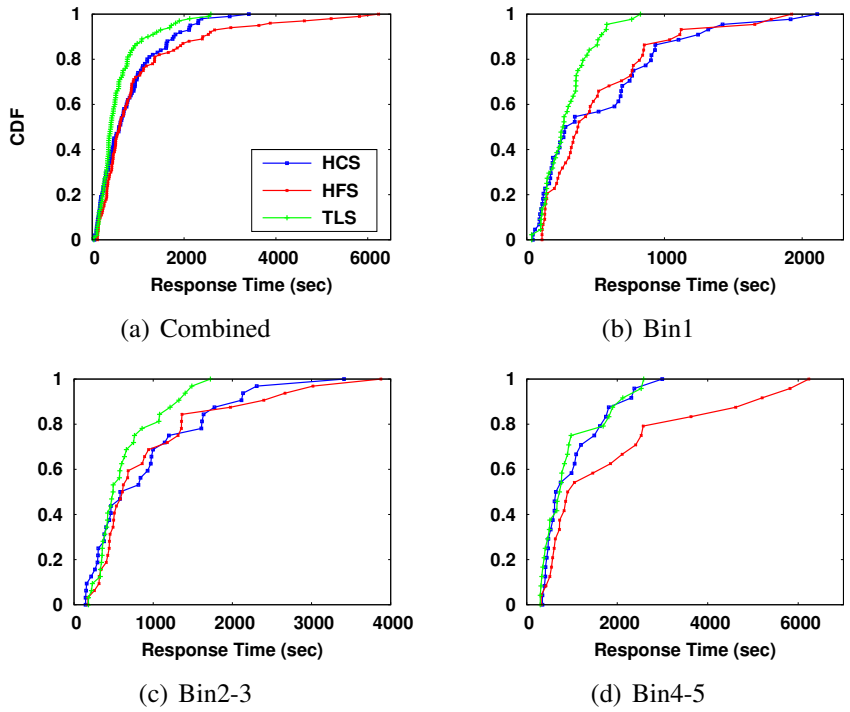

(a) Combined (b) Bin1

(c) Bin2-3 (d) Bin4-5

Figure 5.10: CDF of Query Response Time in Bing Workload

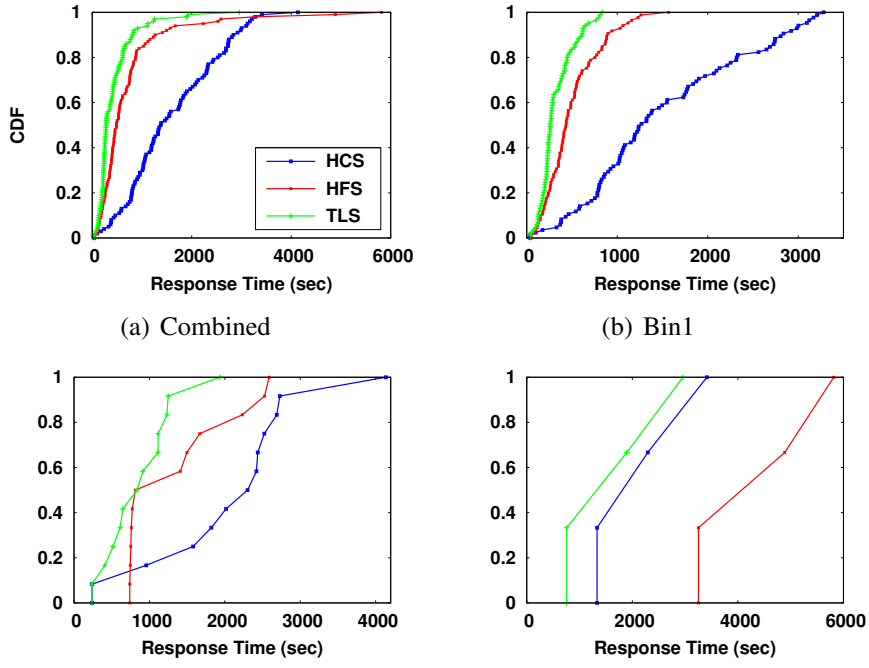

(a) Combined (b) Bin1

(c) Bin2-3 (d) Bin4-5

Figure 5.11: CDF of Query Response Time in Facebook Workload

both HFS and HCS due to the combined benefits from the intra-query and inter-query scheduling techniques. To be specific, our query prediction model provides accurate selectivity estimation and task/job time prediction for the running queries. Based on the prediction results, the inter-query scheduling algorithm firstly selects the queries with smaller WRD for efficiency and assures comparable slowdown among queries for fairness. In addition, LoDFA speedups the progress of a single query once it is assigned with the priority to run. Such combined strategies contribute to the performance advantage of TLS over HCS and HFS for different bins of queries.

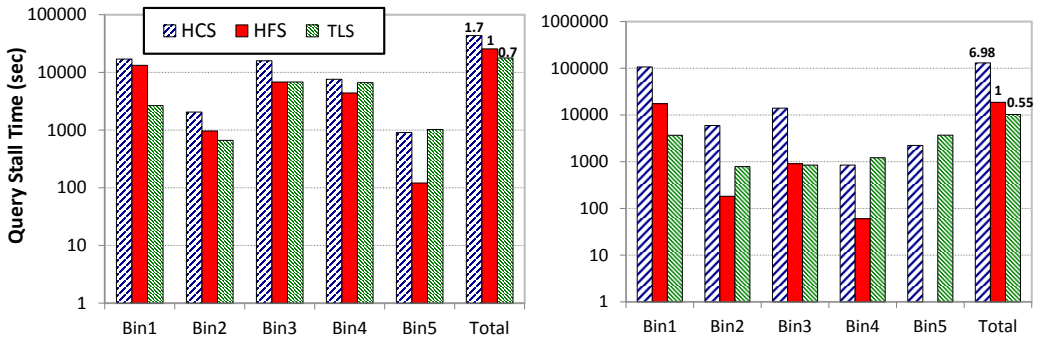

(a) Bing Workload (b) Facebook Workload

Figure 5.12: Aggregated stall times of the query bins in Bing and Facebook workloads (the times are in the logarithmic scale).

Query Execution Stalls

For small queries, the reduction of their response times mainly relies on minimizing execution stalls. To shed light on the reason why TLS can achieve performance improvement, for each query bin, we have collected the aggregated time of the execution stalls experienced by the queries in the bin. We show the aggregated stall times in Figure 5.12 for the three scheduling policies. Compared to HCS and HFS, TLS significantly reduces execution stalls of small queries (e.g., by 84.4% and 96.6% for the queries in Bin1 of the workloads relative to HCS). The last set of bars in each subfigure show the total stall time across all the bins. Compared to HFS and HCS, TLS reduces it by 30.4% and 59.1% for the Bing workload and by 45.1% and 92.1% for the Facebook workload.

We notice that TLS may slightly increase the execution stalls of the bins with large queries, such as Bin5, but the response times of large queries are not impacted by the increase (see Figure 5.11(d)). One reason is that the increase in stall time is not significant (please note Figure 5.12 uses a logarithmic scale to show the times), especially when compared with the total response time of large queries (large queries have large response times). The other reason is that the response time of a large query is more determined by the amount of resources it gets during its execution. A noteworthy observation is that HFS has zero stall for Bin5 in Facebook but performs the worst in terms of response time among three techniques (see Figure 5.11(d)). That is because in HFS even a large query may be allocated with only a tiny portion of total system resources. On the contrary, our inter-query QEF mechanism in TLS guarantees the resources demanded by a large query for fast processing and the intra-query LoDFA allows each single query to perform faster with given resources. Thus, large queries show lower response times with TLS than with other scheduling policies, despite the increases in stall times.

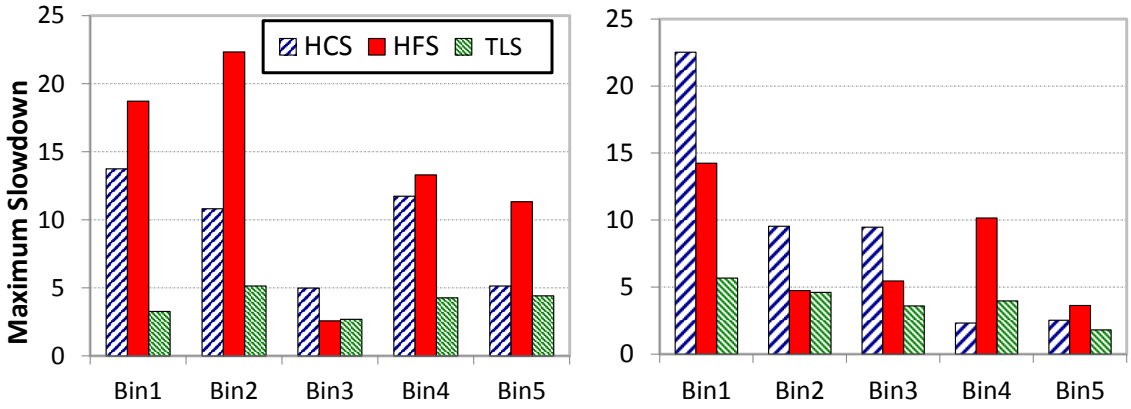

(a) Bing (b) Facebook

Figure 5.13: Maximum Slowdown

Improving Scheduling Fairness

For a system shared by queries from multiple users, it is desirable to schedule the queries fairly. To measure the fairness, we run the concurrent query workloads (Bing and Facebook) and collect the slowdown of each query, which is calculated as the ratio of a query's response time

to its response performance when executing alone. On an ideal system, we expect the queries be slowed down by similar percentages.

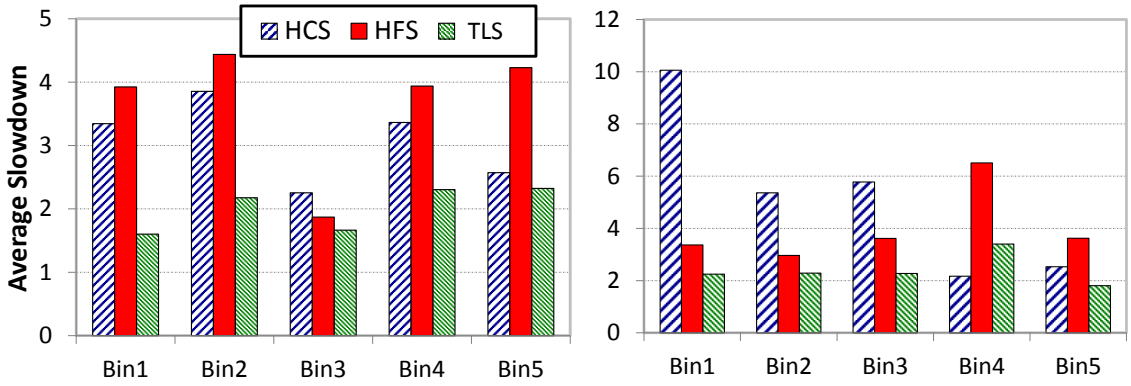

(a) Bing (b) Facebook

Figure 5.14: Average Slowdown

Figure 5.13 shows the maximum slowdown of the queries for each bin in Bing and Facebook workloads. A smaller value of the maximum slowdowns indicates that the queries in the corresponding bin are more fairly scheduled, since it is the upper bound of the slowdown difference between any two queries in the bin. In Figure 5.14, we show the average slowdown of the queries in each bin. By comparing the average slowdowns of different bins, we can estimate how fairly the queries across these bins are scheduled.

Not surprisingly, for both Bing and Facebook workloads, when they run with the HCS or HFS scheduler, the maximum slowdowns of the bins with large queries are usually lower than those of bins with smaller queries. For example, as shown in Figure 5.13, the maximum slowdowns of their first bins are higher than those of any other bins. This indicates that with HCS or HFS the performance of small queries are more subject to unfair scheduling than large queries. Figure 5.13 also shows that, though replacing HCS with HFS generally helps improve the fairness for the bins in Facebook workload, HFS still cannot render satisfactory fairness among different query bins. The main reason is that HFS strives to achieve job-level fairness but lacks the semantic information at query-level. Therefore, HFS cannot achieve good fairness among queries with different input sizes and DAG structures (e.g., tree-shaped and chain-shaped topologies described in Figure 2.7).

However, TLS achieves much lower maximum slowdowns for all the bins than HCS and HFS. This confirms that TLS can improve fairness significantly and consistently, irrespective of the query input sizes.

As shown in Figure 5.14, with HCS, small queries are biased by the scheduler, and they are usually slowed down by higher percentages than large queries. For example, for the Facebook workload, HCS incurs 10.1× average slowdown for the queries in Bin1 but 2.5× for Bin5. Though HFS may improve the fairness, the improvement comes at the cost of the performance of large queries. For example, compared to HCS, HFS significantly increases the average slowdowns of Bin4 and Bin5 in the Facebook workload. However, TLS can improve fairness more effectively than HFS. With TLS, the average slowdowns of different bins show much smaller variations than those with HFS. More importantly, the better fairness comes without degrading the performance. For all the bins, the average slowdowns are much lower than those with either HFS or HCS.

5.5 Related Studies on MapReduce and Scheduling

In this section, we review recent work on query modeling and scheduling in the MapReduce environment.

5.5.1 Query Modeling

Morton et al. [68] proposed the Paratimer model to estimate the progress of Pig queries, which are translated into DAGs of MapReduce jobs. Their model incorporated dataset cardinality and unit processing time. Verma et al. [100, 121] provided a "work/speed" time model for the relationship of execution time and available resources. Both time models require pre-execution profiling or debug runs of the same job in order to acquire the necessary phase information to estimate the job's execution time. Our work leverages selectivity estimation and does not require such pre-execution or debug runs of MapReduce queries.

In [69], Mullin proposed a partial bloom filter based join selectivity estimation algorithm. In [21], Bell et. al presented a piece-wise uniform approach for estimating the frequency distribution

of join attributes by equal-width histograms. In [30], Dell'aquila exploited the canonical coefficient parameters of estimating selectivity factors for relational operations through approximating both the multivariate data distribution and distinct values of attributes. Swami et al. [91] attempted selectivity prediction for multi-join operations with a common key and uniform key distribution. Our work extends this prior study to provide selectivity prediction for multi-join operations on different keys with piece-wise uniform distribution in the MapReduce environment.

Wu et al. [111] proposed AQUA as a comprehensive cost model to estimate CPU, network and I/O costs of database operations and MapReduce jobs. Our work is different from AQUA as a time based model and includes selectivity estimation for different types of query jobs. Li et al. [59] estimated query's resource demands using statistical models for individual operators of database queries. Ganapathi et al. [38, 37] developed a KCCA (Kernel Canonical Correlation Analysis) model based prediction system to solve the database query time estimation. Compared to these studies, we design a multivariate model for queries in MapReduce-based data warehouse systems.

5.5.2 MapReduce Scheduling and Other Related Work

Algorithms for scheduling jobs and/or DAGs of jobs have been studied based on general models. For example, the Johnson's algorithm [49] was proposed to solve two- and three-stage Job-shop problems. HLFET was proposed by Adam et al. [17] as a scheduling algorithm for DAGs of jobs in a multiprocessor environment. Similarly, Hu et al. [43] proposed a polynomial schedule algorithm for in-tree structured DAGs with unit computation cost. These algorithms cannot be directly applied to schedule analytic Hive queries due to the special features of Hive queries and frameworks. For example, Johnson's algorithm is not applicable for query scheduling due to the precedence constraint of jobs. In addition, parallelism level in MapReduce environment is flexible and job nodes in the query DAG are of non-uniform costs, which are different from the scenarios in [17] and [43].

Targeting the scheduling of individual MapReduce jobs, various algorithms were proposed. For example, Zaharia et al. [118] proposed delay scheduling to promote data locality in the scheduling of MapReduce jobs. Wolf et al. proposed a malleable scheduler *Flex* for optimizing the minisum and minimax metrics of response time, stretch, deadlines, etc [108]. They are not aware of the relationship of jobs in a DAG.

In some runtime engines (e.g. Spark [119], Dryad [46], Tez [3]), the structures of DAGs are considered. Shenker et al. [85] implemented Shark as a scalable SQL and Rich Analytics on top of Spark. Yu et al. [117] designed the DryadLINQ model for users to conduct declarative operations on distributed datasets. A DryadLINQ program is translated into an execution plan graph where each vertex is to execute as a Dryad job on the cluster-computing infrastructure. Ke et al. [50] provided a framework called Optimus for dynamically rewriting EPG (Execution Plan Graph) at runtime in DryadLINQ. Their work focuses on rewriting the upper-layer query plan by analyzing real-time statistics passed from low-layer runtime. Compared to these studies, our work leverages semantic information from DAG queries for modeling of job execution time and then employs the model into our two-level scheduler to improve scheduling efficiency.

Recently, FlowFlex extended the Flex scheduler to schedule flows (i.e. DAGs) of MapReduce jobs [70]. It provides a theoretic study and assumes the scheduler already know the amount of work in each job. TLS provides a whole package of solution from job execution time prediction and scheduling algorithms to real implementation. It is also based on richer semantic information, which is used to exploit more performance optimization opportunities. Tez [3] was developed for accelerating query processing in Hive/Hadoop. It supports DAG and task scheduling for every query and adopts a simplistic scheme for determining vertex priority and task parallelism of each vertex. However, it cannot estimate the execution times of the each node and query, and thus cannot correctly identify and schedule vertices on critical execution paths. Specifically, Tez allocates resources randomly among leaf nodes (runnable vertices) in each DAG and treats queries equally, in spite of their large differences in term of resource demands.

5.6 Summary

Many popular data warehouse systems are deployed on top of MapReduce. Complex analytic queries are usually compiled into directed acyclic graphs (DAGs). However, the simplistic job-level scheduling policy in MapReduce is unable to balance resource distribution and reconcile the dynamic needs of different jobs in DAGs. To address such issues systematically, we develop a scheduling framework which includes two main techniques: multivariate DAG modeling and two-level scheduling. Multivariate DAG modeling can accurately predict the changing data sizes and the execution time of jobs in DAG queries. Two-level scheduling is designed to allocate resources and schedule tasks at both inter-query and intra-query levels for efficient and fair execution of concurrent queries. The multivariate model offers important inputs for scheduling decisions in our two-level scheduler. Experiment results demonstrate that our techniques can achieve steady performance improvement over traditional scheduling techniques for representative query benchmarks due to accurate query time estimation, efficient resource allocation and reduced execution stalls. Furthermore, our two-level scheduler also significantly enhances query fairness.

Chapter 6

Conclusion

The dissertation investigates the big data challenges from two major perspectives: first, how to enable applications with fast data retrieval to storage systems; second, how to analyze big data efficiently. To tackle these challenges, I have invested substantial efforts in devising fast PCM-based hybrid storage system and optimizing I/O performance of scientific applications for fast data retrial; and developing a prediction-based scheduling framework on MapReduce-based data warehouse system for efficient data analytics. To this end, this dissertation has made the following three key contributions for addressing big data challenges.

In order to improve the big data storage and retrieval, I devise a PCM-Based Hybrid Storage System to improve I/O performance for traditional hard disk based storage system in Chapter 3. This hybrid storage system involves a novel write cache mapping and management scheme and two wear leveling algorithms for prolonging the life time of phase change memory. The HALO caching scheme introduces an efficient mapping and indexing schemes using advanced data structures such as bucket-based hashing and cuckoo hash table; in addition, a two-way destaging scheme is devised for data spatial and temporal locality optimization. As a result, HALO caching guarantees data reliability and greatly speeds up the I/O performance of diversified workloads (on average, 36.8%). The two novel wear leveling algorithms refer to rank-bank round-robin wear leveling and space filling curve based wear leveling, which prolong the PCM's life time by as much as 21.6 times.

In order to boost data access performance of scientific applications, we profile and address influential factors that can prevent current scientific applications from achieving efficient I/O of underlying parallel storage systems in Chapter 4. Particularly, we select a mission-critical application NASA GEOS-5 climate modeling as our case study. Through comprehensive experimental dissection and analysis, we observe that the hierarchical data aggregation and I/O patterns existent

in legacy applications can cause redundant network traffic and serious single-point contention issues. Therefore, we have modified GEOS-5's current I/O frameworks and enabled the application to exploits the benefits from the state-of-art parallel I/O interfaces such as PnetCDF and ADIOS. Experimental results on the NASA discover cluster shows that our technique can consistently improve the I/O performance of GEOS-5 for at various scales because of the elimination of redundant network aggregation and greatly promoted I/O concurrency.

In order to optimize the big data analytics, I identify the efficiency and fairness problems residing in current MapReduce schedulers and develop a prediction-based two-level query scheduling framework on Hive and Hadoop in Chapter 5. This framework is leveraged for bridging the semantic gap between Hive and Hadoop, conducting accurate resource usage and time estimation of queries, and enabling efficient two-level query scheduling for optimal fairness and response performance among concurrent analytic queries. Specifically, first the multivariate DAG modeling can accurately predict the changing data sizes and the execution time of jobs in DAG queries. Then, based on the predicted information, the two-level query scheduling is proposed to allocate resources and schedule tasks at both inter-query and intra-query levels for efficient and fair execution of concurrent queries. Experiment results demonstrate that our framework can achieve accurate query estimation and significant efficient and fairness improvement over traditional scheduling techniques for representative query benchmarks.

Chapter 7

Future Plan

In this chapter, we discuss some related ideas and topics that can further optimize and extend our accomplished work in different aspects. These issues can help create to a series of opportunities which we will investigate in our future studies.

PCM and storage system: we plan to study dynamically partitioned read/write cache schemes for improving a wider range of workload patterns. Particularly, a workload-aware prefetching scheme can be introduced for expediting the read response performance. In addition, an efficient PCM space management and allocation scheme is also in need. For further reducing memory overhead of cache mapping, a scalable and hierarchical hash table can be introduced. In terms of endurance, we have thought of another critical issue existing in current NVM wear leveling algorithms, namely, the row buffer locality that might be destroyed by the randomized mapping and cache line rotation introduced in traditional wear leveling algorithms such as Start-Gap [77]. Correspondingly, we are designing a bijective-matrix based mapping scheme and a row buffer locality aware rotation algorithm for achieving endurance without sacrificing memory performance.

Application I/O Optimization: it is of good potential to study asynchronous I/O schemes and efficient burst buffering techniques for further I/O performance improvements of scientific applications. To be specific, non-volatile memory technologies such as PCM or FSSD can be integrated into the storage hierarchy of traditional parallel storage systems such as Lustre. Furthermore, our HALO caching and destaging schemes can be adapted to work in cooperation with upper-layer I/O optimization framework for further boosting data depositing and retrieval performance of large-scale applications.

Query scheduling and MapReduce: Recently, Hadoop ecosystem has evolved to version 2.0 - YARN (Yet Another Resource Negotiator) [99]. Therefore, I have just ported my query scheduling framework also to YARN platform. The preliminary results demonstrate that our implementation can also improve query performance significantly compared to traditional scheduling algorithms. In addition, we plan to extend the query prediction model as an accurate real-time query progress indicator with concurrency, data skew and task failure considered. Such optimization can not only provide expectable quality-of-service for users' interactive requests, but also enable the resource scheduler to determine the possible deadline of each request for SLA (Service Level Agreement). Currently the low-latency interactive data processing engines such as Spark [119] and streaming data processing engines such as Storm [2] have sprung up. It is very promising and urgent for us to conduct accurate query resource estimation and smart resource scheduling for such new data analytics paradigms.

Bibliography

[1] Adaptable I/O System. http://www.nccs.gov/user-support/center-projects/adios .

[2] Apache Storm. https://storm.apache.org/.

[3] Apache Tez. http://hortonworks.com/hadoop/tez/.

[4] Are hybrid drives finally coming of age? http://www.researchandmarkets.com/reports/1409321/are_hybrid_drives_finally_coming_of_age.pdf.

[5] Energy Sources. http://energy.gov/science-innovation/energy-sources.

[6] Micron phase change memory. http://www.micron.com/products/phase-change-memory.

[7] NASA Discover. http://www.nccs.nasa.gov/cluster_main.html.

[8] NASA GEOS. http://gmao.gsfc.nasa.gov/systems/geos5.

[9] NETCDF. http://www.unidata.ucar.edu/software/netcdf.

[10] NVIDIA Tesla. http://www.nvidia.com/object/tesla-supercomputing\newline-solutions.html.

[11] The Parallel Virtual File System, version 2. http://www.pvfs.org/pvfs2.

[12] Top 500 supercomputing sites. http://www.top500.org.

[13] TPC. http://www.tpc.org/.

[14] Umass trace repository. http://traces.cs.umass.edu/.

[15] *SNIA BlockIO Traces*. http://iotta.snia.org/tracetypes/3, Online, 2006.

[16] H. Abbasi, M. Wolf, G. Eisenhauer, S. Klasky, K. Schwan, and F. Zheng. Datastager: scalable data staging services for petascale applications. In *Proceedings of the 18th ACM international symposium on High performance distributed computing*, HPDC '09, pages 39–48, New York, NY, USA, 2009. ACM.

[17] Thomas L Adam, K. Mani Chandy, and JR Dickson. A comparison of list schedules for parallel processing systems. *Communications of the ACM*, 17(12):685–690, 1974.

[18] A. Akel, A.M. Caulfield, T.I. Mollov, R.K. Gupta, and S. Swanson. Onyx: A prototype phase change memory storage array. In *HotStorage'11*.

[19] Ganesh Ananthanarayanan, Ali Ghodsi, Andrew Wang, Dhruba Borthakur, Srikanth Kandula, Scott Shenker, and Ion Stoica. Pacman: Coordinated memory caching for parallel jobs. In *USENIX NSDI*, 2012.

[20] M. Baker, S. Asami, E. Deprit, J. Ouseterhout, and M. Seltzer. Non-volatile memory for fast, reliable file systems. *ACM SIGPLAN Notices*, 27(9):10–22, 1992.

[21] David A Bell, DHO Link, and S McClean. Pragmatic estimation of join sizes and attribute correlations. In *ICDE*, pages 76–84. IEEE, 1989.

[22] J. Bent, G. A. Gibson, G. Grider, B. McClelland, P. Nowoczynski, J. Nunez, M. Polte, and M. Wingate. PLFS: a checkpoint filesystem for parallel applications. In *SC '09: Proceedings of the Conference on High Performance Computing Networking, Storage and Analysis*, 2009.

[23] Alan D Brunelle. Blktrace user guide, 2007.

[24] John S. Bucy and G. R. Ganger. Technical report. http://www.pdl.cmu.edu/DiskSim/.

[25] Z. Liu H. Chen B. Neitzel C. Xu, R. Goldsone and W. Yu. Exploiting analytics shipping with virtualized mapreduce on hpc backend storage servers. *Parallel and Distributed Computing, IEEE Transactions on*, 2015.

[26] S. Chen, P.B. Gibbons, and S. Nath. Rethinking database algorithms for phase change memory. *CIDR11*, pages 21–31, 2011.

[27] A. Choudhary, W. Liao, K. Gao, A. Nisar, R. Ross, R. Thakur, and R. Latham. Scalable I/O and analytics. *Journal of Physics*, 180(1), 2009.

[28] Cluster File System, Inc. Lustre: A Scalable, High Performance File System. http://www.lustre.org/docs.html.

[29] Jeffrey Dean and Sanjay Ghemawat. Mapreduce: simplified data processing on large clusters. *Communications of the ACM*, 51(1):107–113, 2008.

[30] Carlo Dellaquila, Ezio Lefons, and Filippo Tangorra. Analytic-based estimation of query result sizes. In *Proceedings of the 4th WSEAS International Conference on Artificial Intelligence, Knowledge Engineering Data Bases*, page 24. WSEAS, 2005.

[31] X. Ding, S. Jiang, F. Chen, K. Davis, and X. Zhang. Diskseen: exploiting disk layout and access history to enhance i/o prefetch. In *USENIX ATC*, 2007.

[32] I.H. Doh, J. Choi, D. Lee, and S.H. Noh. Exploiting non-volatile ram to enhance flash file system performance. In *ACM EMSOFT'07*.

[33] I.H. Doh, H.J. Lee, Y.J. Moon, E. Kim, J. Choi, D. Lee, and S.H. Noh. Impact of nvram write cache for file system metadata on i/o performance in embedded systems. In *ACM SAC'09*.

[34] Jennie Duggan, Ugur Cetintemel, Olga Papaemmanouil, and Eli Upfal. Performance prediction for concurrent database workloads. In *Proceedings of the 2011 ACM SIGMOD International Conference on Management of data*, pages 337–348. ACM, 2011.

[35] M. R. Fahey, J. M. Larkin, and J. Adams. I/O performance on a massively parallel cray XT3/XT4. In *Proc. 22nd IEEE International Symposium on Parallel and Distributed Processing (22nd IPDPS'08)*, 2008.

[36] D. Fotakis, R. Pagh, P. Sanders, and P. Spirakis. Space efficient hash tables with worst case constant access time. *STACS 2003*, pages 271–282, 2003.

[37] Archana Ganapathi, Yanpei Chen, Armando Fox, Randy Katz, and David Patterson. Statistics-driven workload modeling for the cloud. In *ICDEW*. IEEE, 2010.

[38] Archana Ganapathi, Harumi Kuno, Umeshwar Dayal, Janet L Wiener, Armando Fox, Michael Jordan, and David Patterson. Predicting multiple metrics for queries: Better decisions enabled by machine learning. In *Data Engineering, 2009. ICDE'09. IEEE 25th International Conference on*, pages 592–603. IEEE, 2009.

[39] John Gantz and David Reinsel. The digital universe in 2020: Big data, bigger digital shadows, and biggest growth in the far east. *IDC iView: IDC Analyze the Future*, 2012.

[40] Alan F Gates, Olga Natkovich, Shubham Chopra, Pradeep Kamath, Shravan M Narayanamurthy, Christopher Olston, Benjamin Reed, Santhosh Srinivasan, and Utkarsh Srivastava. Building a high-level dataflow system on top of map-reduce: the pig experience. *Proceedings of the VLDB Endowment*, 2(2):1414–1425, 2009.

[41] B.S. Gill and D.S. Modha. Wow: wise ordering for writes-combining spatial and temporal locality in non-volatile caches. In *USENIX FAST'05*.

[42] C. Hill, C. DeLuca, V. Balaji, M. Suarez, and A. D. Silva. The architecture of the earth system modeling framework. *Computing in Science and Engg.*, 6(1):18–28, January 2004.

[43] Te C Hu. Parallel sequencing and assembly line problems. *Operations research*, 9(6):841–848, 1961.

[44] J. H. Laros III, L. Ward, R. Klundt, S. Kelly, J. L. Tomkins, and B. R. Kellogg. Red storm IO performance analysis. In *CLUSTER*, 2007.

[45] E. Ipek, J. Condit, E. B. Nightingale, D. Burger, and T. Moscibroda. Dynamically replicated memory: building reliable systems from nanoscale resistive memories. *ASPLOS'10*.

[46] Michael Isard, Mihai Budiu, Yuan Yu, Andrew Birrell, and Dennis Fetterly. Dryad: distributed data-parallel programs from sequential building blocks. *ACM SIGOPS Operating Systems Review*, 41(3):59–72, 2007.

[47] S. Jiang, X. Ding, F. Chen, E. Tan, and X. Zhang. Dulo: an effective buffer cache management scheme to exploit both temporal and spatial locality. In *USENIX FAST'05*.

[48] S. Jiang and X. Zhang. Lirs: an efficient low inter-reference recency set replacement policy to improve buffer cache performance. In *ACM SIGMETRICS Performance Evaluation Review*, volume 30, pages 31–42. ACM, 2002.

[49] Selmer Martin Johnson. Optimal two-and three-stage production schedules with setup times included. *Naval research logistics quarterly*, 1(1):61–68, 1954.

[50] Qifa Ke, Michael Isard, and Yuan Yu. Optimus: a dynamic rewriting framework for data-parallel execution plans. In *Proceedings of the 8th ACM European Conference on Computer Systems*, pages 15–28. ACM, 2013.

[51] J Keilson and LD Servi. A distributional form of little's law. *Operations Research Letters*, 7(5):223–227, 1988.

[52] C.S. Kim. Lrfu: A spectrum of policies that subsumes the least recently used and least frequently used policies. *IEEE Transactions on Computers*, 50(12), 2001.

[53] S. Lang, P. H. Carns, R. Latham, R. B. Ross, K. Harms, and W. E. Allcock. I/O performance challenges at leadership scale. In *SC'09 USB Key*. ACM/IEEE, Portland, OR, USA, nov 2009.

[54] Eunji Lee, Hyokyung Bahn, and Sam H Noh. Unioning of the buffer cache and journaling layers with non-volatile memory. In *FAST*, pages 73–80. USENIX, 2013.

[55] KH Lee, IH Doh, J. Choi, D. Lee, and SH Noh. Write-aware buffer cache management scheme for nonvolatile ram. In *Proceedings of Advances in Computer Science and Technology*. ACTA Press, 2007.

[56] Rubao Lee, Tian Luo, Yin Huai, Fusheng Wang, Yongqiang He, and Xiaodong Zhang. Ysmart: Yet another sql-to-mapreduce translator. In *Distributed Computing Systems (ICDCS), 2011 31st International Conference on*, pages 25–36. IEEE, 2011.

[57] D. Li, J. Vetter, G. Marin, C. McCurdy, C. Cira, Z. Liu, and W. Yu. Identifying opportunities for byte-addressable non-volatile memory in extreme-scale scientific applications. In *IPDPS*. IEEE, 2012.

[58] J. Li, W. Liao, A. Choudhary, R. Ross, R. Thakur, W. Gropp, and R. Latham. Parallel netCDF: A High Performance Scientific I/O Interface. In *Proc. SC03*, 2003.

[59] Jiexing Li, Arnd Christian König, Vivek Narasayya, and Surajit Chaudhuri. Robust estimation of resource consumption for sql queries using statistical techniques. *Proceedings of the VLDB Endowment*, 5(11):1555–1566, 2012.

[60] Xian Liu and G.F. Schrack. An algorithm for encoding and decoding the 3-d hilbert order. *Image Processing, IEEE Transactions on*, 6(9):1333–1337, sep 1997.

[61] Z. Liu, B. Wang, P. Carpenter, D. Li, J. S. Vetter, and W. Yu. PCM-based durable write cache for fast disk I/O. In *Modeling, Analysis & Simulation of Computer and Telecommunication Systems (MASCOTS), 2012 IEEE 20th International Symposium on*, pages 451–458. IEEE, 2012.

[62] Zhuo Liu, Jay Lofstead, Teng Wang, and Weikuan Yu. A case of system-wide power management for scientific applications. In *Cluster Computing (CLUSTER), 2013 IEEE International Conference on*, pages 1–8. IEEE, 2013.

[63] Zhuo Liu, Bin Wang, Teng Wang, Yuan Tian, Cong Xu, Yandong Wang, Weikuan Yu, Carlos A Cruz, Shujia Zhou, Tom Clune, and Scott Klasky. Profiling and improving i/o performance of a large-scale climate scientific application. In *Computer Communications and Networks (ICCCN), 2013 22nd International Conference on*, pages 1–7. IEEE, 2013.

[64] Zhuo Liu, Jian Zhou, Weikuan Yu, Fei Wu, Xiao Qin, and Changsheng Xie. Mind: A black-box energy consumption model for disk arrays. In *Green Computing Conference and Workshops (IGCC), 2011 International*, pages 1–6. IEEE, 2011.

[65] J. Lofstead, M. Polte, G. Gibson, S. Klasky, K. Schwan, R Oldfield, M. Wolf, and Q. Liu. Six degrees of scientific data: Reading patterns for extreme scale science io. In *In Proceedings of High Performance and Distributed Computing*, 2011.

[66] J. Lofstead, F. Zheng, S. Klasky, and K. Schwan. Adaptable, metadata rich IO methods for portable high performance IO. In *IPDPS'09*, 2009.

[67] The HDF Group. Hierarchical data format version 5, 2000–2010. http://www.hdfgroup.org/HDF5.

[68] Kristi Morton, Magdalena Balazinska, and Dan Grossman. Paratimer: a progress indicator for mapreduce dags. In *Proceedings of the 2010 ACM SIGMOD International Conference on Management of data*, pages 507–518. ACM, 2010.

[69] James K Mullin. Estimating the size of a relational join. *Information Systems*, 18(3):189–196, 1993.

[70] Viswanath Nagarajan, Joel Wolf, Andrey Balmin, and Kirsten Hildrum. Flowflex: Malleable scheduling for flows of mapreduce jobs. In *Middleware 2013*, pages 103–122. Springer, 2013.

[71] T. Nightingale, Y. Hu, and Q. Yang. The design and implementation of a dcd device driver for unix. In *USENIX ATC'99*.

[72] E.J. O'neil, P.E. O'neil, and G. Weikum. The lru-k page replacement algorithm for database disk buffering. In *ACM SIGMOD'93*.

[73] OSDL. *Iometer project*. http://www.iometer.org/, Online, 2004.

[74] R. Pagh and F. Rodler. Cuckoo hashing. *AlgorithmsESA 2001*, pages 121–133, 2001.

[75] Y. Park, S.H. Lim, C. Lee, and K.H. Park. Pffs: a scalable flash memory file system for the hybrid architecture of phase-change ram and nand flash. In *ACM SAC'08*.

[76] Gregory Piatetsky-Shapiro and Charles Connell. Accurate estimation of the number of tuples satisfying a condition. In *ACM SIGMOD Record*, volume 14, pages 256–276. ACM, 1984.

[77] M.K. Qureshi, J. Karidis, M. Franceschini, V. Srinivasan, L. Lastras, and B. Abali. Enhancing lifetime and security of pcm-based main memory with start-gap wear leveling. In *IEEE/ACM Micro'09*.

[78] M.K. Qureshi, V. Srinivasan, and J.A. Rivers. Scalable high performance main memory system using phase-change memory technology. In *ISCA'09*.

[79] L.E. Ramos, E. Gorbatov, and R. Bianchini. Page placement in hybrid memory systems. In *ICS'11*.

[80] M. Rosenblum and J.K. Ousterhout. The design and implementation of a log-structured file system. *ACM SIGOPS Operating Systems Review*, 25(5):1–15, 1991.

[81] S. Saini, J. Rappleye, J. Chang, D.P. Barker, R. Biswas, and P. Mehrotra. I/O Performance Characterization of Lustre and NASA Applications on Pleiades. In *HiPC*, 2012.

[82] S. W. Schlosser, J. Schindler, S. Papadomanolakis, M. Shao, A. Ailamaki, C. Faloutsos, and G. R. Ganger. On Multidimensional Data and Modern Disks. In *FAST*, 2005.

[83] F. Schmuck and R. Haskin. GPFS: A Shared-Disk File System for Large Computing Clusters. In *FAST '02*, pages 231–244. USENIX, January 2002.

[84] Nak Hee Seong, Dong Hyuk Woo, and Hsien-Hsin S. Lee. Security refresh: prevent malicious wear-out and increase durability for phase-change memory with dynamically randomized address mapping. In *ISCA'10*.

[85] Scott Shenker, Ion Stoica, Matei Zaharia, Reynold Xin, Josh Rosen, and Michael J Franklin. Shark: Sql and rich analytics at scale. In *Proceedings of the 2013 ACM SIGMOD International Conference on Management of Data*, 2013.

[86] Liang Shi, Jianhua Li, Chun Jason Xue, and Xuehai Zhou. Hybrid nonvolatile disk cache for energy-efficient and high-performance systems. *ACM Transactions on Design Automation of Electronic Systems (TODAES)*, 18(1):8, 2013.

[87] T. Shimada, T. Tsuji, and K. Higuchi. A storage scheme for multidimensional data alleviating dimension dependency. In *Digital Information Management, 2008. ICDIM 2008. Third International Conference on*, 2008.

[88] Gokul Soundararajan, Vijayan Prabhakaran, Mahesh Balakrishnan, and Ted Wobber. Extending ssd lifetimes with disk-based write caches. In *USENIX FAST'10*.

[89] M. Suarez, A. Trayanov, C. Hill, P. Schopf, and Y. Vikhliaev. MAPL: a high-level programming paradigm to support more rapid and robust encoding of hierarchical trees of interacting high-performance components. In *Proceedings of the 2007 symposium on Component and framework technology in high-performance and scientific computing*, 2007.

[90] G. Sun, Y. Joo, Y. Chen, D. Niu, Y. Xie, Y. Chen, and H. Li. A hybrid solid-state storage architecture for the performance, energy consumption, and lifetime improvement. In *IEEE HPCA'10*.

[91] A. Swami and K.B. Schiefer. On the estimation of join result sizes. *IBM Technical Report*, 1993.

[92] Jian Tan, Xiaoqiao Meng, and Li Zhang. Delay tails in mapreduce scheduling. In *Proceedings of the 12th ACM SIGMETRICS/PERFORMANCE joint international conference on Measurement and Modeling of Computer Systems*, SIGMETRICS '12, pages 5–16, New York, NY, USA, 2012. ACM.

[93] The National Center for SuperComputing. HDF Home Page. http://hdf.ncsa.uiuc.com/hdf4.html.

[94] Ashish Thusoo, Joydeep Sen Sarma, Namit Jain, Zheng Shao, Prasad Chakka, Ning Zhang 0002, Suresh Anthony, Hao Liu, and Raghotham Murthy. Hive - a petabyte scale data warehouse using hadoop. In *ICDE*, pages 996–1005, 2010.

[95] Y. Tian, S. Klasky, H. Abbasi, J. Lofstead, N. Podhorszki R. Grout, Q. Liu, Y. Wang, and W. Yu. EDO: Improving Read Performance for Scientific Applications Through Elastic Data Organization. In *CLUSTER '11: Proceedings of the 2011 IEEE International Conference on Cluster Computing*, 2011.

[96] Y. Tian, S. Klasky, W. Yu, H. Abbasi, B. Wang, N. Podhorszki, R.W. Grout, and M. Wolf. SMART-IO: SysteM-AwaRe Two-Level Data Organization for Efficient Scientific Analytics. In *MASCOTS*, 2012.

[97] Y. Tian, Z. Liu, S. Klasky, B. Wang, H. Abbasi, S. Zhou, N. Podhorszki, T. Clune, J. Logan, and W. Yu. A lightweight I/O scheme to facilitate spatial and temporal queries of scientific data analytics. In *Mass Storage Systems and Technologies (MSST), 2013 IEEE 29th Symposium on*. IEEE, 2013.

[98] Unidata. http://www.hdfgroup.org/projects/netcdf-4/.

[99] Vinod Kumar Vavilapalli, Arun C Murthy, Chris Douglas, Sharad Agarwal, Mahadev Konar, Robert Evans, Thomas Graves, Jason Lowe, Hitesh Shah, Siddharth Seth, et al. Apache hadoop yarn: Yet another resource negotiator. In *Proceedings of the 4th annual Symposium on Cloud Computing*, page 5. ACM, 2013.

[100] Abhishek Verma, Ludmila Cherkasova, and Roy H Campbell. Aria: automatic resource inference and allocation for mapreduce environments. In *Proceedings of the 8th ACM international conference on Autonomic computing*, pages 235–244. ACM, 2011.

[101] A.I.A. Wang, P. Reiher, G.J. Popek, and G.H. Kuenning. Conquest: Better performance through a disk/persistent-ram hybrid file system. In *USENIX ATC'02*.

[102] Bin Wang, Zhuo Liu, Xinning Wang, and Weikuan Yu. Eliminating intra-warp conflict misses in gpu. In *Proceedings of the Conference on Design, Automation and Test in Europe*. EDA Consortium, 2015.

[103] Jue Wang, Xiangyu Dong, Yuan Xie, and Norman P Jouppi. i2wap: Improving non-volatile cache lifetime by reducing inter-and intra-set write variations. In *High Performance Computer Architecture (HPCA2013), 2013 IEEE 19th International Symposium on*, pages 234–245. IEEE, 2013.

[104] Teng Wang, Kevin Vasko, Zhuo Liu, Hui Chen, and Weikuan Yu. Bpar: a bundle-based parallel aggregation framework for decoupled i/o execution. In *Proceedings of the 2014 International Workshop on Data Intensive Scalable Computing Systems*, pages 25–32. IEEE Press, 2014.

[105] Teng Wang, Kevin Vasko, Zhuo Liu, Hui Chen, and Weikuan Yu. Enhance scientific application i/o with cross-bundle aggregation. *International Journal of High Performance Computing Applications*, 2015.

[106] Yandong Wang, Yizheng Jiao, Cong Xu, Xiaobing Li, Teng Wang, Xinyu Que, Cristi Cira, Bin Wang, Zhuo Liu, Bliss Bailey, and Weikuan Yu. Assessing the performance impact of high-speed interconnects on mapreduce. In *Specifying Big Data Benchmarks*, pages 148–163. Springer, 2014.

[107] Yandong Wang, Jian Tan, Weikuan Yu, Xiaoqiao Meng, and Li Zhang. Preemptive reducetask scheduling for fair and fast job completion. In *Proceedings of the 10th International Conference on Autonomic Computing, ICAC*, volume 13, 2013.

[108] Joel Wolf, Deepak Rajan, Kirsten Hildrum, Rohit Khandekar, Vibhore Kumar, Sujay Parekh, Kun-Lung Wu, and Andrey Balmin. Flex: A slot allocation scheduling optimizer for mapreduce workloads. In *Middleware'10*, pages 1–20. Springer, 2010.

[109] Ronald W Wolff. *Stochastic modeling and the theory of queues*, volume 14. Prentice hall Englewood Cliffs, NJ, 1989.

[110] D. Woodhouse. Jffs: The journalling flash file system. In *Ottawa Linux Symposium*, volume 2001, 2001.

[111] Sai Wu, Feng Li, Sharad Mehrotra, and Beng Chin Ooi. Query optimization for massively parallel data processing. In *Proceedings of the 2nd ACM Symposium on Cloud Computing*, page 12. ACM, 2011.

[112] C. Xu, M. G. Venkata, R. L. Graham, Y. Wang, Z. Liu, and W. Yu. SLOAVx: Scalable LOgarithmic AlltoallV algorithm for hierarchical multicore systems. In *Cluster, Cloud and Grid Computing (CCGrid), 13th IEEE/ACM International Symposium on*. IEEE, 2013.

[113] Q. Yang and J. Ren. I-cash: Intelligently coupled array of ssd and hdd. In *IEEE HPCA'11*.

[114] W. Yu, H. S. Oral, J. S. Vetter, and R. Barrett. Efficiency Evaluation of Cray XT Parallel I/O Stack. In *Cray User Group Meeting (CUG 2007)*, 2007.

[115] W. Yu, J. S. Vetter, and S. Oral. Performance characterization and optimization of parallel I/O on the Cray XT. In *IPDPS*, 2008.

[116] W. Yu, J.S. Vetter, R.S. Canon, and S. Jiang. Exploiting lustre file joining for effective collective IO. In *CCGRID*, 2007.

[117] Yuan Yu, Michael Isard, Dennis Fetterly, Mihai Budiu, Úlfar Erlingsson, Pradeep Kumar Gunda, and Jon Currey. Dryadlinq: A system for general-purpose distributed data-parallel computing using a high-level language. In *OSDI*, volume 8, pages 1–14, 2008.

[118] Matei Zaharia, Dhruba Borthakur, Joydeep Sen Sarma, Khaled Elmeleegy, Scott Shenker, and Ion Stoica. Delay scheduling: a simple technique for achieving locality and fairness in cluster scheduling. In *Proceedings of the 5th European conference on Computer systems*, EuroSys'10, pages 265–278, New York, NY, USA, 2010. ACM.

[119] Matei Zaharia, Mosharaf Chowdhury, Michael J Franklin, Scott Shenker, and Ion Stoica. Spark: cluster computing with working sets. In *Proceedings of the 2nd USENIX conference on Hot topics in cloud computing*, pages 10–10, 2010.

[120] W. Zhang and T. Li. Exploring Phase Change Memory and 3D Die-Stacking for Power/Thermal Friendly, Fast and Durable Memory Architecture. In *PACT*, 2009.

[121] Zhuoyao Zhang, Ludmila Cherkasova, Abhishek Verma, and Boon Thau Loo. Automated profiling and resource management of pig programs for meeting service level objectives. In *Proceedings of the 9th international conference on Autonomic computing*, pages 53–62. ACM, 2012.

[122] P. Zhou, B. Zhao, J. Yang, and Y. Zhang. A durable and energy efficient main memory using phase change memory technology. In *ISCA'09*.

[123] Y. Zhou, J.F. Philbin, and K. Li. The multi-queue replacement algorithm for second level buffer caches. In *USENIX ATC'02*.